Aus dem Institut für Transfusionsmedizin und Immunologie
der Medizinischen Fakultät Mannheim
(Direktor: Prof. Dr. med. Harald Klüter)

Analysis of macrophage production and biological activity of chitinase-like protein YKL-39

Inauguraldissertation
zur Erlangung des Doctor scientiarum humanarum (Dr. sc. hum.)
der
Medizinischen Fakultät Mannheim
der Ruprecht-Karls-Universität
zu
Heidelberg

vorgelegt von
Tengfei Liu
aus
Hebei, VR China
2017

Dekan: Prof. Dr. Sergij Goerdt

Referentin: Prof. Dr. Julia Kzhyshkowska

Contents

Figure Index

Table Index

Abbreviation

°C	degrees centigrade
ABCA1	ATP-binding cassette transporter 1
AMCase	Acidic Mammalian Chitinase
ARRDC4	arrestin domain containing 4
BC	buffy coat
BRP–39	breast regression protein-39
CC	Chemokine (C-C motif)
CCL	Chemokine (C-C motif) ligand
CCR	C-C chemokine receptor
CD14	CD14 positive macrophages
CD274	cluster of differentiation 274
CD82	cluster of differentiation 82
CD-MPR	cation-dependent mannose receptor
cDNA	complementary deoxyribonucleic acid
CHI3L1	chitinase-3-like protein 1
CHI3L2	chitinase-3-like protein 2
CHIT1	chitotriosidase
CI-MPR	cation-independent mannose 6-phosphate receptor
CLPs	chitinase-like protein
CRIM1	cysteine rich transmembrane BMP regulator 1
CTLA-4	cytotoxic T-lymphocyte antigen 4
CXC	C-X-C motif chemokine
CXCL	C-X-C motif chemokine ligand
ddH2O	double distilled water
dNTPs	deoxyribonucleotides
EBM	endothelial basal medium
ECM	extracellular matrix
EDTA	ethylene diamine tetra acetic acid
EEA1	early endosome antigen 1
EGF	epidermal growth factor
EGM	endothelial cell growth medium
ELISA	enzyme-linked Immunosorbent Assay
ERK	extracellular signal–regulated kinases

Abbreviation

FACS	fluorescent activated cell sorting
FGF	fibroblast growth factors
GAPDH	glyceraldehyde 3-phosphate dehydrogenase
GC	glucocorticoids
GlcNac	N-Acetylglucosamin
GM-CSF	granulocyte-macrophage colony-stimulating factor
GMP-17	granule membrane protein of 17-kDa
HMVECs	human microvascular endothelial cells
HSD11B1	hydroxysteroid 11-beta dehydrogenase 1
IFNγ	interferon gamma
IGF	insulin-like growth factor-1
IL	interleukin
iNOS	inducible nitric oxide synthase
ITC	isothermal titration calorimetry
LAMP-1	lysosomal-associated membrane protein 1
LMP1	latent membrane protein 1
LPS	lipopolysaccharide
M1	classically activated macrophages
M2	alternatively activated macrophages
mA	microampere(s)
MAPK	mitogen-activated protein kinase
MCP-1	monocyte chemotactic protein 1
M-CSF	macrophage colony-stimulating factor
min	minute(s)
ml	milliliter
mM	millimolar concentration
mm	millimeter
MMP	matrix metalloproteinase
MPR	mannose-6-phosphate receptor
mRNA	messenger RNA
NF-κB	nuclear factor kappa-light-chain-enhancer of activated B cells
ng	nanogram
OA	osteoarthritis
OS	overall survival
p62lck	zeta-interacting protein

Abbreviation

PBMC	peripheral blood mononuclear cell
PBS	phosphate buffered saline
PCR	polymerase chain reaction
PDGF	platelet-derived growth factor
PFA	paraformaldehyde
pg	picogram
PGE	prostaglandin E
RA	rheumatoid arthritis
RELM-alpha	retnla resistin like alpha
RNA	ribonucleic acid
rcf	relative centrifugal force
rpm	revolutions per minute
RT	room temperature
SAGE	serial analysis of gene expression
SGPP2	sphingosine-1-phosphate phosphatase 2
SI-CLP	stabilin-1 interacting chitinase-like protein
siRNA	small interfering RNA
TAMs	tumor-associated macrophages
TGF-beta	transforming growth factor beta
TGFβR1	transforming growth factor, beta receptor I
TGN	trans Golgi network
Th	T helper
TIM	triosephosphateisomerase
TLR	toll-like receptor
TNF-α	tumor necrosis factor alpha
TNFAIP6	TNF-stimulated gene-6
UV	ultraviolet
V	volt(s)
VEGF	vascular endothelial growth factor
VHS	VPS-27, Hrs and STAM
vs	versus
VSMC	vascular smooth muscle cells
YM1	chitinase-like 3
YM2	chitinase-like 4
μg	microgram

Abbreviation

µl	microliter
µm	micrometer

1 Introduction

1.1 Chitinase-like protein family

1.1.1 Chitin, chitinases, and chitinase-like proteins

Chitin is the second most abundant polysaccharide in nature, after cellulose (Tharanathan and Kittur, 2003). It is found in the cell walls of fungi, exoskeletons of crustaceans and insects (Kzhyshkowska et al., 2007; Muzzarelli, 2013). In lower life forms, the deposition of chitin is regulated by the balance of biosynthesis and degradation, in which process chitinases act as key factors (Lee et al., 2011; Patel and Goyal, 2017). The chitinases are produced by the lower life forms as a defense mechanism against infection with chitin-containing organisms (Elias et al., 2005; Mondal et al., 2016). Mammals cannot synthesize chitin, however, several chitinases and chitinase-like proteins (CLPs) were identified in rodents and in human.

Chitinases belong to the Glycoside hydrolase family 18 and possess enzymatic activities, being able to cleave chitin polymers into oligosaccharides of different sizes and release monosaccharides from the end of chitin polymer (Boot et al., 2001; Di Rosa et al., 2016). In human, two functional chitinases: Acidic Mammalian Chitinase (AMCase) and Chitotriosidase (CHIT1) were found. AMCase is induced by IL-13 and is found in allergic inflammation such as asthma (Donnelly and Barnes, 2004; Zhu et al., 2004). Chitotriosidase is expressed by phagocytic cells and is a biomarker for the Gaucher's disease, the lysosomal storage disease that involves the dysfunctional metabolism of sphingolipids (Cox, 2001; Raskovalova et al., 2017).

Chitinase-like proteins are also known as chitinase-like lectins, which have an amino acid sequence similarity to the chitinases but lack enzymatic activity (Kzhyshkowska et al., 2016b). In mammals following CLPs were identified: YKL-40, YKL-39, SI-CLP, YM1 and YM2 (Hu et al., 1996; Jin et al., 1998; Kzhyshkowska et al., 2006b; Owhashi et al., 2000; Volck et al., 1997). Out of them, YKL-39 is present only in human but absent in rodents, while YM1 and YM2 are only present in rodents (Kzhyshkowska et al., 2016b).

1.1.2 Structure and properties of chitinase-like proteins

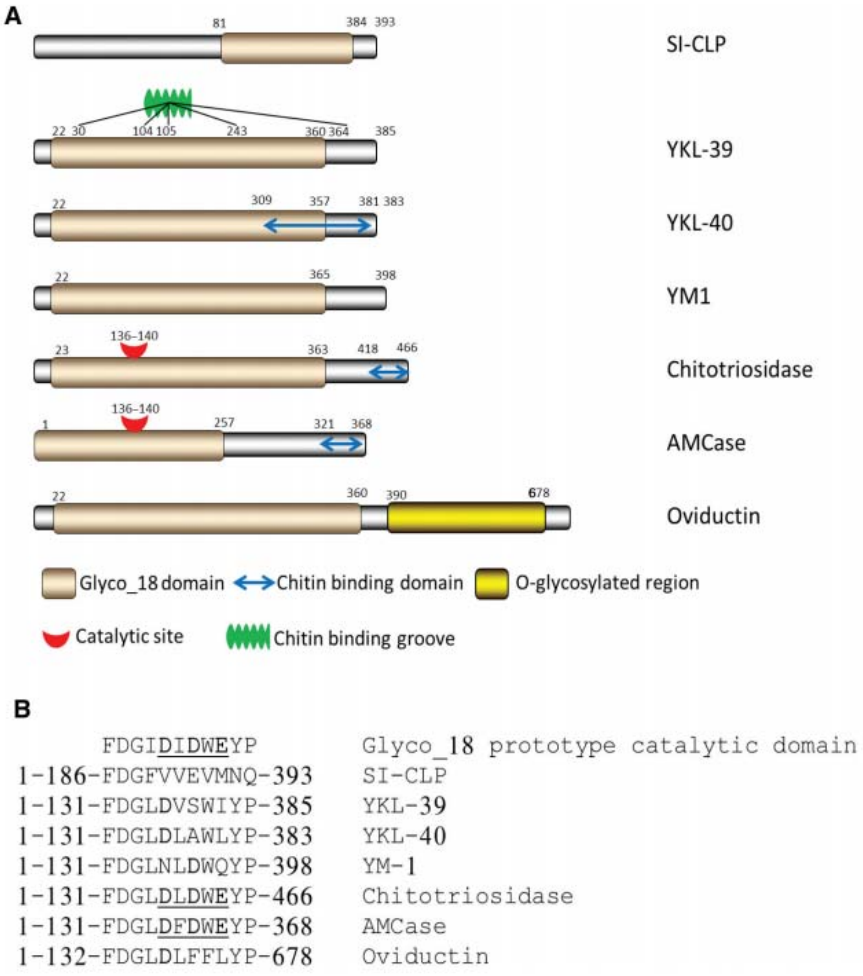

Figure 1. The structure of mammalian chitinases and chitinase-like proteins. A. Domain organization of Glyco_18 containing proteins; **B.** Critical amino acids in catalytic sites of mammalian Glyco_18 containing proteins. Reproduced with permission from (Kzhyshkowska et al., 2016b), Copyright © Portland Press Limited.

CLPs possess the chitin-binding grove in the (α/β)8 TIM-barrel domain, which can bind chitin and chitin oligosaccharides with high affinity (Kzhyshkowska et al., 2016b; Ranok et al., 2015). CLPs lack the enzymatic activity because of the substitution of the critical catalytic residue (glutamic acid) at the end of the DxxDxDxE conserved motif with either leucine, isoleucine or tryptophan (Figure 1) (Kzhyshkowska et al., 2016b). The sugar-binding properties of CLPs are attributed to the Glyco_18 domain of CLPs (Table 1). These properties are critical for the interactions of CLPs with glycoproteins on the cell surface or with specific carbohydrate molecules in the extracellular matrix. The binding ability of YKL-40 for heparin sulfate fragments allows its interaction with syndecan-1 and αvβ3 integrin, which promotes the activation of the ERK1/2 pathway and vascular endothelial growth factor (VEGF)

production in endothelial cells (Francescone et al., 2011; Shao et al., 2009). Moreover, SI-CLP was shown to bind lipopolysaccharide (LPS) *in vitro* and thereby to neutralize the toxic effect of LPS on macrophages (Meng et al., 2010).

Table 1. The lectin properties of CLPs.

CLP	Carbohydrate-binding	Method of analysis	References
YKL-39	Chitooligosaccharides, (GlcNac)5 and (GlcNac)6	Glycan array screen and intrinsic tryptophan fluorescence	(Schimpl et al., 2012)
	Chitooligosaccharides	Isothermal titration calorimetry (ITC)	(Ranok et al., 2015)
YKL-40	Type I collagen	Affinity chromatography and surface plasmon resonance	(Bigg et al., 2006)
	Chitooligosaccharides	Protein X-ray crystallography	(Fusetti et al., 2003)
	(GlcNac)5 and (GlcNac)4	Western blotting	(Renkema et al., 1998)
	Heparin	Heparin affinity and HPLC chromatograph	(Nishikawa and Millis, 2003)
SI-CLP	Galactosamine, glucosamine, chitooligosacharide, (GlcNac)4, ribose and mannose	Isothermal titration calorimetry (ITC)	(Meng et al., 2010)
YM1	Glucosamine, galactosamine and glucosamine polymers	Surface plasmon resonance	(Chang et al., 2001)

1.2 Biological activities of chitinase-like proteins

1.2.1 Growth factor-like activity

CLPs are involved in the regulation of cell growth and proliferation by activating the MAPK and AKT pathways. YKL-40, as the most investigated CLP, was reported to induce the proliferation of human synovial cells and skin fibroblasts by mediating AKT pathways (Recklies et al., 2002). It also has been reported to promote the proliferation of HEK-293 and U-373 MG cells through the activation of the ERK-MAPK pathway (Areshkov et al., 2012). The elevated levels of YKL-40 expression were found to be associated with the proliferation of epithelial cells in colitis-associated cancer (Low et al., 2015). Moreover, YKL-40 was demonstrated to activate AKT/ERK-mediated pathway and to be associated with poor prognosis in cholangiocarcinoma (Thongsom et al., 2016).

Interestingly, as a homolog of YKL-40, YKL-39 was found to activate ERK1/2 phosphorylation in human glioblastoma U87MG cells (Areshkov and Kavsan, 2010) and glioblastoma-astrocytoma epithelial-like cells U-373 cells (Areshkov et al., 2012). The activation of ERK1/2 phosphorylation by YKL-40 resulted in the cell proliferation, while the activation of ERK1/2 phosphorylation by YKL-39 inhibited cell mitogenesis and proliferation (Areshkov et al., 2012). This opposing regulation of MAPK signaling by these two proteins can potentially result in distinct effects on tumor progression. However, YKL-39 protein used by Areshkov et al. was from bacterial source, and it is the only report that showed the negative effect of YKL-39 on cell proliferation. Thus, further studies using mammalian-derived YKL-39 are required to confirm this observation. Moreover, YKL-39 was also shown to act as a growth factor in chondrogenic cells (Miyatake et al., 2013). Collectively, all these studies indicate that CLPs are involved in the regulation of cell proliferation similar to the growth factors.

1.2.2 Chemotactic activity

Several chitinase-like proteins were demonstrated to have chemotactic activities. YM1 has been first identified as eosinophil chemotactic protein (ECF-L) isolated from the culture supernatant of splenocytes of mice (Owhashi et al., 2000). In addition to the chemotactic activity towards eosinophils; YM1 also attracted T lymphocytes and bone marrow polymorphonuclear leukocytes *in vitro* and induced selective extravasation of eosinophils in a mouse model (Owhashi et al., 2000). Zhao et al. showed that YM1 was highly expressed in brain and cerebrospinal fluid (CSF) of Angiostrongylus Cantonese's infected mice and participated in the brain inflammation. Microglia-secreted YM1 secreted was suggested to be involved in eosinophilic meningitis and meningoencephalitis caused by A. Cantonese's infection (Zhao et al., 2013). Moreover, it was found that both YM1 and YM2 are strongly induced in a mouse model for proliferative dermatitis characterized by the accumulation of eosinophils in the skin (HogenEsch et al., 2006).

Human YKL-40 was reported to have chemotactic activity towards different cell types. Nishikawa et al. showed that YKL-40 is associated with vascular smooth muscle cell (VSMC) migration and invasion into the gelatinous matrix (Nishikawa and Millis, 2003). YKL-40 expressed in the human colon cancer SW480 cells enhanced the migration of human monocytes-like cells THP-1 cells and human umbilical vein endothelial cells (HUVEC). The expression of YKL-40 was associated with macrophages infiltration and micro-vessel density (MVD) in the tumors of human colorectal cancer patients and in a xenograft mouse model

(Kawada et al., 2012). Also, Thongsom et al. reported that YKL-40 were shown to promote the growth and migration of cholangiocarcinoma cells *in vitro* (Thongsom et al., 2016). YKL-40 was also found to contribute to the migration of bronchial smooth muscle cells via an indirect way by inducing the expression of IL-8 (Tang et al., 2013).

1.2.3 Induction of cytokine production

Chitinase-like proteins are reported to promote the expression and secretion of various cytokines. YKL-40 was demonstrated to promote cytokine production in different cell types. The expression of MCP-1 and IL-8 was up-regulated in SW480 human colon cancer cells transfected with YKL-40 expressing construct (Kawada et al., 2012). The expression of IL-8 was also up-regulated in YKL-40 stimulated human bronchial epithelial cells (Tang et al., 2013). Moreover, YKL-40 enhanced the expression of CCL2 and CXCL2 in a mouse model of lung cancer (Libreros et al., 2013). Other CLPs also contribute to the production of cytokines. SI-CLP promotes the secretion of IL-1β, IL-6, IL-12 and IL-13 in THP-1 cells treated with PMA (phorbol 12-myristate 13-acetate. In SI-CLP knockout (ko) mice, the serum levels of IL-1β, IL-6, and IL-12 were decreased when compared with wild-type (wt) mice (Xiao et al., 2014).

1.2.4. Angiogenesis

Angiogenesis contributes to the development of abundantly vascularized tumors, such as melanoma, glioblastoma and breast cancer (Riabov et al., 2014). The pro-angiogenic effects of YKL-40 have been demonstrated in several studies. YKL-40 was shown to promote the ability of tube formation in human microvascular endothelial cells (HMVEC) (Kawada et al., 2012; Shao et al., 2009). VEGF production was induced by YKL-40 in U87MG glioblastoma cells, which indirectly promoted HMVEC tube formation *in vitro* (Francescone et al., 2011). siRNA knock-down of YKL-40 resulted in suppressed tumor angiogenesis both in endothelial cells and *in vivo* (Shao et al., 2009). A correlation between blood vessel density and YKL-40 expression level was also observed in human glioblastoma (Shao, 2014) and human breast cancer (Shao et al., 2009). Since anti-VEGF antibody failed to block migration of HMVEC cells as well as tube formation induced by YKL-40, it was hypothesized that the pro-angiogenic effects of YKL-40 were independent of VEGF (Shao et al., 2009). Overall, all these studies indicate that YKL-40 act as a major factor in angiogenesis.

1.3 Chitinase-like proteins in disease

1.3.1 Chitinase-like proteins in cancer

Accumulating data reveals that CLPs are playing a role in the progression of different types of cancer. Elevated levels of circulating YKL-40 are related to poor outcome or short disease-free survival in glioblastoma, melanoma, ovarian, breast, colon, lung, and prostate cancers in humans (Cintin et al., 1999; Høgdall et al., 2009; Hormigo et al., 2006; Iwamoto et al., 2011; Johansen et al., 2007; Libreros and Iragavarapu-Charyulu, 2015; Ma et al., 2015; Schmidt et al., 2006; Shao et al., 2011; Wan et al., 2017). Moreover, in breast cancer, elevated serum levels of YKL-40 were used as a prognostic biomarker (Shao et al., 2011). The adhesive and invasive abilities of U87MG glioblastoma cells were significantly inhibited when endogenous expression of YKL-40 was blocked (Ku et al., 2011). YKL-40 was also induced during pulmonary melanoma metastasis and this induction was mediated by the semaphorin 7a (Ma et al., 2015). Overexpression of YKL-40 and YM1/2 was observed in the pre-neoplastic phase of latent membrane protein 1 (LMP1) viral oncogene-expressing transgenic mouse model, which is associated with carcinogenic progression (Qureshi et al., 2011). Targeting of YKL-40 as a potential therapeutic approach has been evaluated in melanoma and glioblastoma mouse models. Application of anti-YKL-40 antibody in the U87 glioblastoma mouse models resulted in the suppression of the xenograft tumor growth as well as angiogenesis (Faibish et al., 2011). However, an opposite result was seen in BALB/c-scid mice injected with human melanoma cells; the tumor growth was enhanced after anti-YKL-40 antibody treatment (Salamon et al., 2014). The contradictory results between glioblastoma and melanoma mouse models can be explained by the different mouse strains and antibodies used in the studies. SI-CLP was shown to induce the secretion of IL-1β, IL-6, IL-12, and IL-13 in PMA-treated THP-1 cells suggesting it may serve as a regulator of inflammation and in the tumor microenvironment (Xiao et al., 2014). The regulatory effect of SI-CLP is not clear yet since the cytokines induced by SI-CLP can either promote (IL-1β, IL-6, IL-13) or suppress (IL-12) tumor progression (Xiao et al., 2014)

The information about the potential role of YKL-39 in cancer is very limited. Serial Analysis of Gene Expression (SAGE) revealed that YKL-39 expression is elevated in II–IV grades of glial tumors (Kavsan et al., 2004). The expression of YKL-39 was detected in the majority of glioblastomas (19 of 27 samples analyzed) by Northern blot analysis and demonstrated on the protein level by Western blotting (Kavsan et al., 2008). However, the cell types overexpressing YKL-39 in glioblastoma remain to be identified.

1.3.2 Chitinase-like proteins in chronic inflammation and neurodegeneration

The elevated plasma levels of YKL-40 were detected in number of chronic inflammatory diseases, such as rheumatoid arthritis (RA), osteoarthritis (OA), systemic lupus erythematosus, inflammatory bowel disease, sarcoidosis and chronic obstructive lung disease (Johansen et al., 2005; Kawada et al., 2008; Létuvé et al., 2008; Vind et al., 2003; Vos et al., 2000). The elevated levels of circulating YKL-40 correlated with the degree of liver fibrosis (Kumagai et al., 2016; Nøjgaard et al., 2003). Elevated serum level of YKL-40 is considered as a potential biomarker of inflammation in patients with psoriasis (Baran et al., 2017) and with Kawasaki disease (Kim et al., 2017). Also, it was described that elevated circulating levels of YKL-40 are associated with Alzheimer's disease and multiple sclerosis (Baldacci et al., 2017a; Baldacci et al., 2017b; Comabella et al., 2010; Craig-Schapiro et al., 2010; Muszyński et al., 2017). A relationship between serum level of YKL-40 and carotid atherosclerosis has also been reported (Bakırcı et al., 2015; Michelsen et al., 2010).

The role of SI-CLP in the regulation of inflammation is still controversial. SI-CLP is the only known member of CLPs family induced by IL-4 and glucocorticoids in macrophages (Kzhyshkowska et al., 2006b). The expression of SI-CLP was detected in the peripheral blood leukocytes (PBLs) of patients with chronic inflammatory disorders of the respiratory tract (Kzhyshkowska et al., 2006b). Moreover, Xiao et al. found that knockout of SI-CLP resulted in the decrease of IL-1β, IL-6, IL-12, and IL-13 expression and lower susceptibility of mice to collagen-induced arthritis (CIA) (Xiao et al., 2014).

YKL-39 is expressed by synoviocytes and chondrocytes and it is considered as a biomarker for osteoarthritis (Hu et al., 1996; Knorr et al., 2003; Steck et al., 2002). Moreover, increased YKL-39 mRNA levels were also detected in microglia of Alzheimer patients (Colton et al., 2006). The detection of YKL-39 in cerebrospinal fluid was suggested to be a potential prognostic biomarker in the early stage of multiple sclerosis (Hinsinger et al., 2015; Møllgaard et al., 2016). Also, YKL-39 mRNA levels were significantly increased in the hippocampus of simian immunodeficiency virus encephalitis (SIVE) and HIV encephalitis (HIVE) (Sanfilippo et al., 2017). These data suggested the role of YKL-39 in both neurodegeneration and chronic inflammatory diseases of the brain.

1.4 Macrophages

1.4.1 General overview

Macrophages are versatile cells of the immune system present in almost all tissues (Ginhoux and Jung, 2014). Tissue macrophages can originate from three different sources: embryonic yolk sac macrophages, fetal liver monocytes, and adult bone marrow derived monocytes (van de Laar et al., 2016). There is experimental evidence suggesting that sac macrophages are main precursors for brain microglia (Ginhoux et al., 2010), fetal liver monocytes for Kuffer cells and lung alveolar macrophages (Hoeffel et al., 2012; Schneider et al., 2014), and adult bone marrow-derived monocytes for intestinal, dermal and cardiac macrophages (Bain and Mowat, 2012; Epelman et al., 2014a; Tamoutounour et al., 2013). Depending on their origin and localization, macrophages display high structural and functional heterogeneity (Ginhoux and Jung, 2014; Varol et al., 2015). Circulating blood monocytes migrate into tissue sites and differentiate into tissue-specific macrophages in response to the composition of tissue microenvironment (Epelman et al., 2014b). The tissue-specific environmental cues and ontogeny-related signals directly affect macrophage activation (Ginhoux et al., 2016). It is widely accepted that macrophages are involved in various physiological and pathological processes. Macrophages play a crucial role in acute and chronic inflammatory responses by producing enzymes, enzyme inhibitors, cytokines, plasma proteins (coagulation factors, complement components, and apolipoprotein E) and low molecular weight substances (reactive oxygen and derivatives of arachidonic acids) (Duque and Descoteaux, 2015). Pathological programming of macrophages is crucial for the developed of major life-threatening disorders including cancer and cardiovascular disorders (Dehne et al., 2017; Gisterå and Hansson, 2017; Goswami et al., 2017; Kzhyshkowska et al., 2012). Macrophages regulate intratumoral immune responses and progression of atherosclerosis not only by the secretion of cytokines, growth factors, enzymes and extracellular matrix proteins but also by selective scavenging of these mediators (Kzhyshkowska et al., 2012; Rhee, 2016; Riabov et al., 2014).

Major stimuli responsible for macrophage phenotype formation include cytokines, hormones, immune complexes and pathogen-derived products. The molecular factors that characterize specific type of macrophage activation include transcription factors, surface-expressed receptors, secreted cytokines, enzymes and components of extracellular matrix (Murray et al., 2014) (Figure 2).

Classical activation of macrophages (M1) is induced by pro-inflammatory stimuli such as Interferon-γ (IFN-γ), lipopolysaccharides (LPS), tumor necrosis factor (TNF-α) and CpG DNA (Gordon, 2003; Martinez and Gordon, 2014). M1 macrophages polarization is characterized by the production of high levels of pro-inflammatory cytokines (such as IL-1β, TNF-α, IL-6, and IL-12), strong microbicidal properties, high production of reactive nitrogen and oxygen intermediates, and promotion of Th1 responses (Mantovani et al., 2004; Martinez and Gordon, 2014). Switching of the tolerogenic phenotype of TAM to the M1 phenotype has been proposed as a promising key of anti-cancer immunotherapeutic treatment strategy (Mills et al., 2016).

Alternative activation of macrophages (M2) is induced by Th2 cytokines, hormones, immune complexes and tumor-derived growth factors. According to the most recent classification (Murray et al., 2014), the subtypes of M2 macrophages were described in response to the specific stimuli or their combinations, such as M(IL-4), M(Ic), M(IL-10), M(GC+TGF-beta) and M(GC) (Figure 2B). M2 macrophages are involved in response to parasite invasion, tissue remodeling, wound healing and tumor promotion (Duque and Descoteaux, 2015; Mantovani et al., 2004; Martinez and Gordon, 2014). The M2 polarization of macrophages leads to the secretion of numerous chemokines and cytokines, such as TGF-beta, IL-10, and CCL17 (Rőszer, 2015). In addition, M2 express high levels of scavenger receptors (Kzhyshkowska et al., 2016a). The molecules secreted by alternatively activated macrophages have the primary function to resolve inflammation and promote tissue repair (Gordon, 2003; Mantovani et al., 2013; Pellicoro et al., 2014).

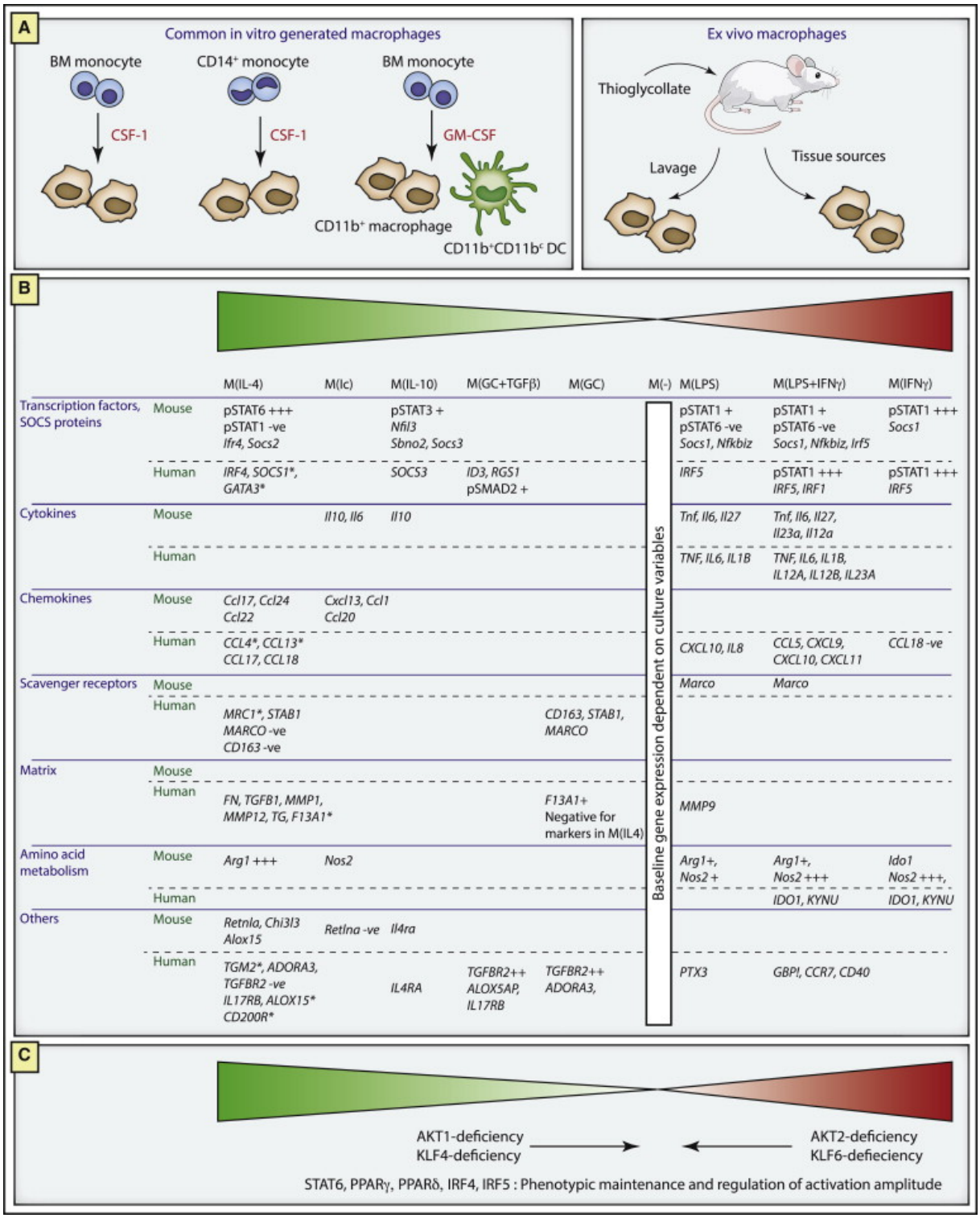

Figure 2. The activation of macrophage and related stimulations. A. Examples of widely used macrophage preparations. **B.** Marker systems for activated macrophages. **C.** Use of genetics to aid in macrophage activation studies. Reproduced with permission from (Murray et al., 2014), Copyright © Elsevier.

Additionally, macrophages are not terminally differentiated and have been demonstrated to be highly plastic cells (Stout and Suttles, 2004). It has been demonstrated in our laboratory that polarized M1, and M2 macrophages can be re-polarized by Th2 or Th1 cytokines and revert

to their functional state (Gratchev et al., 2006; Kzhyshkowska et al., 2016a). Recently, transcriptional profiling revealed a spectrum of macrophage activation that extends beyond traditional M1 versus M2-polarization model (Xue et al., 2014). The new concept of a spectrum of macrophage activation presenting the commonly observed activation states is illustrated in Figure 2 (Murray et al., 2014).

1.4.2 Macrophages as source of chitinase-like proteins

Macrophages as important regulatory cells serve as major source of all murine and human chitinase-like proteins. (Table 2). In human, the expression of YKL-40 was found in microglia from Alzheimer's disease patients (Colton et al., 2006); macrophages in pulmonary sarcoid granulomas (Johansen et al., 2005); and tumor-associated macrophages (TAMs) in human small cell lung cancer (Junker et al., 2005). The expression of SI-CLP was detected in peripheral blood mononuclear cells from rheumatoid arthritis (RA) patients (Xiao et al., 2014). Elevated levels of YKL-39 gene expression were detected in microglia of Alzheimer's patients (Colton et al., 2006). In *in vitro* experimental models, expression of CLPs depends on the activation state of macrophages (M1 or M2). YKL-40 expression is elevated during the differentiation process of human macrophages, and macrophage differentiation factors GM-CSF or M-CSF were shown to induce YKL-40 expression (Kunz et al., 2015; Rehli et al., 1997; Rehli et al., 2003). It was identified that in human monocyte-derived macrophages IFN-γ and LPS are strong inducers of YKL-40 gene expression (Di Rosa et al., 2013; Kzhyshkowska et al., 2006b). It was demonstrated in our laboratory that expression of SI-CLP is induced by IL-4 and dexamethasone both on the mRNA and protein levels in human monocyte-derived macrophages (Kzhyshkowska et al., 2006b). Further, it was found that the combination of IL-4+TGF-beta but not IL-4 alone induces expression of YKL-39 gene in monocyte-derived macrophages (Gratchev et al., 2008b). However, expression of YKL-39 on the protein level both *in vitro* and *in vivo* remained to be identified and has not been analyzed up to date due to the lack of antibodies. The information about the expression of CLPs in various types of macrophages is summarized in Table 2.

Table 2. Expression of chitinase-like proteins in macrophages.

CLP	Macrophage type	Method of analysis	References
YKL-40	Human primary monocyte-derived macrophages stimulated by IFN-γ	RT-PCR	(Kzhyshkowska et al., 2006b)
	Microglia in Alzheimer's disease patients	RT-PCR	(Colton et al., 2006)
	Human peritumoral macrophages and murine lung macrophages	RT-PCR	(Junker et al., 2005)
	Human macrophages in pulmonary sarcoid granulomas	Immunohistochemical staining	(Johansen et al., 2005)
	Peritumoral macrophages in human small cell lung cancer	Immunohistochemical staining	(Junker et al., 2005)
	Human primary monocyte-derived macrophages stimulated by GM-CSF or M-CSF	RT-PCR/ELISA/ Immunofluorescence staining	(Kunz et al., 2015)
	Murine pulmonary macrophages	RT-PCR/ELISA	(Sohn et al., 2010)
	Human M1 polarized macrophages stimulated by LPS and IFN-γ	RT-PCR	(Di Rosa et al., 2013)
SI-CLP	Human primary monocyte-derived macrophages stimulated by IL-4+dexamethasone	RT-PCR/Western blotting/Immunofluorescence staining	(Kzhyshkowska et al., 2006b)
	Murine bone marrow–derived macrophages	RT-PCR/Western blotting	(Xiao et al., 2014)
	PMA-treated THP-1 macrophages	RT-PCR/Western blotting	(Xiao et al., 2014)
	THP-1, Mono-Mac-6 cells	RT-PCR/Western blotting	(Kzhyshkowska et al., 2006b)
YKL-39	Human primary monocyte-derived macrophages stimulated by TGF-beta and IL-4	RT-PCR	(Gratchev et al., 2008b)
	Alternatively activated microglia in Alzheimer's disease patients	RT-PCR	(Colton et al., 2006)

1.4.3 Secretory pathways in macrophages

There are three major secretory pathways in macrophages responsible for the release of endogenously synthesised proteins to the extracellular space: 1) constitutive secretory pathway which continuously releases vesicles loaded with proteins to the cell surface; 2) regulatory secretory pathway which releases secretory vesicles in response to a specific stimulus; 3) lysosomal secretory pathway which releases vesicles fused with lysosomes (Blott and Griffiths, 2002; Kienzle and von Blume, 2014; Luzio et al., 2014; Ponpuak et al., 2015). For the constitutive secretion pathway, proteins are packed into vesicles in the Golgi apparatus, and these secretory vesicles are transported to the cell surface and fused with the plasma membrane, followed by the release of the content to the extracellular space (Alberts et al., 2002; Kienzle and von Blume, 2014). For the regulated secretion, proteins are stored in secretory vesicles, which later fuse with the plasma membrane in response to specific secretion signals, such as reactive oxygen species (ROS) (Blott and Griffiths, 2002; Kurz et al., 2008; Luzio et al., 2014). Macrophages utilize lysosomal pathway for the secretion of lysosomal enzymes (Aggarwal and Sloane, 2014; Kzhyshkowska and Krusell, 2009; Liu et al., 2004). Mannose 6-phosphate receptors (MPRs), are known as classical intracellular sorting receptors, which mediate the transport of newly synthesized lysosomal hydrolases or proteins from Golgi to the lysosomal secretory pathway (Hasanagic et al., 2015). The sorting process requires the generation of phosphor-mannosyl residues on the lysosomal protein which act as high-affinity ligands for the recognition by MPRs and binding of these molecules to MPRs in Golgi (Braulke and Bonifacino, 2009; Hasanagic et al., 2015). The mannose 6-phosphate tags are recognized in the trans-Golgi network (TGN) by a cation-independent mannose 6-phosphate receptor (CI-MPR) or a cation-dependent mannose receptor (CD-MPR), which both mediate the recruitment of lysosomal proteins to clathrin-coated vesicles in TGN. Later, the MPR-protein complex is delivered to late endosomes by these carrier vesicles. The release of proteins from MPRs are induced by the acidic pH of endosomes; subsequently, proteins are transported to lysosomes, while MPRs return to the TGN for other rounds of sorting (Braulke and Bonifacino, 2009). GGAs (Golgi-localizing, gamma-adaptin ear homology domain, ARF-binding proteins) were also reported to mediate the sorting of mannose 6-phosphate receptors (Ghosh et al., 2003b; Stahlschmidt et al., 2014). The acidic-cluster-dileucine signals on the cytosolic tails of CI-MPR and CD-MPR bind to the VHS domain of the GGAs, which direct the proteins from TGN to the endosomal-lysosomal system (Guo et al., 2014). Moreover, GGAs comprise clathrin adaptor properties which recruit clathrin for MPR sorting

in the TGN (Stahlschmidt et al., 2014). In addition, it was reported that the binding capability of GGAs and ubiquitination are necessary for the delivery of both biosynthetic and endosomal ubiquitinated cargo to the lysosome (Babst, 2004).

Several studies suggested that Glyco_18 domain containing proteins are sorted via the endosomal/lysosomal system and secreted by macrophages (Kzhyshkowska et al., 2007; Renkema et al., 1997). By immunoelectron microscopy, chitotriosidase was detected in lysosomal vesicles comparably to cathepsin D (Renkema et al., 1997). It was demonstrated in our laboratory that stabilin-1 interacts with GGA adaptors in endosomes and the trans-Golgi network. Stabilin-1 is further involved in sorting and lysosomal delivery of SI-CLP in alternatively activated macrophages (Kzhyshkowska et al., 2004; Kzhyshkowska et al., 2006b). More information about stabilin-1 and its interaction with SI-CLP is provided in the next chapter.

1.4.4 Stabilin-1 as sorting receptor for SI-CLP

Stabilin-1 was originally identified as the MS-1 antigen (Goerdt et al., 1991), which is primarily expressed on tissue macrophages and sinusoidal endothelial cells (Kzhyshkowska, 2010; Politz et al., 2002). It was also demonstrated that the expression of stabilin-1 on alternatively activated macrophages is induced by IL-4 and dexamethasone *in vitro* (Goerdt et al., 1993; Politz et al., 2002). In addition, several studies reported stabilin-1 was found on tumor-associated macrophages (TAMs) in mouse and human cancers including breast cancer, melanoma, and glioblastoma (David et al., 2012; Riabov et al., 2016; Schledzewski et al., 2006).

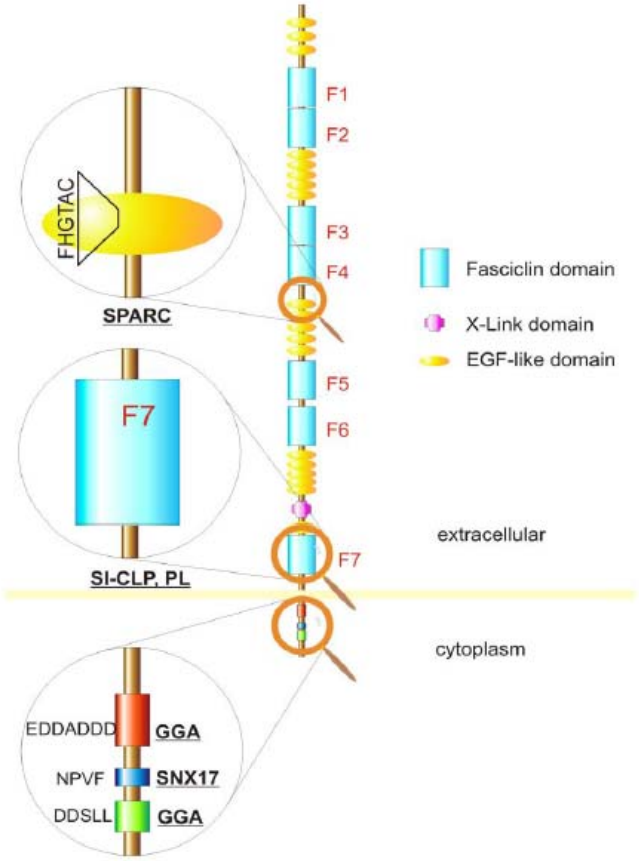

Figure 3. Schematic presentation of stabilin-1 binding sites for the ligands and domain organization. The extracellular domain of stabilin-1 contains 7 fasciclin domains (F1-F7, shown in blue cylinders) and EGF-like domains (shown in yellow ovals). The X-link domain is shown in pink. SI-CLP and PL bind to F7; SPARC binds to the EGF-like domain located between F4 and F5. The cytoplasmic tail comprises a DDSLL motif and a novel acidic cluster EDDADDD which interacting with intracellular sorting adaptors: GGA1, GGA2, and GGA3L; the NPVF site interacting with sorting nexin 17 (SNX17). Reproduced with permission from (Kzhyshkowska, 2010), Copyright © 2010 Julia Kzhyshkowska.

Stabilin-1 is a type-1 transmembrane protein containing a transmembrane domain, a cytoplasmic tail and an extracellular fragment which contains 7 fasciclin domains, 18 epidermal growth factor (EGF)-like domains, and an X-link domain (Figure 3) (Kzhyshkowska, 2010). The extracellular domain interacts with different ligands, such as SI-CLP, SPARC, acLDL and PL (Kzhyshkowska, 2010; Kzhyshkowska et al., 2006b) (Figure 3). The functions of stabilin-1 include the mediation of the endocytic and phagocytic clearance of "unwanted-self" components, such as SPARC (Kzhyshkowska et al., 2006c); transcytosis of growth hormone family member placental lactogen (PL) (Kzhyshkowska et al., 2008); the intracellular sorting and lysosomal delivery of endogenously synthesized SI-CLP (Kzhyshkowska et al., 2006b) (Figure 4). It was also demonstrated in our laboratory that stabilin-1 is a specific marker for TAMs in breast cancer patients and supports tumor growth

in a mammary adenocarcinoma mouse model (Riabov et al., 2016). However, whether stabilin-1 can interact with other chitinase-like protein is not known. Therefore, the intracellular sorting mechanism of stabilin-1 needs to be further investigated.

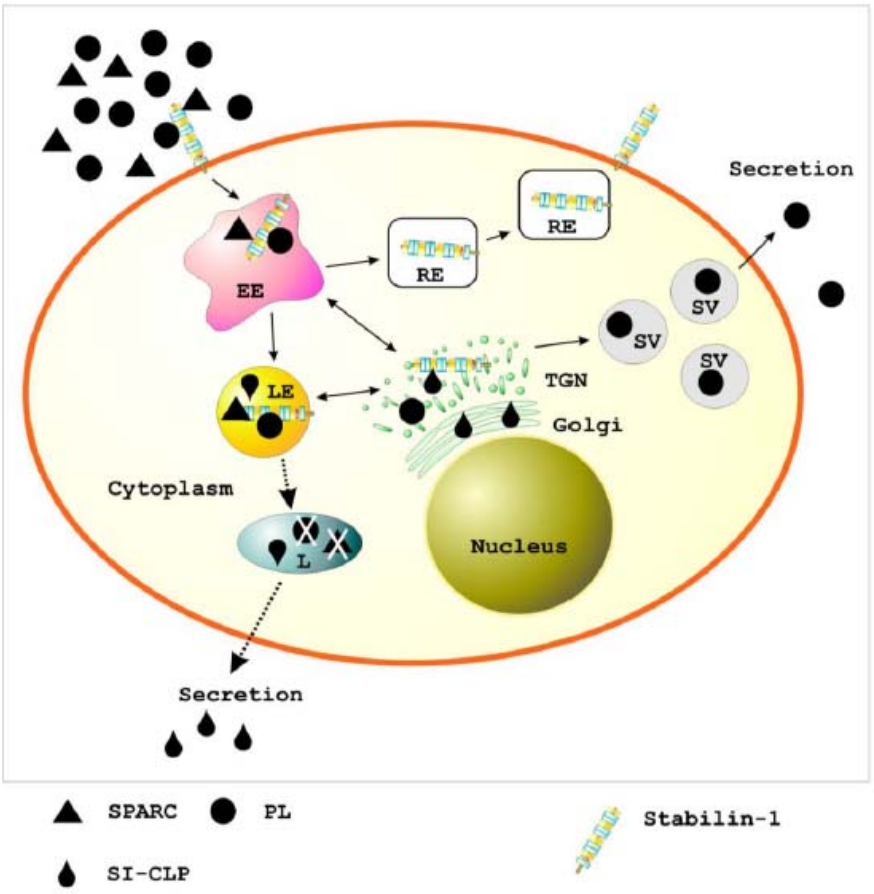

Figure 4. Schematic presentation of stabilin-1 trafficking pathways in macrophages. Stabilin-1 shuttles between endosomes and biosynthetic compartment via TGN. Newly synthesized SI-CLP is recognized by stabilin-1 in TGN and delivered to early and late endosomes, which targeting to lysosomes. Reproduced with permission from (Kzhyshkowska, 2010), Copyright © 2010 Julia Kzhyshkowska.

Stabilin-1 is shuttling between endosomal and biosynthetic compartments (Kzhyshkowska et al., 2006a), and its interaction with GGA adaptors indicates its functional homology with CI-MPR, a sorting receptor for lysosomal hydrolases (Ghosh et al., 2003a; Robinson and Neuhaus, 2016). Thus, the function of stabilin-1 in lysosomal secretion was further studied. The interaction of stabilin-1 and SI-CLP as a ligand-receptor couple was demonstrated in our laboratory, which is the only known example of protein-protein interaction between a transmembrane receptor and mammalian chitinase-like protein (Kzhyshkowska et al., 2006b). Intracellular localization studies by confocal microscopy suggested that SI-CLP is sorted into late endosomes, LAMP-1 positive lysosomes, and CD63 positive secretion lysosomes. A

co-localization of stabilin-1 and SI-CLP was found in TGN of macrophages, which were stimulated with IL-4 and dexamethasone; this process was impaired by the knockdown of stabilin-1 by siRNA (Kzhyshkowska et al., 2006b). In addition, it was observed that stabilin-1 mediates re-localization of recombinant SI-CLP-FLAG in H1299 cells, which lack the endogenous lysosomal sorting machinery for this protein. The interaction with SI-CLP is mediated by the extracellular fasciclin domain 7 (F7) of stabilin-1 that has been demonstrated in an *in vitro* binding assay (Kzhyshkowska et al., 2006b). However, whether stabilin-1 can mediate intracellular sorting of other chitinase-like proteins is not known yet.

1.5 The aim and objectives of the thesis

The major aims of this thesis project include the identification of YKL-39 production in primary human macrophages, the analysis of its intracellular sorting mechanisms, and the identification of its biological activities towards monocytes, endothelial cells and tumor cells.

The main objectives of this project were:

1) To analyze the expression of YKL-39 in human primary macrophages;
2) To analyze the intracellular localization of YKL-39 in human primary macrophages;
3) To analyze the role of stabilin-1 in the interaction and intracellular sorting of YKL-39;
4) To analyze the effect of YKL-39 on monocyte migration and activation *in vitro*;
5) To analyze the effect of YKL-39 on angiogenesis *in vitro;*
6) To analyze the effects of YKL-39 tumor cell proliferation and apoptosis.

2. Materials & Methods

2.1 Chemicals, materials and reagents

Product	Company
0.05% Trypsin/EDTA solution	Biochrom
10x Earle's Balanced Salt Solution (EBSS)	Sigma Aldrich
10x Incomplete PCR buffer	BIORON
30% Acrylamide/Bis Solution	Bio-rad
4'.6-diamidino-2-phenylindole (DAPI)	Roche Diagnostics
50x Tris-Acetate EDTA (TAE) buffer	Eppendorf
Acetic acid	Merck
Agarose	Bioron
Amersham Hyperfilm ECL	GE Healthcare
Ammonium persulfate (APS)	Merck Millipore
Ampicillin	Sigma Aldrich
BL21-(DE3)-RIL-Codon-Plus E.coli	Stratagene
Bovine Serum Albumin (BSA)	Sigma Aldrich
BSA loading controls	Bio Rad
CD14 MicroBeads	Miltenyi Biotec
Dako Pen	Dako
Dako Fluorescent Mounting Medium	Dako
Deoxyribonucleotides (dNTPs) 10M	Fermentas
DEPC Water	Thermo Fisher Scientific
Dexamethasone	Sigma Aldrich
Dimethylsulfoxide (DMSO)	Sigma Aldrich
DMEM medium+Gluta MAX	Thermo Fisher Scientific
DMSO	Sigma Aldrich
DNA ladder	Thermo Fisher Scientific
DNA Loading Dye (6x)	Thermo Fisher Scientific
DNase Buffer (10x)	Thermo Fisher Scientific
DNase I RNase free 1U/µl solution	Fermentas
DRAQ5	Biostatus Ltd.
EDTA	Invitrogen
EDTA-free Protease Inhibitor Cocktail Tablets	Roche
Ethanol	Roth
Expand High Fidelity PCR Kit	Roche
Fetal calf serum (FCS)	Biochrom
FuGENE HD transfection reagent	Promega
Gel Blue stain reagent	Pierce
Gel Red	Biotium
Glycerol	Sigma Aldrich
Isopropanol	Merck Millipore
Laemmli sample buffer	Bio Rad
LB broth with agar	Sigma Aldrich

Matrigel (growth factor reduced)	Corning
MAX Efficiency DH5α Competent E. coli	Thermo Fisher Scientific
Methanol	Merck
Nitrocellulose blotting membrane	GE Healthcare
Non-Fat Dry Milk	Bio Rad
Oligo(dt) primer	Thermo Fisher Scientific
OptiMEM	Thermo Fisher Scientific
Page Ruler Plus Prestained Protein Ladder (10-250 kD)	Fermentas
Paraformaldehyde (PFA)	Sigma Aldrich
Phosphate buffered saline (D-PBS), sterile 1x	Invitrogen
PCR primers	Eurofins MWG Operon
PCR probes	Eurofins MWG Operon
Penicillin/Streptomycin	Biochrom
Percoll	GE Healthcare Life Sciences
Phenylmethylsulfonyl fluoride (PMSF)	Sigma Aldrich
Plasmid DNA- Mini/Midi/Maxiprep Kit	Qiagen
Ponceau S solution	Sigma Aldrich
Protein Assay Reagent	Bio-Rad
Protein G Sepharose	GE Healthcare
Rapid DNA ligation kit	Fermentas
Recombinant human MCP-1 (CCL2)	R&D
Recombinant human YKL-39 protein	Sinobio
Recombinant Human IL-4	Peprotech
Recombinant human M-CSF	Peprotech
RPMI medium	Life Technologies
Staurosporine	Sigma Aldrich
Sepharose 4B	GE Healthcare
Sensimix II Probe Kit	Bioline
SOC medium	Invitrogen
Sodium Chloride	Sigma Aldrich
Sodium dodecyl sulfate (SDS) 10%	Bio-Rad
Sodium pyruvate (100mM)	Sigma Aldrich
TEMED	Sigma Aldrich
TGS (Tris/Glycine/SDS) buffer 10x	Bio-Rad
Tris-HCl buffer 0.5M, pH 8.8	Bio-Rad
Tris-HCl buffer 1.5M, pH 6.8	Bio-Rad
Triton X-100	Sigma Aldrich
Trypan blue solution	Sigma Aldrich
Tween 20	Sigma Aldrich
β-mercaptoethanol	Sigma Aldrich

2.2 Consumables

Product	Company
0.22 µm filter	Fisherbrand
22x22 mm coverslips	Marienfeld
3MM blotting papers	GE Healthcare
CASY cups	Omni Life Sciences
Cryovials	Nunc
Elisa plate sealers	R&D systems
Elisa Plates	R&D systems
GeneChip® Human Gene 2.0 ST Array	Affymetrix
Glass slides	Servoprax
LS columns	Miltenyi Biotec
Parafilm	American National Can
PCR tubes	Star Labs
Petri dishes	Nunc
Pipettes tips	Eppendorf
Pipettes	Eppendorf
Plastic wrap	Toppits
Western film	GE Healthcare
Safe-Lock Eppendorf Tubes, 1.5ml	Eppendorf
Scalpel	Feather
Sterile pipette tips	Star Labs, Nerbeplus
Tubes	Falcon
Trans-well 5 µm	Corning

2.3 Equipment

Product	Company
Agarose electrophoresis unit	VWR
Autoclave VX-95	Systec
Balance	Kern
CASY Cell Counter	Schärfe System
Cell culture hood	Thermo Fisher Scientific
Cell culture incubator	Heraeus Instruments
Centrifuge 5415 D	Eppendorf
Centrifuge 5804 R	Eppendorf
Confocal laser scanning microscope SP8	Leica Microsystems
Electrophoresis comb	Peqlab
Electrophoresis power supply	Peqlab
FACS Canto II	BD Biosciences
Freezer (-20°C)	Liebherr
Freezer (-80°C)	Sanyo
Fridge (4°C)	Liebherr
Ice machine AF100	Scotsman
Inverted microscope	Leica Microsystems

LightCycler 480 Instrument	Roche Diagnostics
MACS manual cell separator	Miltenyi Biotec
Gel dryer model 583	Bio-Rad
Magnetic stirrer MR3000	Heidolph
Microwave oven	Sharp
Neubauer haemocytometer	Assistent
Pipette Controller	Accu Jet Pro, Brand
Roller	Ortho Diagnostic Systems
Rotator	Neolab
SDS-PAGE chamber	Peqlab
SDS-PAGE gel comb	Peqlab
SDS-PAGE power unit Power-Pac 200	Bio-Rad
SDS-PAGE unit	Biometra
Shaker KS 260 basic	IKA
Sorvall RC5C Plus ultracentrifuge	Thermo Fisher Scientific
Staining Dish	Neolab
Staining rack	Neolab
Tecan Infinite 200	Tecan
Thermomixer 5436	Eppendorf
Thermomixer comfort	Eppendorf
Tweezers	Neolab
Ultracentrifuge tubes 50ml	Thermo Fisher Scientific
UV fluorescent light	Peqlab
Vortex Genie 2	Scientific Industries
Water bath	Memmert
Water bath VWB12	VWR
X-ray cassette	Kodak
X-ray film processor CAWOMEN 2000 IR	CAWO Solutions

2.4 Kits

Product	**Company**
E.Z.N.A. Total RNA Kit I	Omega Biotech
Plasmid Isolation Kit	Qiagen
QIAquick PCR Purification Kit	Qiagen
RevertAid H Minus First Strand Synthesis Kit	Thermo Fisher Scientific
RNAeasy Mini Kit	Qiagen
Human YKL-39/CHI3L2 ELISA Kit (Sandwich ELISA)	Lifespan BioSciences

2.5 Buffers and solutions

Fixation solution (4% PFA)	40 g of paraformaldehyde (PFA) powder were weighed under the fume hood and dissolved in 700 ml PBS in a large beaker. The solution was stirred at room temperature, and pH value was adjusted to 11.4 with 1 N NaOH buffer. Then the pH value was adjusted to 7.4 with 1 N HCl buffer with stirring. The volume was adjusted to 1 L with PBS. Afterward, the PFA solution was filtered with a 0.22 µm filter, aliquoted into 50 ml Falcon tubes, and stored in -20 °C.
Permeabilization solution (0.5% Triton X-100 in PBS)	2.5 ml of Triton X-100 was pipetted into 500 ml PBS; the pipette was left in the beaker for 30 min. The solution was stirred for 1h and stored at RT.
1 x TAE buffer	20 ml of 50 x TAE buffer was added into 900 ml ddH_2O. The volume was adjusted to 1 L with ddH_2O.
Blocking solution (3% BSA)	1.5 g BSA powder was dissolved in 50 ml of PBS in a falcon tube. The falcon tube was left on a tube roller mixer overnight.
Washing buffer for ELISA (0.05% Tween 20 in PBS)	500µl of Tween 20 was pipetted into 1L of PBS. The beaker was stirred on a magnetic stirrer for 30 min, and the solution was stored at RT.
LB medium	20 g of LB broth powder was dissolved in 1 L ddH_2O. The mixture was autoclaved for 15 min at 121°C for sterilization. The solution was cooled, and antibiotics were added.
LB agar	35 g of LB broth with agar powder was dissolved in 1 L of ddH_2O. The mixture was autoclaved for 15 min at 121°C to sterilize. The solution was cooled, and antibiotics were added. The solution was poured into Petri dishes and left to solidify under a laminar flow hood. After the agar had solidified, the plates were sealed with Parafilm and stored at 4°C.

10% APS	10g of ammonia persulfate was dissolved in 100 ml of ddH_2O and stored in -20°C.
Running buffer for SDS-PAGE	100 ml of 10x TGS was adjusted to 1 L with ddH_2O.
Towbin buffer	200 ml of 100% methanol, 100 ml of 10 x TGS were adjusted to 1 L with ddH_2O.
Loading/lysis buffer for SDS-PAGE	0.5 ml of β-mercaptoethanol was mixed with 9.5 ml of 2x Laemmli Sample Buffer.
Gel drying solution	70 ml of 100% methanol, 70 ml of 100% acetic acid, and 10 ml of glycerol were mixed and adjusted to 1 L with ddH_2O.
Protease inhibitor cocktail mini solution (50x)	1 tablet of protease inhibitor cocktail was dissolved in 1 ml of sterile PBS.
Protease inhibitor cocktail solution	1 ml of protease inhibitor cocktail mini was added into 24 ml of PBS.
Sepharose washing buffer	5 M NaCl and 1 % Triton X-100 were prepared and in 1 L PBS.
Sepharose storage buffer	500 µl glycerol, 200 µl protease inhibitor cocktail mini were adjusted to 10 ml with PBS.
MACS-buffer	2.5 g BSA, 2 ml 0.5 M EDTA were dissolved in 500 ml PBS. The mixture was filtered through 0.22 µm filter to a sterile flask.
ELB complete buffer	125 mM NaCl, 50 mM HEPES-buffered saline (pH 7.0), 0.1% NP-40, 0.5 mM EDTA and 0.5 mM DTT were prepared and dissolved in 1L ddH_2O.

2.6 Molecular biology techniques

2.6.1 Plasmids

Table 3. List of plasmids.

Name	Internal number	Company
pGEX4T1	p36	GE Healthcare
pLP-IRESneo Acceptor Vector	p64	Clontech
pLP-IRESneo-hSt1	p295	constructed
pGEX4T1-hSt1-Fas7	p395	constructed
pGEX4T1-hSt1-P9	p396	constructed
pSNAP-tag	p789	BioLabs
pGEX4T1-hSt1-C	p818	constructed
pSNAP-tag-YKL-39-FLAG	p825	constructed

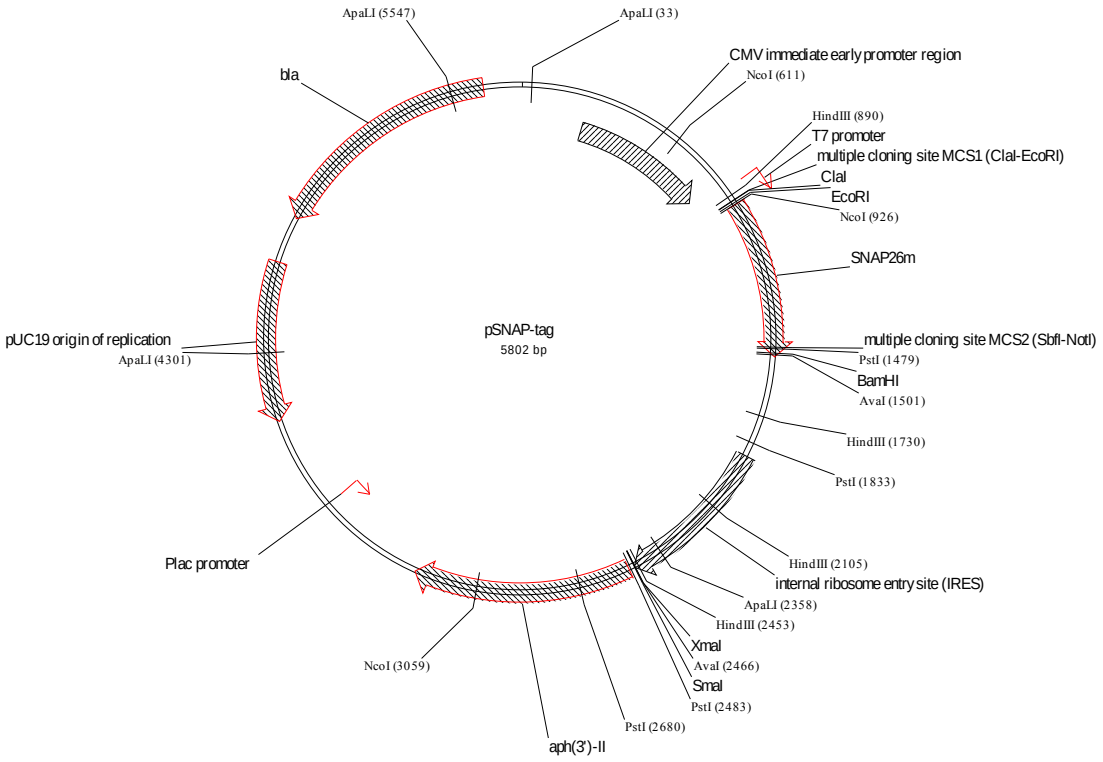

Figure 5. The vector plasmid of pSNAP-tag. Plasmid map of vector pSNAP-tag was painted using Vector NTI Advance Version 11.5 from Life Technologies.

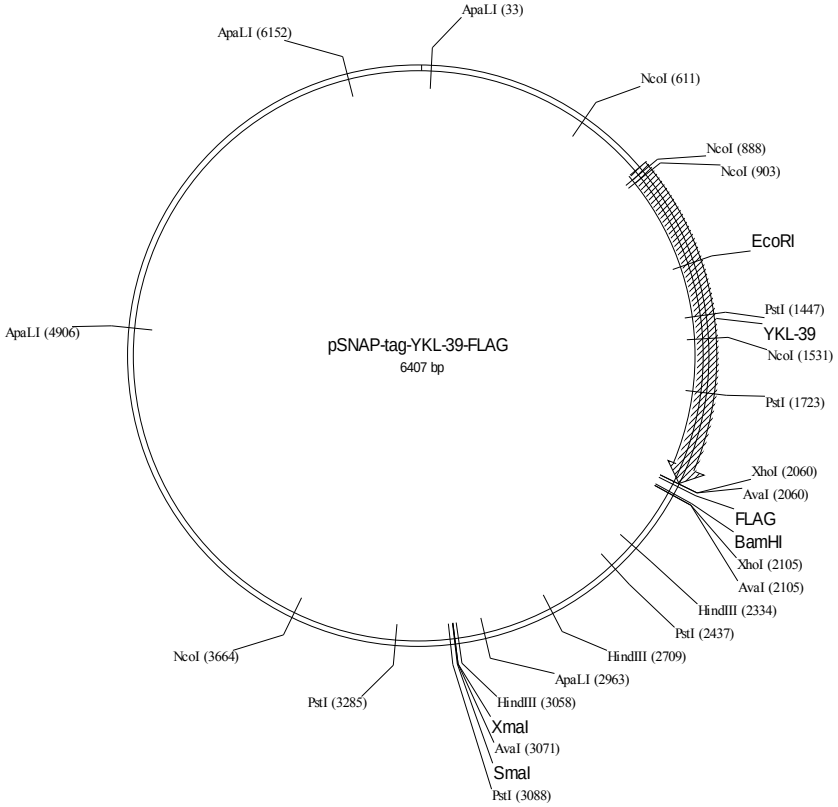

Figure 6. The plasmid pSNAP-tag-YKL-39-FLAG. Plasmid map of pSNAP-tag-YKL-39-FLAG was painted using Vector NTI Advance Version 11.5 from Life Technologies.

2.6.2 Transformation of the chemically competent cells

Competent *E.coli* DH5α cells from Thermo Fisher Scientific were utilized in this step.

1) The cells were thawed on ice.
2) 50 µl of competent cells were mixed with 3 µl of pSNAP-tag or pSNAP-tag-YKL-39-FLAG plasmid in a pre-chilled Eppendorf tube by pipetting, and the samples were incubated on ice for 30 min.
3) The samples were subjected to heat shock for 42 s in 42°C water bath.
4) The samples were incubated for 5 min on ice.
5) 250 µl of SOC-medium was added to each sample.
6) The samples were incubated on a thermomixer for 1 h at 37°C on a shaker at 400 rpm.
7) The samples were centrifuged at 6000 rpm for 3 min.
8) 200 µl of the supernatant was removed, and the pellet was re-suspended.
9) The samples were streaked onto LB-agar plates and were incubated at 37°C overnight upside down.

2.6.3 Bacteria culture

1) Mini culture: One single colony was selected from the LB-agar plate with a pipette tip, the pipette was placed in 15 ml Falcon tube with 3 ml of LB-medium and 3 µl of ampicillin solution (100 µg/ml). The mixture was incubated at 37°C in a shaking incubator at 200 rpm overnight.
2) Enlarge culture: 100 µl of mini-preparation culture was added into an Erlenmeyer flask with 200ml of LB-medium and 200 µl of ampicillin (100 µg/ml). The mixture was incubated overnight at 37°C in a shaking incubator at 150 rpm overnight.

2.6.4 Isolation of plasmid DNA

Plasmid DNA preparations were performed using the Plasmid Midi Kit from Qiagen.

1) The cultures were pelleted in 2 x 50 ml Falcon tubes by centrifuging at 6000 g for 15 min at 4°C.
2) The pellets were re-suspended in 2 ml of P1 solution, and the mixture was vortexed for 1 min.
3) 4 ml of P2 was added to the tube, and the tube was vigorously inverted for 5 times. The mixture was incubated for 5 min at RT.
4) 4 ml of pre-chilled P3 was added to the mixture, and the tube was vigorously inverted 5 times. The sample was incubated for 15 min on ice.
5) The tube was centrifuged at 4°C for 30 min at 20,000 g. The supernatant was removed to a new tube, and the sample was centrifuged for 15 min at 20,000 g.
6) 100-tip column was equilibrated by running through 5 ml of buffer QBT.
7) The supernatant was applied to the column.
8) The column was washed twice with 10 ml of buffer QC.
9) DNA was eluted into a new 50 ml Falcon tube with 5 ml of Buffer QN.
10) 3.5 ml isopropanol was added to the sample.
11) The sample was mixed and centrifuged at 4°C for 30 min at 15,000 g.
12) The pellet was washed with 2 ml of 70% ethanol, and the sample was centrifuged for 10 min at 15000 g.
13) The pellet was air dried for 10 min and dissolved with 100 µl ddH_2O.

2.6.5 Agarose gel electrophoresis

1) 1% agarose gel was prepared by dissolving 0.5 g agarose in 50 ml 1x TAE buffer. The mixture was microwaved to melt gel.

2) The mixture was cooled down, and 5 µl of Gel Red was added.
3) The mixture was poured into the gel tray equipped with a comb for 30 min. Then the gel was placed into the electrophoresis unit filled with 1x TAE buffer.
4) 2 µl of loading dye was added to 2µl of each sample. The mixture was loaded onto the gel. 5 µl of DNA ladder was added to the first line of the gel to verify the size of testing plasmids.
5) Electrophoresis was carried out at 100 V for 40 min.
6) The results were visualized by UV illumination.

2.6.6 Total RNA isolation

For RNA Isolation, E.Z.N.A. Total RNA kit I from Omega was used.

1) The lysis buffer was prepared by adding 20 µl of β-mercaptoethanol to 1 ml of TRK buffer.
2) 350 µl of lysis buffer was added to each 3-5x10^6 cells.
3) The cells were disrupted by passing through a Nr.19 needle with a 10 ml syringe for 10 times.
4) 350 µl of 70 % ethanol was added to the lysate. The sample was mixed and applied to HiBind RNA spin columns.
5) The column was centrifuged at 10,000 g for 1 min. The flow-through was discarded, and the column was washed with 500 µl of RNA wash buffer I and then washed twice with 500 µl of RNA wash buffer II (each wash was followed by a centrifugation step at 10,000g).
6) The column was placed in a fresh RNase-free centrifuge tube, and 40 µl of DEPC-treated water which pre-heated to 70°C was added to the column for eluting.
7) The sample was incubated for 5 min and centrifuged at maximum speed for 1min.
8) The concentration of isolated RNA was determined by TECAN Infinite 200 PRO. The quality of the RNA sample was analyzed with 1 % agarose gel.
9) The isolated RNA samples were stored at -80 °C.

2.6.7 cDNA synthesis

For cDNA synthesis, RevertAid H Minus First Strand Synthesis Kit from Fermentas was used.

Before cDNA synthesis, all RNA samples were digested with DNase I to remove contamination of genomic DNA.

For DNA digestions, following components were mixed:

Total RNA	5 µl (1 µg)
10x DNAseI buffer with $MgCl_2$ (Fermentas)	1 µl
RNAse free DNAse I (Fermentas)	1 µl
Distilled water (RNase-free)	3 µl

1) Digestion was done at 37°C for 40 min in Thermoblock followed by enzyme inactivation at 70°C for 10 min.
2) 1 µl of Oligo dTs primer was added to each sample.
3) The volume of the reaction was adjusted to 12 µl with ddH_2O and incubation at 70°C for 5 min.
4) The samples were placed on ice for 1 min. Then the following components were added to each sample and mixed:

5x reaction buffer	4 µl
Ribolock RNase inhibitor	1 µl
10 mM dNTP mix	2 µl
RevertAid H minus reverse transcriptase	1 µl

5) The samples were incubated at 42°C for 1 h in a Thermo block, and then the enzymatic activity was stopped by incubation at 70°C for 10 min.
6) The cDNA samples were diluted 10 times with ddH_2O and stored at -80 °C.

2.6.8 Real-time qPCR with Taqman probe

Table 4. List of primers for Real-Time PCR. All ready-made mixes were ordered from Life Technologies.

Name of genes	Primer sequence(5'-3') or assay code
Human GAPDH (Eurofins MWG Operon.)	Forward: TCCATGACAACTTTGGTATCGT
	Reversed: CAGTCTTCTGGGTGGCAGTGA
	Probe: AAGGACTCATGACCACAGTCCATGCC
YKL-39	Hs00970220_m1
TNFAIP6	Hs00200178_m1
HSD11B1	Hs00194153_m1
ABCA1	Hs01059111_m1
CD274	Hs01125301_m1
CD82	Hs01017982_m1
SGPP2	Hs00544786_m1
CRIM1	Hs00212750_m1
ARRDC4	Hs00411771_m1

Each reaction mixture for real-time qPCR was prepared in a 1.5ml Eppendorf tube by mixing:

TaqMan Gene Expression Master Mix	5 µl
20 x TaqMan Assay	0.5 µl
diluted cDNA sample	1 µl
ddH_2O	3.5 µl

Each cDNA sample was analyzed in triplicates. Amplification was performed using LightCycler 480 from Roche. The following program was used:

1) Denaturation: 95°C for 10 min 1 cycle.
2) Annealing and elongation: 1 min at 60°C,
   followed by denaturation at 95°C for 15 s; 50 cycles.
3) Cooling: 37°C; 10 min.

In all experiments, GAPDH was used as the reference gene. The probe for GAPDH contained JOE on 5' end and BHQ1 quencher at 3' end of the sequence.

2.6.9 RNA preparation for Affymetrix chip assay

Total RNA was prepared using E.Z.N.A. Total RNA Kit I as described above.

1) The volume of RNA sample was adjusted to 100 µl with DEPC-treated water.

2) 12 µl of 10 x DNase I buffer with $MgCl_2$ and 10 µl of RNase-free DNase I was added to sample and mixed by pipetting.
3) DNA digestion was done at 37°C for 40 min in a Thermo block followed.

For RNA cleans up procedure, Rneasy kit from Qiagen was used.

1) 350 µl of RLT buffer and 250 µl of 100% ethanol were added to each sample, and the mixture was mixed by pipetting.
2) The sample was applied to the RNeasy mini column, which placed in a 2ml collection tube and centrifuged at 10,000 g for 1 min.
3) After centrifugation, the flow-through was discarded, and the column was washed twice with 500 µl of RPE buffer (each wash was followed by a centrifugation step at 10,000g).
4) After the last centrifugation step, the column was placed in RNAse free tube. RNA was eluted with 40µl of DEPC-treated water, and the samples were incubated for 5 min.
5) Samples were centrifuged at maximum speed for 1 min. The RNA concentration was determined by measuring the absorption peak at a 260nm wavelength with Tecan Infinite 200 PRO.

2.6.10 Hybridization of gene chip microarray data

RNA was tested by capillary electrophoresis by Agilent 2100 Bioanalyzer (Agilent) to confirm the quality of RNA. Hybridization of probes was done using arrays of human HuGene-2.0-st-type from Affymetrix. Biotinylated antisense cRNA was prepared according to the Affymetrix standard labeling protocol with the GeneChip WT Plus Reagent Kit and the GeneChip Hybridization, Wash and Stain Kit (both from Affymetrix, Santa Clara, USA). The hybridization on the chip was performed in a GeneChip Hybridization Oven 640, and then dyed in the GeneChip Fluidics Station 450 and scanned with a GeneChip Scanner 3000. All of the equipment used was from the Affymetrix-Company (Affymetrix, High Wycombe, UK). All the necessary procedures needed for hybridization and scanning of chips were performed by technical assistants Ms. Maria Muciek and Ms. Carolina De La Torre in the Affymetrix Core Facility of Medical Research Center, Medical Faculty Mannheim.

2.7 Protein related techniques

2.7.1 SDS-PAGE

1) The gel casting unit was assembled. 12 % separation gel was prepared according to the Table 5 and poured between the two glass plates to cover 80 % of the unit. 500 µl of 100 % methanol was added on top of the separation gel. The separation gel was left to polymerize until it was solid.
2) Stacking gel was prepared according to the Table 5 and poured on top of the separation gel. A comb was inserted into the stacking gel to form loading wells. The gel was left to polymerize until it was solid.
3) The gel casting unit was transferred to the electrophoresis unit and filled with 1x TGS running buffer.
4) Protein samples were mixed with 2x Laemmli buffer supplemented with β-mercaptoethanol and heated at 95°C for 3 min.
5) 20-25 µl prepared samples were added to the wells with Hamilton glass syringe. 5 µl of protein ladder was pipetted into the first well.
6) Electrophoresis was performed at a constant current of 20 mA for 1 gel and 40 mA for 2 gels.
7) The program was run until the target protein reach to the middle of the gel.

2.7.2 Western blotting

1) The gel was placed in a plastic container filled with blotting buffer. Filter papers and a nitrocellulose membrane were cut to the gel size.
2) The Western Blot cassette was arranged in the following order: Spongy pad/ 2x Filter papers/ gel/ Nitrocellulose membrane/ 2x Filter papers/ Spongy pad. The cassette was placed in the blotting device, which filled with blotting buffer.
3) The blotting process was run at a constant current of 150 mA overnight.
4) The membrane was washed in a plastic container with PBS and then stained with Ponceau S solution for 10 min to visualize the protein bands.
5) The membrane was washed and replaced into blocking buffer (6% non-fat milk in PBS) and then incubated for 1 h.
6) The membrane was further incubated with primary antibody diluted in 1% non-fat milk/PBS on a shaker for 2 h at RT.

7) The membrane was washed 4 times with 0.1% Tween 20/PBS on a shaker (each time 5 min). The membrane was then incubated with the secondary antibody diluted in 1% milk/PBS for 45min at RT on a shaker.
8) The membrane was washed 4 times with 0.1% Tween 20/PBS on a shaker (each time 10 min).
9) 4 ml Western HRP substrate from Luminata Forte was added to cover the membrane, and the membrane was incubated for 3 min.
10) The membrane was packed in a plastic film and exposed with Kodak Bio-Max light film in dark room for different time points, ranging from 30 sec to overnight. Afterward, the film was developed in an X-ray film instrument.

Table 5. The composition of SDS-PAGE gels.

Ingredients	**12% Separating gel/25ml**	**Stacking gel/5 ml**
ddH_2O	5.7 ml	2.7 ml
30% Acrylamide mix	12.5ml	0.83 ml
Tris	6.3 ml (1.5 M, pH-8.8)	1.26 ml (1,0 M, pH 6.8)
10 % SDS	250 µl	50 µl
10 % APS	250 µl	50 µl
TEMED	10 µl	5 µl

2.7.3 Blue gel staining

1) After SDS-PAGE, the gel was removed from the glass plate, placed in a plastic container, and then washed twice with ddH_2O on a shaker (each time 15 min).
2) 50 ml Gel Blue Stain Reagent was added to the container.
3) The container was placed on a shaker for 40 min.
4) The gel was washed twice with ddH_2O on a shaker (each time 15 min).
5) The gel was stored in ddH_2O and kept at 4°C overnight.
6) Stained gels were incubated in gel drying solution at 4°C overnight.
7) The gel was dried in a gel dryer with a vacuum at 80°C for 2 h.

2.7.4 Enzyme-linked Immunosorbent Assay (ELISA)

Protocol for ELISA kit is from Lifespan BioSciences Company.

1) The Capture Antibody was diluted to working concentration according to manufacturer instruction in PBS without carrier protein. 96-well plates were coated with 100µl per well of capture antibody and incubated overnight.

2) The plate was washed with HydroFlex ELISA microplate washer (350 µl wash buffer 4 times) and blocked with 100µl 1% BSA/PBS for 1 h.
3) 50 µl of sample or 100µl of standards diluted in Reagent Diluent was added per well. The plate was covered with an adhesive strip, and the sample was incubated for 2 h. The plate was washed with HydroFlex ELISA microplate washer (350µl wash buffer 4 times).
4) The Detection Antibody was diluted to working concentration according to manufacturer instruction. 100 µl of Detection Antibodies were added to each well, and the plate was incubated for 2 h.
5) The plate was washed with HydroFlex ELISA microplate washer (350µl wash buffer 4 times).
6) Streptavidin-HRP was diluted to working concentration according to manufacturer instruction. 100 µl of Streptavidin-HRP was added to each well, and the plate was incubated for 20 min in the dark.
7) The plate was washed with HydroFlex ELISA microplate washer (350µl wash buffer 4 times).
8) The Substrate Solution was prepared by mixing 5ml of Reagent A with 5ml of Reagent B. 100µl of Substrate Solution was added to each well, and the plate was incubated for 20 minutes in the dark.
9) 50µl of Stop solution was added to each well to stop the reaction.
10) The absorbance at 450nm was read on a Tecan Infinite 200 PRO reader.

2.7.5 Purification of GST-fused proteins

Transformation of DNA into BL21-(DE3)-RIL-Codon-Plus E.coli

1) The Cells were thawed on ice.
2) 50 µl aliquot of cells was mixed with 1 µl of the plasmid in a pre-chilled Eppendorf tube.
3) The sample was incubated for 15 min on ice and then heat shocked at 42°C for 30 s.
4) Afterward, the sample was incubated on ice for 5 min.
5) 400 µl of SOC-medium was added to the cells and mixed by pipetting.
6) The sample was incubated at 37°C for 30 min.
7) The cells were streaked out on LB-agar plates.
8) Incubation was done at 37°C overnight.

Mini expression test

Mini cultures were made to exam the protein expression in different clones.

1) Colonies of each construct and 1 GST control clone were placed in a 15 ml Falcon tube using a pipette tip. 3 ml of LB-medium with 3 µl of ampicillin (100 µg/ml) was added to each tube.
2) The samples were incubated at 37°C, 220 rpm on a shaker overnight.
3) 7 ml of LB-medium with 100 µg/ml ampicillin was added to a Falcon tube for each sample, and 120 µl of overnight culture was added.
4) The OD600 of culture was measured until it reached a value of 0.6. 2 µl of IPTG (1 M) was added to each sample.
5) The samples were incubated at 37°C, 200 rpm for 3 h on a shaker.
6) 500 µl of stimulated culture was added to a new Eppendorf tube. The samples were centrifuged for 5 min at 5,000 rpm. The supernatant was aspirated.
7) 500 µl of Laemmli sample buffer with 2% β-mercaptoethanol was added to each pellet and mixed.
8) The mixture was run on a 12% SDS-PAGE gel and stained blue as described in this study.

Large-scale protein purification: Day 1

1) 100 ml of LB medium supplemented with 100 µg/ml ampicillin was added to a large Erlenmeyer flask and mixed with 200 µl of the BL21-(DE3)-RIL-Condon-Plus *E.coli* culture chosen from the last step.
2) The mixture was incubated at 37°C, 200 rpm overnight on a shaker.
3) Two flasks filled with 500 ml of LB medium (100 µg/ml ampicillin) were warmed up to 37°C in a water bath. 10 ml of overnight culture was pipetted into each flask.
4) The cultures were incubated at 37°C on a shaker at 250 rpm for 1 h.
5) The OD values of cultures were measured until they reached 0.5.
6) Negative control samples were taken: 500 µl of culture was added to an Eppendorf tube and centrifuged for 5 min at 5000 rpm, and the pellet was lysed in 500 µl of Laemmli sample buffer with 2% β-mercaptoethanol.
7) The cultures were stimulated with 250 µl of IPTG (1 M) per 500 ml of culture.
8) The cultures were incubated at 37°C, 250 rpm for 2.5 h on a shaker.

9) Positive control samples were taken: 500 µl of culture was added to an Eppendorf tube and centrifuged for 5 min at 5000 rpm, and the pellet was lysed in 500 µl of Laemmli sample buffer with 2% β-mercaptoethanol.
10) The stimulated culture was poured into 50 ml tubes. The cultures were centrifuged for 15 min at 6000 g and 4°C.
11) The pellets were re-suspended in 10 ml of the Protease inhibitor cocktail solution and froze at -80°C.

Large-scale protein purification: Day 2

1) Large scale samples were thawed on ice.
2) The following reagents were added to a 10 ml total sample volume:

Protease inhibitor cocktail (mini)	100 µl
PMSF	100 µl
DNase (1mg/ml)	100 µl
$MgCl_2$ (1 M)	130 µl
$MnCl_2$ (1 M)	13 µl

3) The samples were incubated 15 min on ice.
4) The samples were vortexed and sonified with the following program:

Amplitude	**Time**
10%	5x 15 s
20%	5x 15 s
50%	1x 15 s

*The samples were kept on ice at all times.

5) The following reagents were added to a 10 ml total sample volume:

NaCl (5 M)	1 ml
20% Triton X-100 in PBS	500 µl
Protease inhibitor cocktail (mini)	100 µl

6) The samples were incubated for 10 min on ice.
7) Test samples were collected (P1): 40 µl of the suspension was mixed with 250 µl Laemmli sample buffer with 2% β-mercaptoethanol.
8) The suspensions were added to 50 ml ultracentrifuge tubes.
9) The samples were centrifuged for 30 min at 16,000 rpm at 4°C.

10) The Sepharose 4B was washed and equilibrated as following: 300 µl of Sepharose 4B was added to an Eppendorf tube; 1 ml of PBS was added; The sample was centrifuged for 3 min at 6,000 rpm at 4°C; The supernatant was removed; The sample was washed twice with PBS; then washed twice with Sepharose washing buffer; then the supernatant was removed.
11) Test samples were collected (P2): 40 µl of the suspension was mixed with 250 µl of Laemmli sample buffer with 2% β-mercaptoethanol.
12) The supernatant was pipetted into 15 ml Falcon tubes, and 100 µl of Protease inhibitor cocktail (mini) was added.
13) Test samples were collected (P3): A small sample of the pellet was mixed with 1 ml of Laemmli sample buffer with 2% β-mercaptoethanol.
14) The Sepharose 4B was dissolved in 1 ml of the supernatant.
15) The samples were rotated for 1.5 h at 4°C. Then the samples were centrifuged at 4°C for 10 min at 1,200 rpm.
16) The lysates were transferred into fresh 15 ml Falcon tubes and frozen at -80°C.
17) Test samples were collected (P4): 40 µl of lysate was mixed with 250 µl of Laemmli sample buffer with 2% β-mercaptoethanol.
18) The sepharose beads were washed 3 times with wash buffer, and the mixtures were centrifuged at 4°C for 15 min at 1,200 rpm.
19) The sepharose beads were transferred to an Eppendorf tube with 1ml of wash buffer, and the mixtures were centrifuged at 6,000 g for 3 min.
20) 1 ml of Sepharose storage buffer was added.
21) Test samples were collected (P5): 30 µl of Sepharose suspension was mixed with 30 µl of Laemmli sample buffer with 2% β-mercaptoethanol.
22) The Sepharose suspension was aliquoted into 100 µl aliquots and froze at -80°C.
23) 25 µl of samples P1-P5 were run on a 12% SDS-PAGE gel and stained as described to determine if stimulation was successful and purification.

Pull-down assay

Bait protein was purified using the protein purification protocol and immobilized on Sepharose 4B. Commercial YKL-39 protein was used as prey proteins to determine possible binding partners and fragments.

1) Proteins (the protein being studied and GST as a negative control) bound to Sepharose 4B were thawed on ice.
2) The samples were washed 3 times with 1 ml ELB complete buffer, each time the samples were centrifuged at 4°C, 6,000 rpm for 5 min.
3) Beads were resuspended in 100 µl of ELB complete buffer per reaction and aliquoted.
4) 1 µg commercial YKL-39 protein was added to each aliquot to have the same amount of protein in each sample.
5) ELB complete buffer was added to a total volume of 400 µl.
6) The samples were incubated at 4°C with rotation for 3 h.
7) The samples were washed 5 times with 1 ml of ELB complete buffer by centrifuging at 4°C for 5 min at 6,000 rpm.
8) After the final wash, the ELB complete buffer was removed, and 50 µl of Laemmli sample buffer supplemented with 2% β-mercaptoethanol was added.
9) The samples were stored at -20°C.

2.8 Cell culture techniques

2.8.1 Cultivation of cell lines and primary cells

Table 6. Cultivation conditions of cell lines and primary cells.

Cell line / primary cell	Growth medium	Growth conditions	Cell type
HEK 293T/17	DMEM complete and 1mM sodium pyruvate	37°C, 5% CO_2	Human embryonic kidney cells
MCF-7	DMEM complete	37°C, 5% CO_2	Human breast adenocarcinoma
Human CD14+ monocytes	X-VIVO10 (supplemented with 1ng/ml M-CSF and 10^{-8} M dexamethasone)	37°C, 7,5% CO_2	Human monocyte

*Complete medium contained 10% FCS and 100 µg/ml penicillin/streptomycin.

2.8.2 Cell thawing

1) A T-75 flask was prepared with 10 ml medium.
2) The vial with frozen cells was put into 37°C water bath to thaw the cells.
3) The melted cells were added to 5 ml warm culture medium in a 15ml Falcon tube.
4) The Falcon tube was centrifuged for 8 min at 1200 rpm.
5) The supernatant was discarded, and the pellet was re-suspended with 1 ml of medium and added into the flask.
6) The flask was put into the 37°C incubator with 5% CO_2 and 95% humidity.

2.8.3 Splitting of adherent cells

Cells were cultivated in T-75 flasks and were split when their confluence reached 80-90%.

1) A 15 ml Falcon tube was used for each flask of cells.
2) The medium was aspirated from the flasks. The cells were washed with 10 ml of PBS. 2 ml of Trypsin/EDTA solution was added to each flask, and the flasks were incubated at 37°C for 3 min.
3) 2 ml of medium was added to the flask to stop the T/E reaction.
4) The contents of each flask were added to the corresponding Falcon tube, and the tubes were centrifuged at 1200 rpm for 8 min.
5) T-75 flasks were prepared with 10 ml medium.

6) The supernatant was aspirated from the pellets. The pellets were re-suspended in 1 ml of medium, and the cells were counted.
7) New T-75 flasks were prepared and filled with 10 ml medium.
8) The cell suspension was added to each new T75 flask. The flasks were put into the 37°C incubator with 5% CO_2 and 95% humidity.

2.8.4 Cell cryopreservation

1) T/E solution and freezing medium (FCS with 10% DMSO) were warmed in 37°C water bath.
2) The medium was aspirated, and the cells were washed with 10 ml of PBS.
3) 2 ml of T/E was added to each flask. The flasks were incubated at 37°C for 3 min.
4) 2 ml of medium was added to stop the T/E reaction.
5) 10ml of PBS was added to each flask to wash and detach the cells.
6) The cell suspension was added to a new 15 ml Falcon tube.
7) The samples were centrifuged at 1200 rpm for 8 min.
8) The supernatant was aspirated. The cell pellet was re-suspended with 1.5 ml of freezing medium (FCS+ 10% DMSO).
9) The suspension was put into the cryovials, and the vials were transferred into the Cryo Freezing Container with 250 ml of isopropanol. The container was placed into the -80°C freezer.
10) The samples were transferred to liquid nitrogen tanks on the next day.

2.8.5 Cell counting

HEK293 cells were counted using a Neubauer hemocytometer.

1) The supernatant was aspirated.
2) The cell pellet was re-suspended in 1 ml of medium.
3) 10 µl of cells were mixed with 10 µl of Trypan blue solution in an Eppendorf tube.
4) 10 µl of the mixture was pipetted into the hemocytometer chamber via capillary action.
5) Using a microscope, cells without trypan blue staining in the four large corner squares were counted. Cells overlapping on the top and left boundaries were counted while cells overlapping the bottom and right boundaries were not.
6) The number of cells per ml was calculated using the following equation:
   (Number of cells in the 4 corner squares/4) x 10^4 x 2

2.8.6 Transfection methodology for HEK 293 cells

Transient transfection

1) A new 6-well plate was prepared (each well was filled with 3ml DMEM complete medium), $2x10^5$ healthy HEK293 cells were seeded in each well. The cells were cultured in 37°C incubator with 5% CO_2 and 95% humidity until the cell confluence reach 80%.
2) The old medium was exchanged with 3ml new warm medium before the experiment.
3) Three sterile Eppendorf tubes were prepared:
   a): 96 µl Optimem+3 µl Fugene HD+1 ug plasmid- pSNAP-tag (p789);
   b): 96 µl Optimem+3 µl Fugene HD+1 ug plasmid-YKL-39-FLAG (p825);
   c): 92 µl Optimem+6 µl Fugene HD+2 ug plasmid-YKL-39-FLAG (p825).
4) The mixtures were incubated for 15min at RT.
5) The reaction mixture was added into corresponding well, and the plate was put into the cell incubator.
6) The cells were cultured for 48 h.

Stable transfection

1) A new 6-well plate was prepared (each well was filled with 3ml DMEM complete medium), $2x10^5$ healthy HEK293 cells were seeded in each well. The cells were cultured in 37°C incubator with 5% CO_2 and 95% humidity until the cell confluence reach 80%.
2) The old medium was exchanged with 3ml new warm medium before the experiment.
3) Three sterile Eppendorf tubes were prepared:
   a): 96 µl Optimem+3 µl Fugene HD+1 ug plasmid- pSNAP-tag (p789);
   b): 96 µl Optimem+3 µl Fugene HD+1 ug plasmid-YKL-39-FLAG (p825);
   c): 92 µl Optimem+6 µl Fugene HD+2 ug plasmid-YKL-39-FLAG (p825).
4) The mixtures were incubated for 15min at RT.
5) The reaction mixture was added into corresponding well, and the plate was put into the cell incubator. The cells were cultured for 48 h in DMEM complete medium.
6) The medium was exchanged to selection medium (DMEM complete medium supplemented with 800 ng/ml G418). The selection medium was exchanged every 2-3 days.

7) Cells were grown for 7 days in selection medium until all the control non-transfected HEK293 cells were dying.
8) Survived transfected cells from 6 well plate was harvested. The cell suspension was prepared to contain 60-90 cells in 10 ml medium, and 100 µl of the suspension was added to each well in a 96-well plate. 96-well plates were incubated at 37°C, 5% CO2.
9) Cells were grown for 4-5 days, and the single resistant colonies from 96-well plate were split to 12-well plate. Cells were grown for 2 days and passage into 6-well plates with cover glasses for further analysis of recombinant protein expression using IF and were transferred into T-25 flasks for the propagation of positive clones and analysis of recombinant protein expression using Western Blot.
10) The positive clones were cultured in T-75 flasks. The early passages were frozen and stored in liquid nitrogen.

2.8.7 Isolation of CD14+ monocytes from human blood (buffy coats)

20-50 ml fresh buffy coats in protective bags were obtained from German Red Cross Blood Donor Service Baden-Württemberg–Hessen.

1) Blood was transferred from plastic bag to a T-75 flask and diluted 1:1 with PBS (without Ca^{2+} and Mg^{2+}).
2) 30ml of diluted blood was layered on top of 15 ml Biocoll solution. The tubes were centrifuged at 420 rcf, for 30 min without breaks.
3) The upper layer (serum) was discarded and second layer (enriched PBMC fraction) was transferred to a new 50 ml falcon tube. The mixture was filled up to 50 ml with PBS and centrifuged at 420 rcf for 10 min with breaks.
4) The supernatant was discarded and the cell pellet was re-suspended in 3 ml of PBS and then filled up to 50 ml with PBS. The Falcon tubes were centrifuged at 420 rcf for 10 min.
5) The percoll gradient was prepared by mixing 13.5 ml percoll, 15 ml MEM medium, 1.5 ml 10 x Earle's Balanced Salt solution.
6) The cell pellet was re-suspended in 4 ml PBS and layered on top of the Percoll gradient. Cells were centrifuged at 420 rcf for 30 min without breaks.
7) The upper layer (PBS) and second layer (cells enriched for monocytes) were collected and transferred to new 50 ml falcon tube and filled up to 50 ml with PBS and then centrifuged at 420 rcf for 10 min with breaks.

8) The supernatant was discarded. The cell pellet was re-suspended in 2 ml PBS and transferred into a new 15 ml falcon tube. The volume was filled to 10 ml. Cells were counted, and the rest of them were centrifuged at 420g, for 10 min with breaks. Cell counting was performed on CASY Cell Counter.
9) The supernatant was discarded. The cell pellet was re-suspended CD14+ microbeads and MACS buffer according to the formula: (95 µl of MACS buffer + 5 µl CD14 microbeads) per $1x10^7$ cells.
10) The cells were incubated for 25 min on a rotator at 4°C. The tubes were filled up to 10 ml with MACS buffer and centrifuged at 420 rcf for 10 min. The cell pellet was re-suspended in 1 ml of MACS buffer.
11) The separation column was placed in the magnetic separation unit and washed with 3 ml MACS buffer. A new collecting tube has been put under the columns, and the cell suspension was applied onto the column.
12) The column was washed 3 times, each time 3 ml MACS buffer. The column was removed from magnetic separation unit and placed on a new 15 ml falcon tube.
13) CD14+ monocytes were eluted from the column with 10 ml MACS buffer. Cells were centrifuged at 420 rcf for 10 min.
14) The cell pellet was resuspended in X-VIVO 10 medium at a concentration of $1x10^6$ cells/ml.

2.8.8 Primary human macrophages culture

1) Isolated monocytes were cultured in 6-well plate with X-VIVO 10 medium supplemented by M-CSF 1ng/ml and Dexamethasone 10^{-8} M. 3-5 ml of cell suspensions were applied to each well ($1x10^6$ cells/ml).
2) Cytokine stimulations were performed immediately after monocyte plating. Following stimulations were used: IL-4 (10 ng/ml) or IL-4 (10 ng/ml) +TGF-beta (10ng/ml).
3) Cells were differentiated for 6, 12, 18 and 24 days at 37°C and 7,5% CO_2 without changing medium.

2.9 Immunological methods

2.9.1 Antibodies

Primary antibodies

Table 7. Primary antibodies. N/A: not applied

Name of antigen and isotype controls	Species	Company/Lab	Catalog number	IF dilution	WB dilution
CD63	Mouse	BD	556019	1:100	N/A
EEA1	Mouse	Santa Cruz	sc-53939	1:25	N/A
FLAG	Rabbit	Sigma	F7425	1:10	1:800
IgG2a (isotype control)	Rat	eBioscience	14-4321	1:160	N/A
IgG1κ (isotype control)	Mouse	BD	557273	1:200	N/A
LAMP-1	Mouse	Santa Cruz	sc-18821	1:50	N/A
p62lck	Mouse	BD	610833	1:25	N/A
Stabilin-1	Rabbit	Our laboratory	RS-1	1:800	N/A
TGN46	Mouse	BD	AHP500G	1:500	N/A
YKL-39	Mouse	Our lab and Institute for Molecular Immunology, Helmholtz Center Munich	Clone 3E4	N/A	1:10
YKL-39	Rat	Our lab and Institute for Molecular Immunology, Helmholtz Center Munich	Clone 18H10	1:1-1:5	1:10

Secondary antibodies and labeling agents

Table 8. Secondary antibodies and labeling agents. N/A: not applied

Antibody/labeling agent	**Species**	**Company**	**Catalog number**	**IF dilution**	**WB dilution**
α-goat-IgG (H+L) Cy5	donkey	Dianova	705-175-147	1:400	N/A
α-mouse-IgG (H+L) Alexa 488	donkey	Dianova	715-545-151	1:400	N/A
α-rabbit-IgG (H+L) Cy3	N/A	Dianova	711-165-152	1:400	N/A
α-rabbit-IgG (H+L) Alexa 488	donkey	Dianova	711-486-152	1:400	N/A
α-rat-IgG (H+L) Alexa 488	N/A	Molecular Probes	a-21208	1:400	N/A
α-rat-IgG (H+L) Cy3	donkey	Dianova	712-165-153	1:400	N/A
DRAQ5	N/A	Cell Signaling	4084s	1:1000	N/A
HRP labeled anti-mouse	goat	Dianova	115-035-133	N/A	1:5000
HRP labeled anti-rabbit	donkey	Amersham	NA934	N/A	1:5000
HRP labeled anti-rat	goat	Santa Cruz	Sc-2303	N/A	1:5000

2.9.2 Immunofluorescence staining

Preparation of cells on coverslips

The stably transfected cells were seeded in 6-well plate ($3x10^5$ cells per well) with coverslips for culture. Then the cells were PFA fixed and subjected to immunofluorescence staining.

1) The supernatants were removed, and the cells were washed twice with 2 ml PBS.
2) The cells on coverslips were fixed with 1 ml 2 % PFA for 10 min.
3) The PFA was removed. 1 ml 0.5% TritonX-100/PBS was added to each well. The samples were incubated for 15 min.
4) The Triton-X 100 solution was aspirated away. The cells were fixed with 1 ml 4% PFA for 10 min.

5) The cells were washed 5 times with 2 ml PBS on a shaker (each time 10 min).

Cytospin preparation

1) The chambers with filter, metal clips and slides were put into the centrifuge.
2) The cell suspensions were pipetted into each chamber, and the samples were centrifuged at 700 rpm for 4 min.
3) The slides with cells were air-dried on a filter paper.
4) The cells on slides were fixed with 2 % PFA for 10 min.
5) The slides were incubated in 0.5% TritonX-100/PBS for 15 min.
6) Then the cells on slides were fixed with 4% PFA for 10 min.
7) The slides were washed 5 times with PBS on a shaker (each time 10 min).

Immunofluorescence staining

1) A circle was drawn with dako pen around the cells on the slides.
2) The slides were washed twice with 2 ml PBS on a shaker (each time 5 min).
3) The slides were washed with 2 ml 0.1% Tween20/PBS for 30 s.
4) The slides were blocked with 1 ml 3% BSA/PBS for 1 h in a humid chamber.
5) The slides were washed with 2 ml 0.1% Tween 20/PBS for 30 s.
6) Primary antibody was diluted with 1% BSA/PBS, and 100 µl dilution was added on to the cells of each slide, and the samples were incubated for 1.5 h in a humid chamber.
7) The slides were washed for three times with 2 ml PBS (each time 5 min).
8) The secondary antibody was diluted with 1% BSA/PBS, 100 µl dilution was added on to the cells of each slide, and the samples were incubated for 45 min in a humid chamber.
9) The slides were washed for four times with 2 ml PBS (each time 5 min).
10) One drop of aqueous fluorescent mounting media was pipetted on the cells. The coverslips were added on the top of the slides.

Confocal laser scanning microscope

Confocal microscopy analysis was performed using Leica TCS SP8 laser scanning spectral confocal microscope, equipped with a 63×1.32 objective. As a source of excitation an argon laser emitting at 488 nm, a krypton laser emitting at 568 nm and a helium/neon laser

emitting at 633 nm were used. Data were acquired and analyzed with Leica Confocal Software. All two- or three-color images were acquired using sequential scan mode.

2.10 Functional assays

2.10.1 Migration assay

1) Freshly isolated human CD14+ monocytes were resuspended in X-VIVO 10 medium at a concentration of $1x10^7$ cells/ml.
2) 600 µl control medium or 600 µl chemoattractant medium (supplied with 100 ng/ml MCP-1 or 100 ng/ml human recombinant YKL-39) were added in the lower chamber of transwell.
3) 100 µl cell suspension ($1x10^6$ cells) was added to the upper insert and transferred to the plate.
4) The plate was incubated at 37°C for 1 h or 3 h.
5) The insert was removed from the plate, and the cells were fixed with 4% PFA for 10 min.
6) The insert was washed twice with PBS.
7) Cells on the insert were fixed with 100% pre-chilled methanol for 5 min.
8) Non-migrated cells were scraped with a moist cotton swab.
9) The insert was washed twice with PBS.
10) The cells on the membrane were stained with hemalum solution for 30 s.
11) The insert was washed twice with PBS.
12) The insert was air-dried. Pictures of the membrane in 10 random fields were taken using 40x magnification.
13) Migrated cells on the membrane were counted with Image J Software.
14) At the same time, cell numbers in the lower chamber were counted by Casy Model TT cell counter, using the following equation: *number of cells obtained/100.*

2.10.2 Tube formation assay

1) Matrigel was thawed one day before experiment at 4°C.
2) The 96-well plate and the pipet tips were pre-chilled at -20°C for 2 h.
3) 50 µl Matrigel were added to each well of the pre-chilled 96-well plate on ice. The polymerization of Matrigel was done in 37°C incubator for 1 h.

4) 100 µl HUVEC cells suspension (1.7 x 10^4 cells) were added to each well; cells were suspended in endothelial cell growth medium (EGM) containing VEGF, endothelial basal medium (EBM), 100ng/ml or 1 µg/ml YKL-39 protein. The plate was incubated at 37 °C, 5% CO_2 overnight.
5) The tube visualizations were analyzed using a light microscope. 10 pictures were taken from each well. The tube numbers and lengths were counted using the AxioVision Image software.

2.10.3 Apoptosis and Proliferation

DNA fragmentation assay

1) MCF-7 cells (2x10^4 per well) were seeded in 24 well plates.
2) The cells were stimulated with 0.5µM Staurosporine, 100ng/ml YKL-39 or serum free medium for 6, 12, 24 and 48h.
3) DNA from treated cells were isolated and analyzed by 1% agarose gel with the participation of gel red.
4) The results were visualized by Multi Doc-It Imagine system (UVP).

Proliferation assay

The Click-iT EdU Alexa Fluor 488 Flow Cytometry Assay Kit was used. All procedures were performed according to the manufacturer's instructions.

1) 3 x 10^5 cells/per well were seeded in 6 well plate with the corresponding medium for 24 or 48 h.
2) 10 µM/ml EdU was added to each well, and the 6 wells plates were incubated at 37°C, 5% CO_2 for 1 h.
3) The cells were harvested in FACS tubes, and then cells were washed with 2 ml of FACS buffer.
4) 100 µl of fixative solution (Click-iT component D) was added to each FACS tube and mixed with the cells.
5) The cells were incubated for 15 min, RT.
6) 1ml of 1% BSA/PBS was added to each FACS tube.
7) Centrifugation at 1,200 rpm for 8 min and discard the supernatants.
8) 100 µl of saponin-based permeabilization and wash reagent (Click-iT component E) was added to each FACS tube. Vortexed and incubated at room temperature for 15 min.

9) 500 µl of Click-iT reaction cocktail was added to each FACS tube and incubated at room temperature for 30 min without light.
10) The cells were washed by 3 ml of saponin-based permeabilization and wash reagent.
11) Centrifugation at 1,200 rpm for 8 min and discard the supernatants.
12) Re-suspend the cells in 200 µl of saponin-based permeabilization and wash reagent.
13) The cell suspension was analyzed by a BD FACS Canto II.

2.11 Statistical analysis

The significance of the difference between groups of experimental data in RT-qPCR analysis and ELISA, migration assay and tube formation assay was determined using Student's paired t-test. A p-value less than 0.05 were considered statistically significant. All statistical analysis was performed in GraphPad Prism 6.

Statistical analysis of microarray data was done by Dr. Carsten Sticht from the Affymetrix Core Facility of Medical Research Center, Medical Faculty Mannheim. A Custom CDF Version 19 with ENTREZ based gene definitions was used to annotate the arrays. The Raw fluorescence intensity values were normalized applying quantile normalization and RMA background correction. One-way-ANOVA was performed to identify differential expressed genes using a commercial software package SAS JMP10 Genomics, version 6, from SAS (SAS Institute, Cary, NC, USA). A false positive rate of a=0.05 with FDR correction was taken as the level of significance. Plots (3D Scatterplots and Venn diagrams) were made with JMP. Heat maps were generated in Morpheus application from Broad Institute.

3 Results

3.1 YKL-39 expression in human macrophages

3.1.1 Long-term macrophage cultivation

It was previously identified in our laboratory that the expression of YKL-39 mRNA is induced by IL-4 and TGF-beta in primary human macrophages after 6 days cultivation (Gratchev et al., 2008b). Tissue macrophages have been shown to be long-living cells (Hashimoto et al., 2013; Murphy et al., 2008; Yona et al., 2013). However, whether YKL-39 is expressed in long-term cultivated macrophages was unknown. To analyze the expression of YKL-39 at late stages of macrophage maturation, a model system for the long-term differentiation of human monocyte-derived macrophages was established.

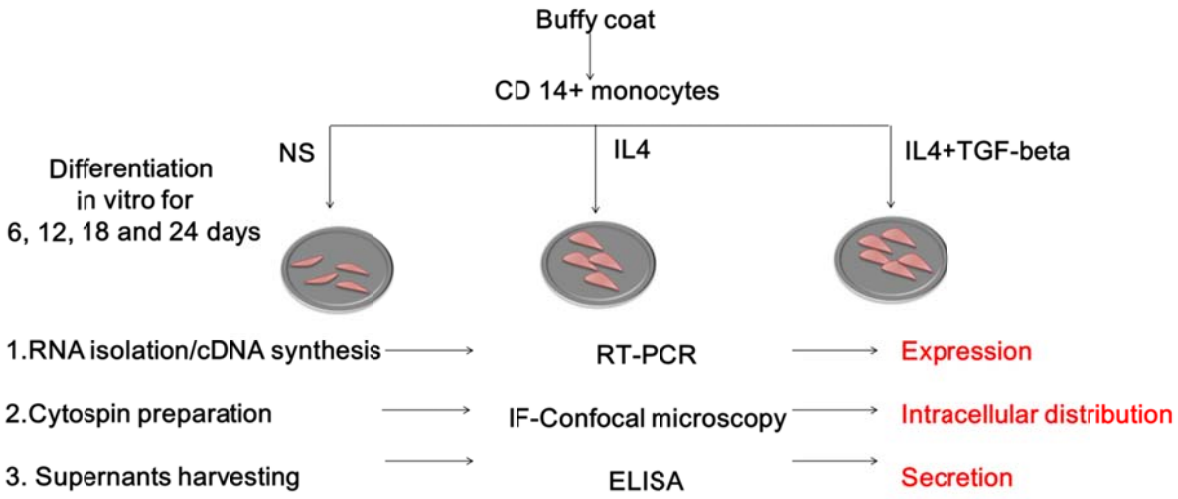

Figure 7. Schematic presentation of the model system for the analysis of YKL-39 expression and intracellular distribution in macrophages.

Human CD14+ monocytes isolated out of buffy coats were cultivated in X-VIVO 10 medium supplemented by 1 ng/ml M-CSF to optimize viability of macrophages during long-term cultivation. Dexamethasone was added at the concentration of 10^{-8} M that corresponds to the physiological levels of glucocorticoids. Three macrophage subpopulations were generated with different stimulations: 1) no cytokine stimulation; 2) stimulated with IL-4; 3) stimulated with IL-4+TGF-beta. Each subpopulation was cultivated for 6, 12, 18 and 24 days. The general experimental design is illustrated by Figure 7.

3.1.2 YKL-39 mRNA expression

The mRNA expression of YKL-39 was analyzed in primary human macrophages by RT-qPCR. The highest level of YKL-39 mRNA expression was detected in macrophages stimulated with TGF-beta in combination with IL-4, but not with IL-4 alone on all days (Figure 8). YKL-39 was not expressed in non-stimulated macrophages, while IL-4 had an only slight stimulatory effect compared to the non-stimulated cells on days 6, 12, 18 and 24. YKL-39 expression was significantly up-regulated by the stimulation of IL-4 and TGF-beta on day 6, 12, 18 and 24. The highest effects of TGF-beta were detected on day 12 of macrophage cultivation. The level of up-regulation induced by the TGF-beta in combination with IL-4 compared to IL-4 alone was from 4.26 (BC880-1) times to 16.72 (BC880-2) times in individual macrophage cultures (Figure 8). In 5 out of 6 analyzed individual macrophage cultures, the levels of YKL-39 under IL-4+TGF-beta stimulation were decreased after 18 and 24 days, and in one individual culture (BC880-1), levels of YKL-39 were up-regulated on day 18 and decreased only on day 24.

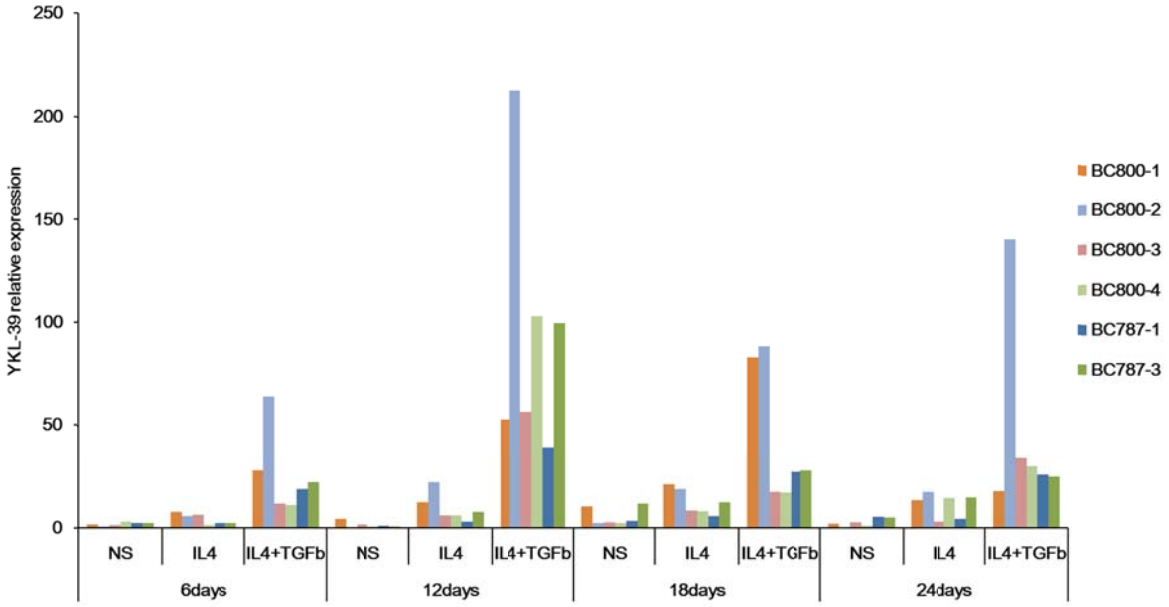

Figure 8. Real-time qPCR analysis of YKL-39 expression in human macrophages. Human CD14+ monocytes were cultured for 6, 12, 18 and 24 days (non-stimulated macrophages were used as a control). Six individual donors with differential response are presented. The gene expression levels of YKL-39 were normalized to GAPDH mRNA expression.

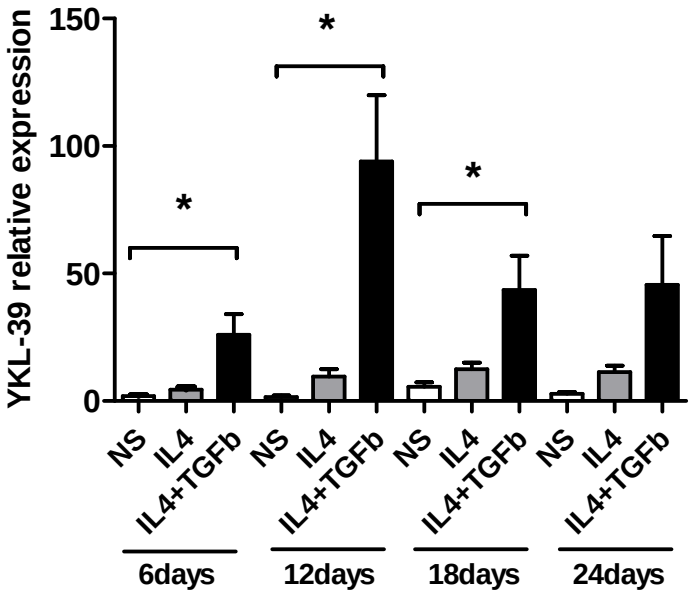

Figure 9. Relative expression of YKL-39 mRNA in human macrophages. Human CD14+ monocytes were cultured for 6, 12, 18 and 24 days (non-stimulated macrophages were used as a control). The graph represents mean values from six individual donors with standard deviations. The expression levels of YKL-39 were normalized to GAPDH mRNA expression. For statistical analysis Student's t-test was used (* $p < 0.05$).

Figure 9 illustrates the expression of YKL-39 by macrophages in response to IL-4 and IL-4+TGF-beta. YKL-39 was significantly up-regulated by IL-4+TGF-beta in macrophages compared to IL-4 stimulated macrophages (5.87 times on day 6, 9.77 times on day 12, 3.49 times on day 18), while no significant difference was found on day 24. In summary, the RT-qPCR demonstrated that IL-4 and TGF-beta induce expression of YKL-39 on the mRNA levels in long-term macrophage cultures suggesting that YKL-39 can be expressed on the long-living tissue macrophages also *in vivo*.

3.1.3 YKL-39 protein expression

The next aim was to detect the expression of YKL-39 on the protein level. YKL-39 monoclonal antibodies were generated in cooperation with Dr. Elisabeth Kremmer, Institute of Molecular Immunology, Helmholtz Zentrum München, Germany. Reactivity of monoclonal antibodies for immunofluorescence was evaluated by indirect immunofluorescence using YKL-39 transient transfection TS/A cells from previous studies in our laboratory (Bin Song, unpublished data). In this study, the expression of the YKL-39 protein in macrophages was detected by rat mAb 18H10.

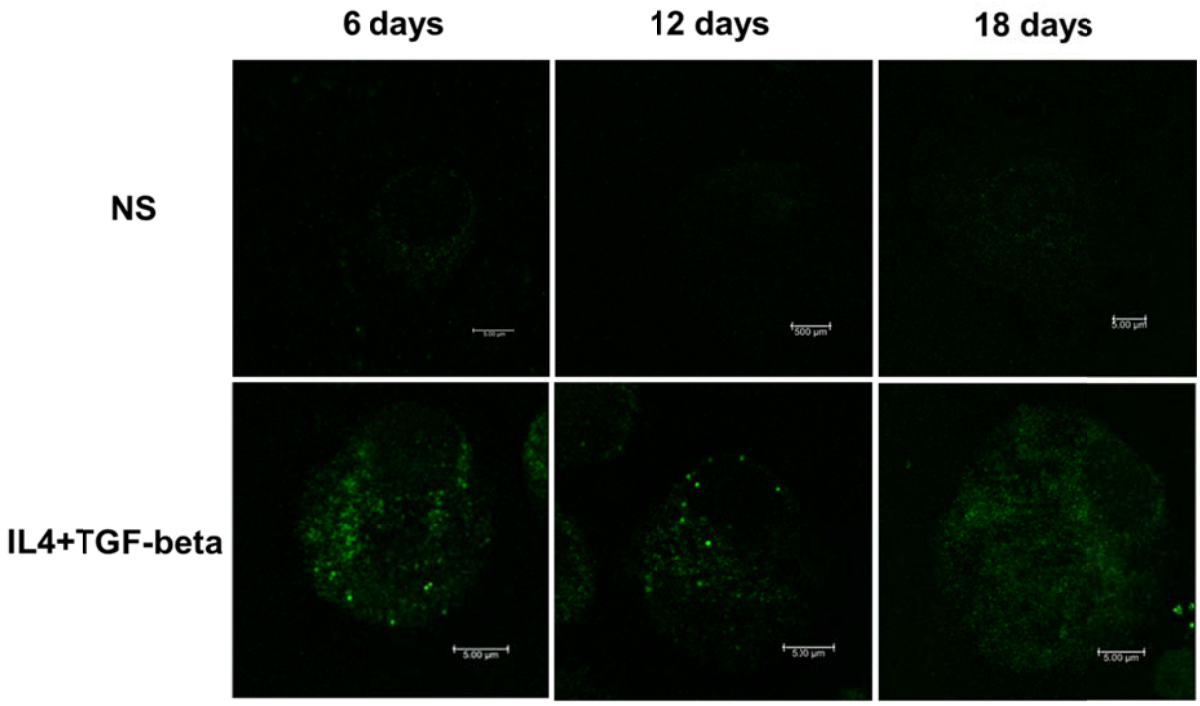

Figure 10. YKL-39 protein is up-regulated in IL-4+TGF-beta stimulated macrophages. Human CD14+ macrophages were cultivated without additional cytokine stimulation (NS) or stimulated with IL-4+TGF-beta for 6, 12 and 18 days. YKL-39 protein was identified by immunofluorescent staining using rat mAb 18H10 and anti-rat Alexa488-conjugated secondary antibody (green) and visualized by confocal microscopy. Scale bars: 5 µm.

Immunofluorescence results indicate that YKL-39 protein is induced by the stimulation of IL-4 and TGF-beta (Figure 10). The expression of YKL-39 was detected on day 6, 12 and 18 that corresponded to the expression levels of YKL-39 mRNA identified by RT-qPCR (Figure 9). On the protein level, the similar tendency for the elevated expression of YKL-39 on day 12 was observed.

3.2 Intracellular localization and trafficking of YKL-39

3.2.1 Localization of YKL-39 in alternatively activated macrophages

Macrophages are professional secretory cells that utilize both conventional and lysosomal secretory pathways (Kzhyshkowska and Krusell, 2009). Previous work in our laboratory demonstrated that SI-CLP is sorted into the endosomal/lysosomal system and secreted by human monocyte-derived macrophage (Kzhyshkowska et al., 2006b). Thus, it was hypothesized that YKL-39 could be secreted by human macrophages similar to SI-CLP. In this study, macrophages were stimulated with IL-4 and TGF-beta for 12 days to achieve the highest expression levels of YKL-39. The localization of YKL-39 in the intracellular vesicles was analyzed by indirect immunofluorescence and confocal microscopy.

The rare event of co-localization was observed for YKL-39 with early endosomal marker EEA1 or late endosomal marker p62lck suggesting that YKL-39 is targeted to the endosomal/lysosomal system; however, only transiently present in the endosomes (Figure 11A and B). Strong co-localization was identified for YKL-39 and major lysosomal marker LAMP-1, indicating that YKL-39 is accumulated in the lysosomes (Figure 11C). To identify whether YKL-39 is targeted for the secretion, co-localization of YKL-39 with CD63, used as a specific marker for secretory lysosomes in macrophages, was examined. YKL-39 was indeed present in CD63 positive lysosomes of primary macrophages (Figure 11D). The pattern of intracellular YKL-39 distribution was similar to the pattern previously demonstrated for SI-CLP (Kzhyshkowska et al., 2006b), suggesting that YKL-39, at least partially, can be secreted by the lysosomal secretory pathway.

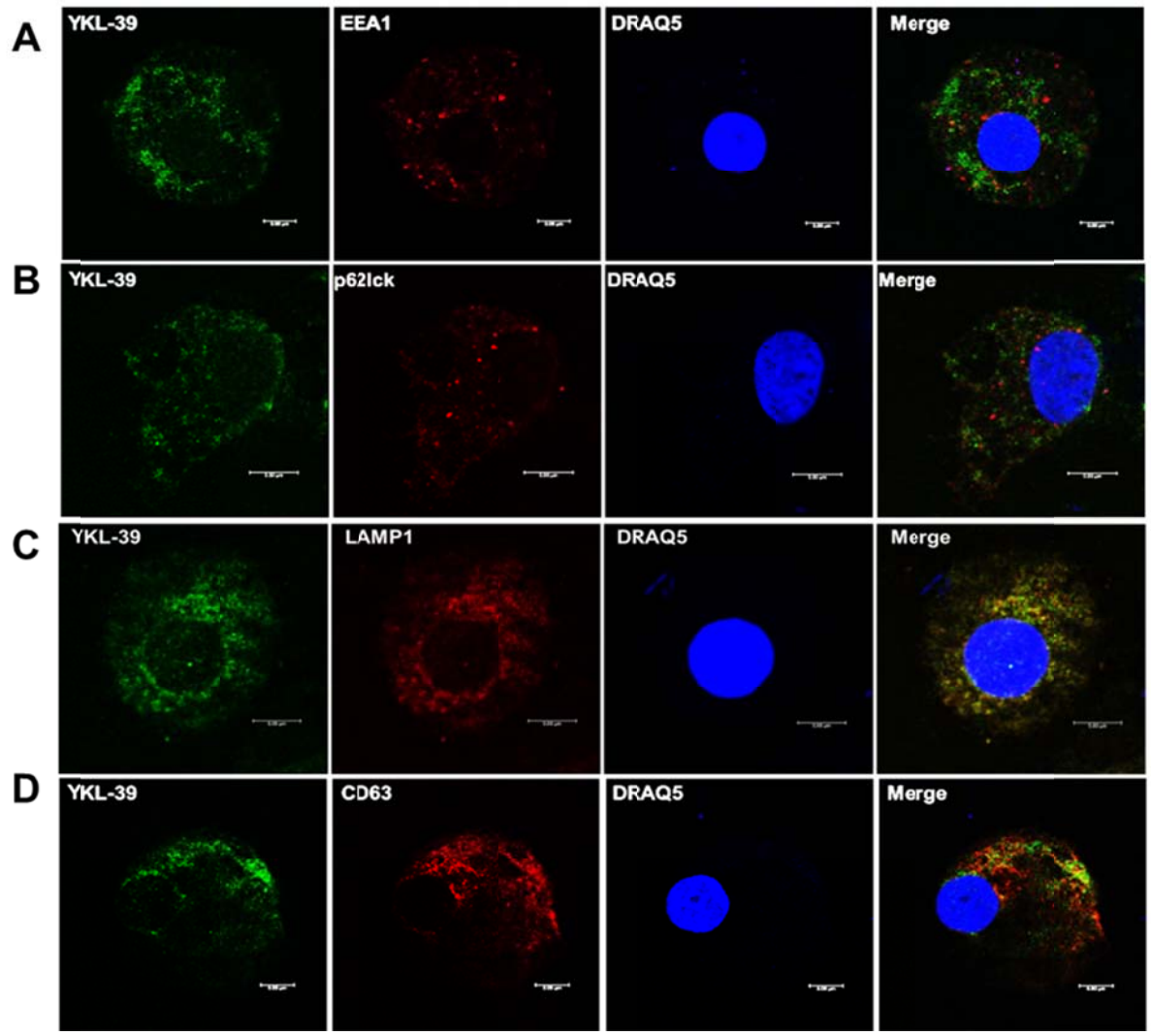

Figure 11. Intracellular distribution of YKL-39 in human macrophages. Human CD14+ monocytes were stimulated with IL-4+TGF-beta for 12 days. YKL-39 was detected with rat mAb 18H10 and anti-rat Alexa488-conjugated secondary antibody (green). Other proteins are visualized in red and nuclear are visualized in blue. Merge of green and red is shown in yellow. **A.** Co-localization of YKL-39 and EEA-1(early endosomes); **B.** Co-localization of YKL-39 and p62lck (late endosomes); **C.** Co-localization of YKL-39 and LAMP-1 (lysosomes); **D.** Co-localization of YKL-39 and CD63 (secretory lysosomes). Scale bars: 5 μm.

3.2.2 Stabilin-1 mediated intracellular sorting of YKL-39

Satbilin-1 was previously identified in our laboratory as a sorting receptor for SI-CLP in alternatively activated macrophages (Kzhyshkowska et al., 2006b). Here it was hypothesized that stabilin-1 can act as sorting receptor for YKL-39. To test this hypothesis, the co-localization of YKL-39 and stabilin-1 was examined in IL-4+TGF-beta stimulated human macrophages. It was found that YKL-39 partially co-localizes with stabilin-1 in the trans-Golgi network (TGN) (Figure 12A) and in the stabilin-1 positive vesicles around the nuclear area (Figure 12B). Taking into consideration that YKL-39 was very rarely present in the EEA1 positive early endosomes (Figure 11A), co-localization of YKL-39 and stabilin-1 was found in the secretory but not in the endocytic pathway, providing the argument towards the role of stabilin-1 as the intracellular sorting receptor for YKL-39 in macrophages.

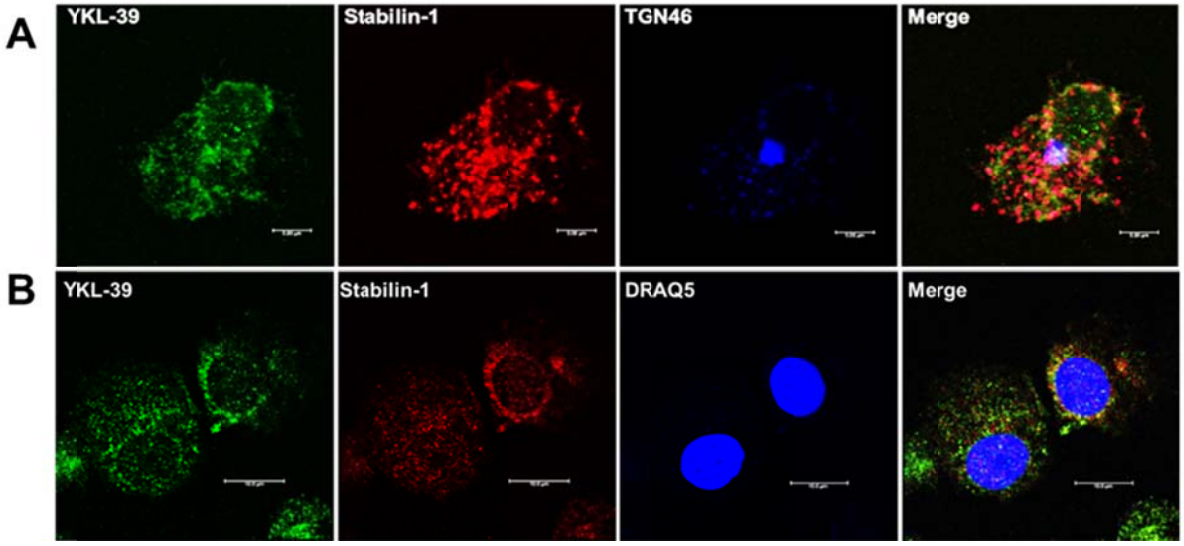

Figure 12. YKL-39 co-localized with stabilin-1 in primary human macrophage. Human CD14+ monocytes were stimulated with IL-4+TGF-beta for 12 days. YKL-39 was detected with rat mAb 18H10 and anti-rat Alexa488-conjugated secondary antibody (green). Stabilin-1 was visualized in red, TGN46 and cell nuclear are visualized in blue. Merge of green and red is shown yellow; red and blue in pink; green, red and blue in white. **A.** YKL-39 was found in TGN and co-localized with stabilin-1; **B.** YKL-39 partially co-localized with stabilin-1 around cell nuclear.

3.2.3 The effect of overexpression of stabilin-1 on YKL-39 trafficking

In order to find further confirmation for the role of stabilin-1 in the intracellular sorting of YKL-39; the model HEK293 cell lines stably expressing recombinant YKL-39 were generated and used to analyze the effect of stabilin-1 on the intracellular distribution of YKL-39. HEK293 cells were transfected with pSNP-YKL-39-FLAG or control empty vector. Stable single-cell-derived clones expressing YKL-39 were identified using a-FLAG immunofluorescent staining and confocal microscopy (data not shown). The list of positive clones is provided in Table 9.

Table 9. Stable transfected HEK293 cells.

Expression construct	Clone names	Percentage of positive cells	Expression level
pSNAPtag-YKL-39-FLAG (P825)	P1B2	60%	strong
	P1C12	60%	strong
	P1F7	80%	strong
	P1F10	50%	strong
	P2E6	30%	strong
pSNAP-tag (P789)	VectorE4		

Effect of stabilin-1 over-expression on YKL-39 trafficking in HEK293 cell line

To analyze whether stabilin-1 is directly involved in sorting process of YKL-39, HEK293-YKL-39-FLAG stable transfected cells (clone P1B2) were seeded on coverslips and transiently transfected with stabilin-1 expressing construct pLP-IRESneo-hSt1 or empty vector pLP-IRESneo. After 48 h transfection, cells were examined by immunofluorescence/confocal microscopy. It was found that recombinant YKL-39 was localized as nuclear globular structures in HEK293 cells, which indicated that YKL-39 is miss-sorted in these cell lines; the transient overexpression of stabilin-1 resulted in the relocalization of YKL-39-FLAG into stabilin-1 positive cytoplasmic structures (Figure 13).

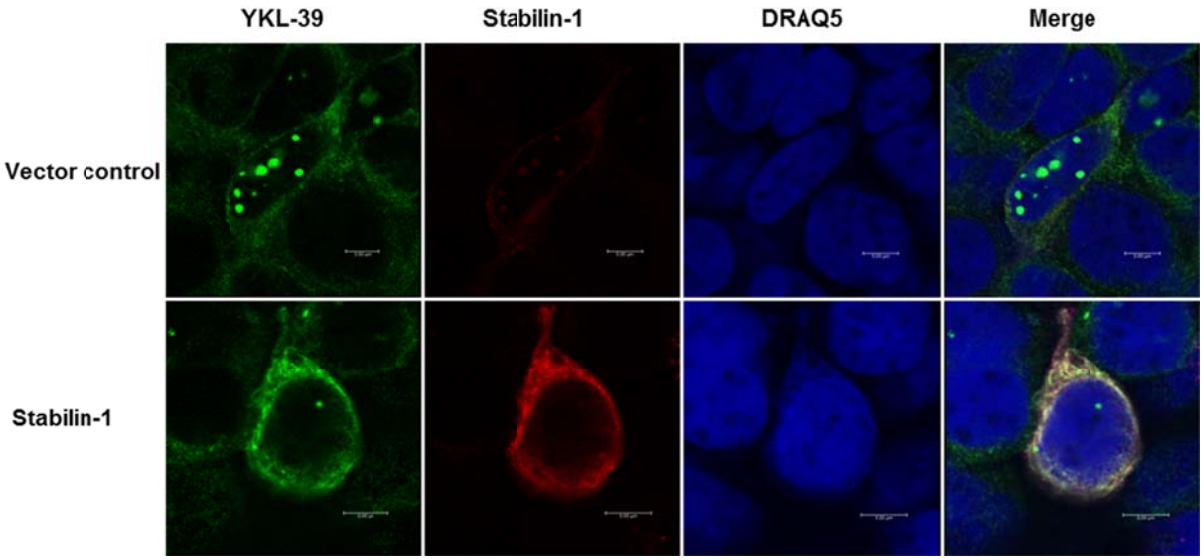

Figure 13. Effect of stabilin-1 over-expression on the localization of YKL-39 in HEK293 cells. HEK293-YKL-39 stable cells were grown on coverslips and transfected with stabilin-1 expressing plasmid. Stabilin-1 was detected with rabbit mAb RS-1 and anti-rabbit Cy3-conjugated secondary antibody (red), and YKL-39 was detected with rat mAb 18H10 and anti-rat Alexa488-conjugated secondary antibody (green). Recombinant YKL-39 is miss-sorted in globular structures localized in the nuclear area. Transient over-expression of stabilin-1 resulted in relocalization of YKL-39 in the cytoplasm. Scale bars: 5 μm.

Identification of stabilin-1 and YKL-39 interaction in vitro

It was previously demonstrated in our laboratory that stabilin-1 directly interacts with SI-CLP and this interaction is mediated by the fasciclin domain 7 of stabilin-1 (Kzhyshkowska et al., 2006b). To analyze the interaction of stabilin-1 with YKL-39, GST pull-down assay was performed using purified YKL-39 and immobilized sepharose beads with the stabilin-1 fragments. Following fragments of stabilin-1 were produced in bacterial expression system and immobilized on the sepharose 4B beads: GST-fused P9 domain of stabilin-1 (GST-St-P9), GST-fused F7 domain (GST-St1-F7) and GST-fused cytoplasmic tail of stabilin-1 (GST-St1-C) (Figure 14B). Purified in the same system, GST was used as the negative control in the pull-down assay.

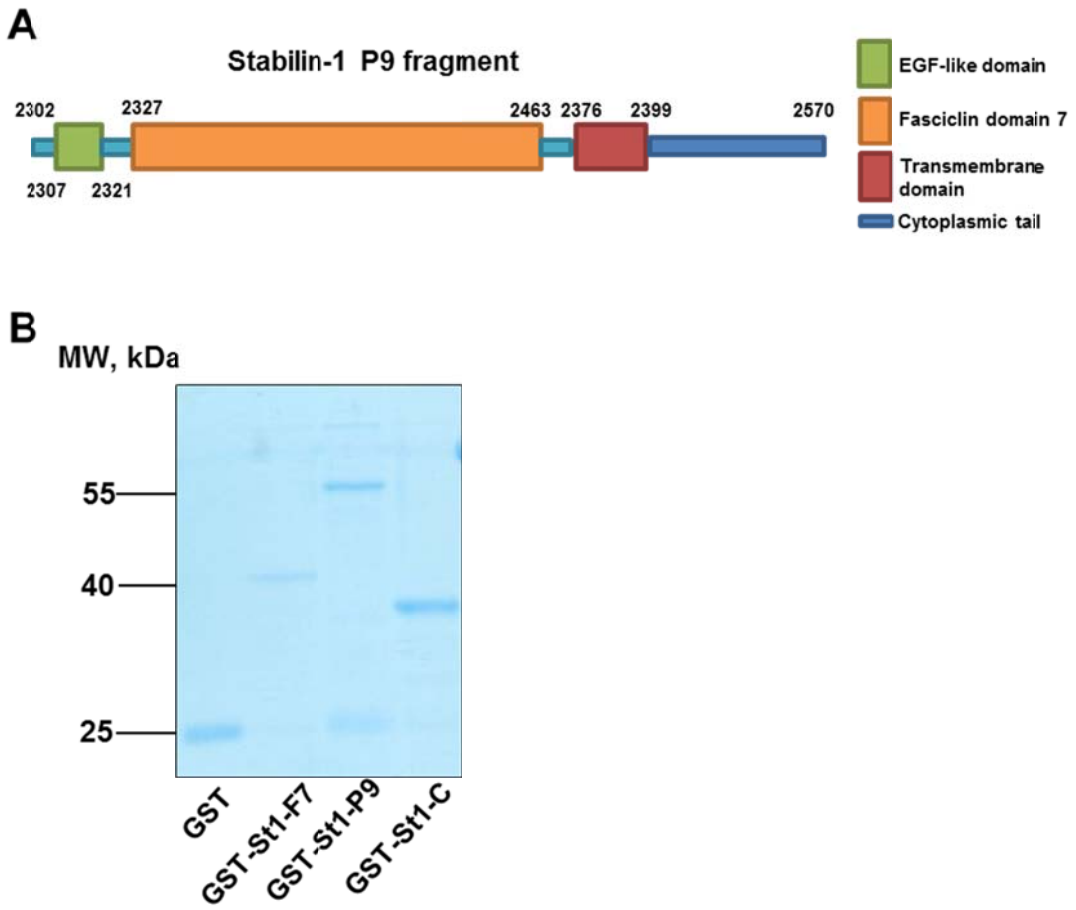

Figure 14. Schematic presentation of stabilin-1 fragment and control for the amounts of GST-fused proteins used in the pull-down assay. A. Schematic presentation of stabilin-1 P9 fragment. **B.** Control of GST-fused protein amounts used in the pull-down assay.

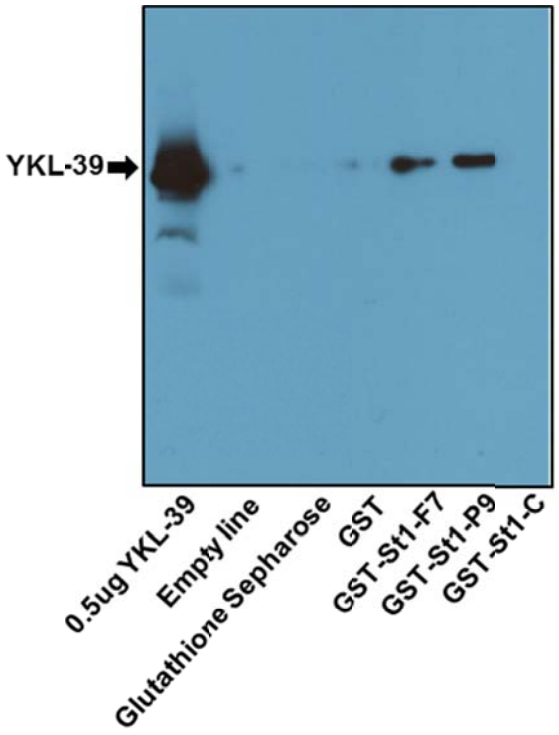

Figure 15. Identification of YKL-39 as stabilin-1 interacting protein using GST pull-down assay. Purified YKL-39 (0.5 μg) was used as a positive control for Western blotting. 1 μg of the recombinant YKL-39 was used in each pull-down assay. YKL-39 was identified by Western blotting using mouse 3E4 antibody. Interaction of YKL-39 was identified for the F7 and P9 fragments of stabilin-1. No interaction was identified in case of empty sepharose beads, GST or cytoplasmic tail stabilin-1.

It was found that human recombinant YKL-39 binds to the GST-fused P9 fragment of stabilin-1 that contains fasciclin domain 7 (GST-St-P9), and to the fasciclin domain 7 itself (GST-St1-F7), but not to the cytoplasmic tail of stabilin-1 (GST-St1-C) or to the GST alone (Figure 15). The pull-down assay demonstrated that fasciclin domain 7 of stabilin-1 is responsible for the interaction with YKL-39, similarly to the previously identified interaction with SI-CLP. Identified direct interaction of stabilin-1 with YKL-39 provided further evidence for the role of stabilin-1 as sorting receptor for YKL-39 in macrophages.

3.3 Analysis of YKL-39 secretion in long-term macrophage cultures

After the identification of YKL-39 in the secretory pathway in macrophages (Section 3.2), the next step was to identify whether YKL-39 is secreted by macrophages. The presence of YKL-39 in the macrophage-conditioned medium was analyzed on day 6, 12, 18 and 24. The concentrations of YKL-39 in the conditioned medium were identified by ELISA.

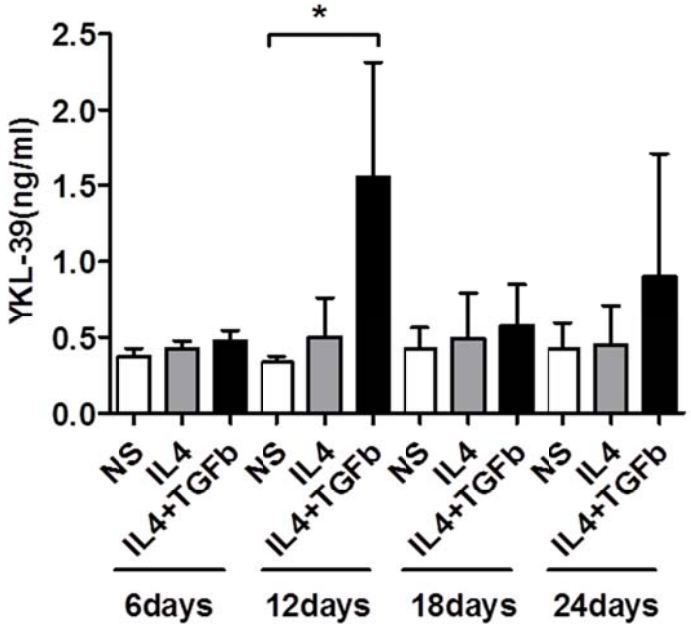

Figure 16. ELISA analysis of YKL-39 secretion in long-term macrophage cultures. Human CD14+ monocytes, non-stimulated (NS) or stimulated with IL-4 or IL-4+TGF-beta were cultured for 6, 12, 18 and 24 days. Highest levels of secreted YKL-39 were detected in the conditioned medium of IL-4+TGF-beta stimulated macrophages on day 12. For the statistical analysis Student's paired t-test was used (* $p < 0.05$). The mean values from four individual donors with standard deviations are presented.

The maximum level of YKL-39 protein (1.5 ng/ml) was detected on day 12 in IL-4+TGF-beta stimulated macrophages (Figure 16) that correlated with the RNA expression levels (Figure 9). On day 18, the decrease of extracellular YKL-39 levels was detected, while on day 24 the concentration was slightly increased. The dynamic changes in the extracellular levels of YKL-39 can be explained by additional factors involved in its intracellular retention or internalization of already released YKL-39. In conclusion, it was demonstrated that YKL-39 is secreted by human macrophages stimulated by IL-4+TGF-beta in long-term culture condition.

3.4 Effect of human recombinant YKL-39 protein on the recruitment of monocytes

As a homolog of YKL-40, YKL-39 was suggested also promote the migration of monocytes. The ability of YKL-39 to induce migration of human primary monocytes was analyzed in the trans-well system using purified YKL-39 as chemotactic factors. As a positive control the monocyte chemotactic agents MCP-1 was used in parallel. It was found that YKL-39 mediates monocytes migration *in vitro* (Figure 17). Amounts of migrated cells were

quantified on the lower surface of the membranes and in the lower chambers. In both cases, the stimulatory effect of YKL-39 was detected after 1 h and 3 h of incubation. On the membranes, YKL-39 stimulated migration of monocytes 1.84 times ($p<0.01$) after 1 h and 1.98 times ($p<0.01$) after 3 h compared to control group. Quantification of monocytes migrated in the lower chamber demonstrated event stronger chemotactic effect of YKL-39: 1.91 times ($p<0.01$) after 1 h and 5.6 times ($p<0.01$) after 3 h compared to control group. Effect of YKL-39 on the migration of monocytes in the lower chamber after 3 h was comparable with the effect of MCP-1 (65 % of MCP-1). The migration assay demonstrated that YKL-39 has a chemotactic activity toward primary monocytes *in vitro* suggesting that it can act as a recruitment agent for the circulating monocytes into the tissues.

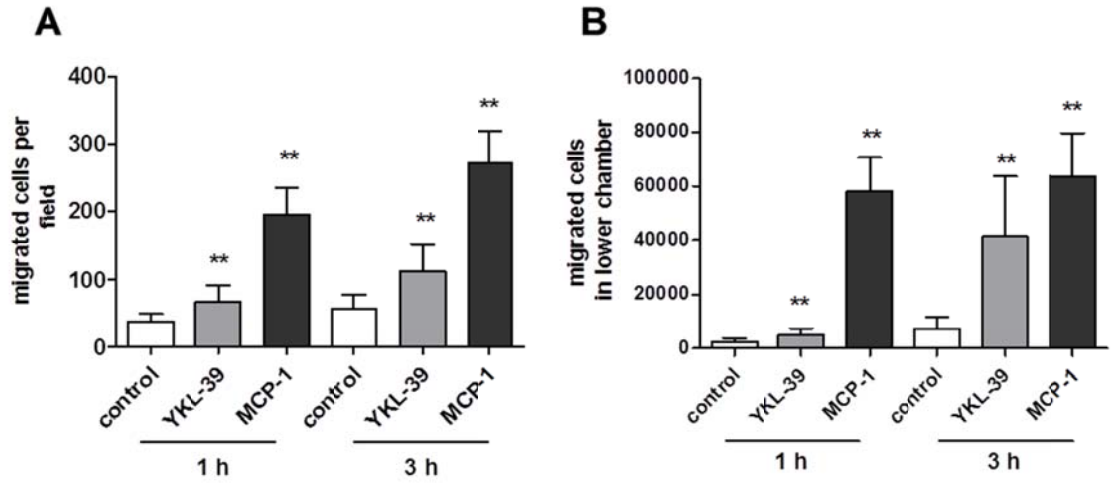

Figure 17. Effect of recombinant YKL-39 on monocytes migration. Peripheral blood–derived CD14+ monocytes were loaded in the upper chamber of a transwell system; YKL-39 (100 ng/ml) or MCP-1 (100 ng/ml) was added to the lower chamber. Cells on the transwell membrane per field or total migrated cell numbers in the lower chamber were quantified. **A.** Migrated cells on the membrane (average of 10 randomly selected fields); **B.** Total cell numbers in the lower chamber after migration. The total amount of donors analyzed (n=9). For statistical analysis, Student's t-test was used.* denotes the statistical significance of YKL-39 or MCP-1 with control group (**$p<0.01$,*$p<0.05$).

3.5 Tube formation assay

It was previously demonstrated that YKL-40 acts as an angiogenic factor to promote tumor angiogenesis (Shao et al., 2009). It was also reported that over-expression of YKL-40 in HCT-116 and MDA-MB-231 cells promote angiogenesis in mouse models for breast adenocarcinoma and colorectal carcinoma (Shao, 2014). Moreover, YKL-40 was found to enhance the migration of VSMC cells which support angiogenesis (Nishikawa and Millis, 2003). It was hypothesized that YKL-39, similarly to YKL-40, can have a pro-angiogenic

activity. To test this hypothesis, tube formation assay using HUVEC cells was performed. Representative images are presented on Figure 18A. EGM (VEGF-containing endothelial cell growth medium), was used as a positive control. The tube formation induced by recombinant YKL-39 were 5.95 (100 ng/ml) and 5.98 (1 µg/ml) times higher than that were observed in the negative control group (Figure 18B). YKL-39 was found to induce endothelial cell tube formation on the level similar the positive control: 68.9 % (100 ng/ml) and 69.2 % (1 µg/ml) of positive control.

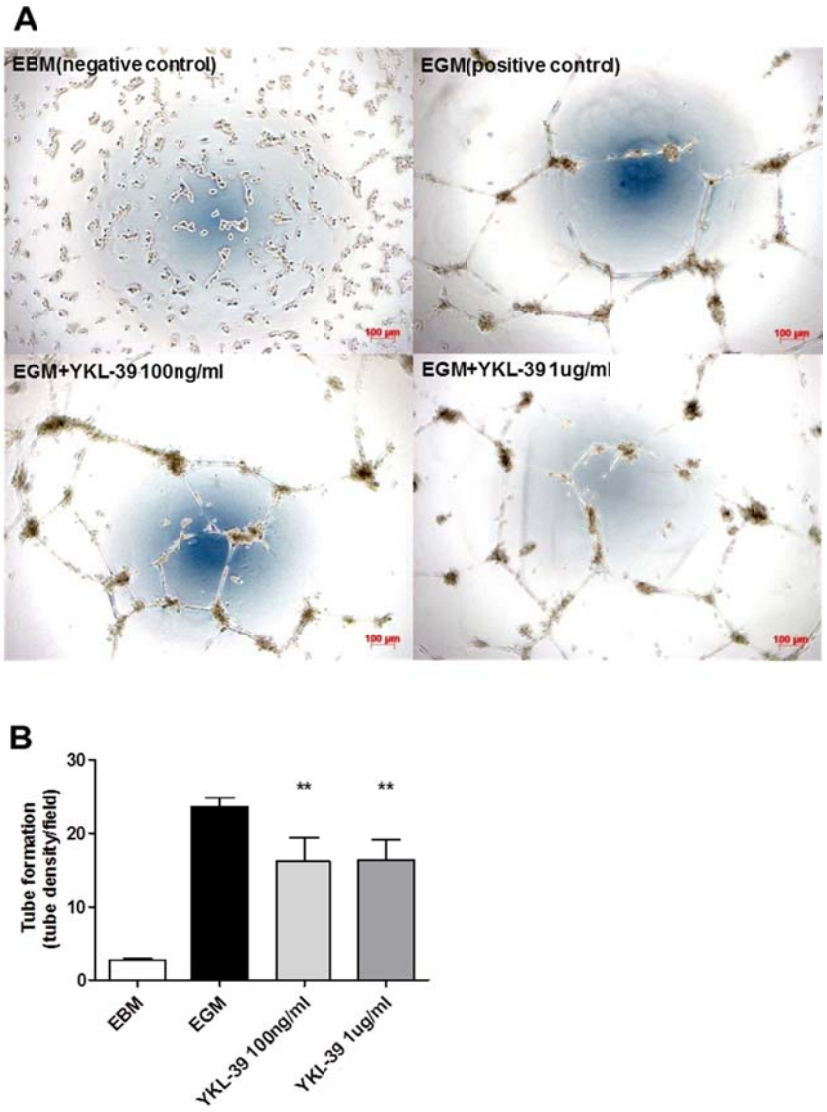

Figure 18. YKL-39 stimulates endothelial cell tube formation in vitro. Human microvascular endothelial cells (HUVECs) were loaded on a layer of Matrigel and cultured overnight in the presence of human YKL-39 (100 ng/ml or 1 µg/ml). EBM: negative control group, EGM: positive control group. Vessel-like tubes were quantified. **A.** Representative images for tube formation. Scale bars: 100 µm. **B.** Tube density per field. **p<0.01 compared with EBM control group

These data supported the hypothesis that YKL-39 can stimulate angiogenic responses in endothelial cells, suggesting YKL-39 expression can induce angiogenesis in tumor microenvironment.

3.6 Gene expression profile of monocytes stimulated with YKL-39

3.6.1 Affymetrix microarray analysis of monocytes stimulated with YKL-39

After the identification of chemotactic effects of YKL-39 on monocytes, the next question was raised whether YKL-39 can affect the transcriptional program of human monocytes. Therefore, Affymetrix microarray analysis was performed to identify the effects of YKL-39 on the gene expression profile of human primary CD14+ monocytes.

Freshly isolated monocytes out of five individual donors were stimulated with YKL-39 at the concentration of 100 ng/ml or 1 μg/ml for 24 h. For each donor, three different groups were analyzed: blank control, YKL-39 100 ng/ml, YKL-39 1 μg /ml (Figure 19). The comparison was made between non-stimulated monocytes, and monocytes stimulated with YKL-39 100 ng/ml (comparison 1), and between non-stimulated monocytes and monocytes stimulated with YKL-39 1 μg /ml (comparison 2). For each stimulation, additionally, to the statistical threshold ($p<0.05$), an arbitrary cut-off was introduced. Thus, only the genes in which the difference of the signal intensity between the control group and the YKL-39-stimulated group higher than 0.5 were taken from the profile. In the comparison 1, there were no genes correspond to these criteria. Therefore, eight up-regulated genes from comparison 2 have been selected for further analysis (Figure 19).

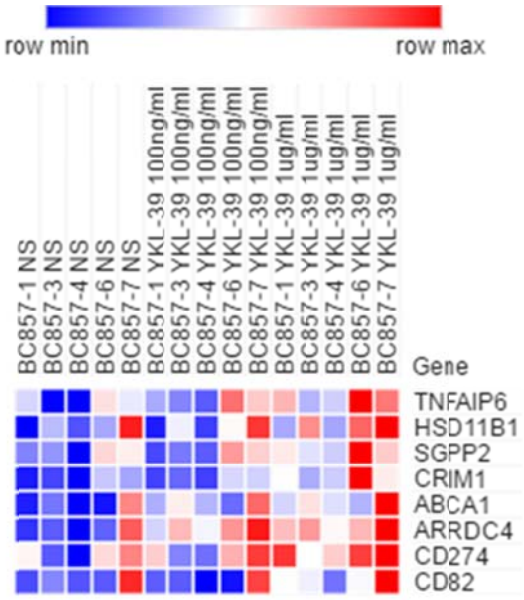

Figure 19. List of the most strongly up-regulated genes in monocytes after YKL-39 stimulation. Human CD14+ monocytes were stimulated with YKL-39 (100 ng/ml or 1 µg /ml) for 24 h; non-stimulated monocytes (NS) were used as negative control. Gene expression comparison of YKL-39 stimulation (100 ng/ml or 1 µg /ml) from five individual donors was performed by Affymetrix chip microarray assay (BC 857-1, 857-3, 857-4, 857-6, 857-7 refers to different donor used in the test).

Following genes were selected: TNFAIP6, HSD11B1, SGPP2, CRIM1, ABAC1, ARRDC4, CD274, and CD82. The relative expression of each gene in monocytes non-stimulated and stimulated with YKL-39 is presented in different colors; blue refers to the low expression, and red refers to the high expression of specific genes (Figure 19). It was found that monocytes from different donors do not respond equally to YKL-39 stimulation, the gene expression profile was different in each donor. For example, donor BC857-7 is more sensitive to YKL-39 stimulation.

3.6.2 Validation of microarray data by RT-qPCR

To confirm the results obtained from microarray analysis, RT-qPCR analysis was performed. The same samples that have been used for Affymetrix analysis where stimulation with YKL-39 for 24 h and compared to the samples from the same donors stimulated with YKL-39 for 6 h. The analysis was performed for monocytes stimulated with 2 concentrations of YKL-39: 100 ng/ml and 1 µg/ml. The expressions of followed eight genes were analyzed: TNFAIP6, HSD11B1, SGPP2, CRIM1, ABAC1, ARRDC4, CD274 and CD82 (Figure 20).

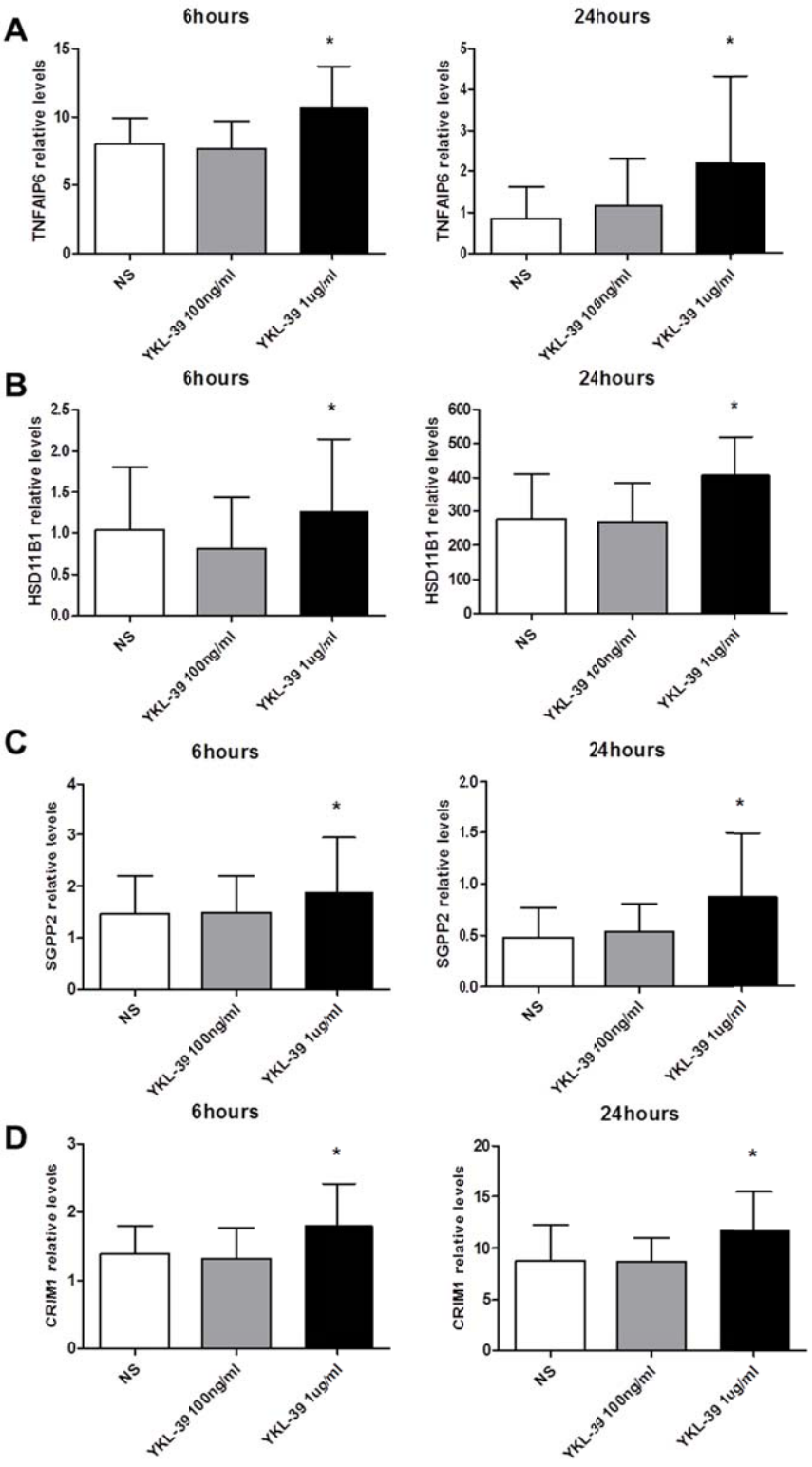
A
6hours
24hours
TNFAIP6 relative levels
B
HSD11B1 relative levels
C
SGPP2 relative levels
D
CRIM1 relative levels
NS
YKL-39 100ng/ml
YKL-39 1ug/ml
*

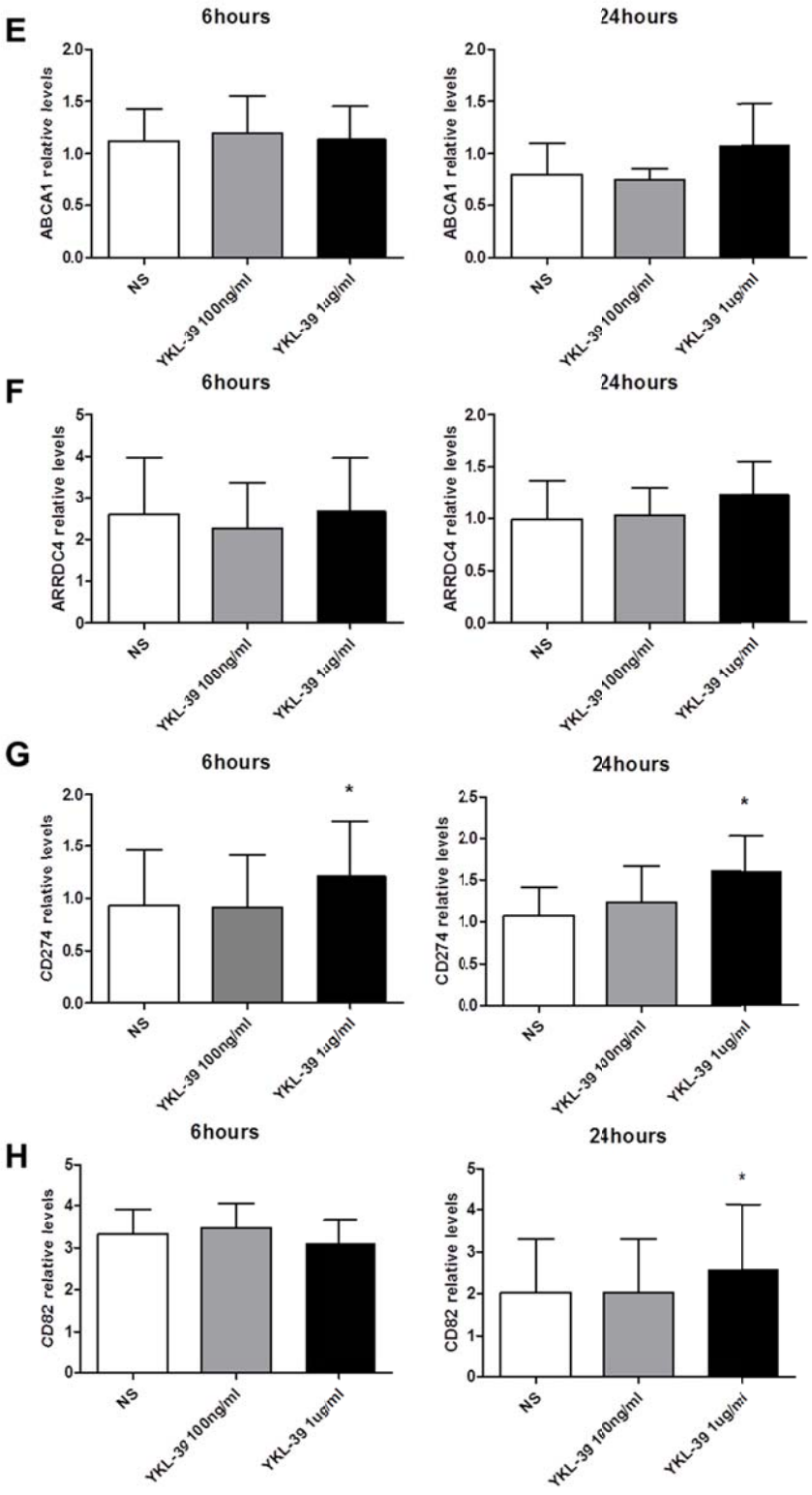

Figure 20. RT-qPCR validation of YKL-39-induced gene expression in monocytes identified by Affymetrix chip assay. A. TNFAIP6 expression; **B.** HSD11B1 expression; **C.** SGPP2 expression; **D.** CRIM1 expression; **E.** ABCA1 expression; **F.** ARRDC4 expression; **G.** CD274 expression; **H.** CD82 expression. All graphs represent mean values with standard deviations from 5 individual donors. For statistical analysis Student's t-test was used (* $p < 0.05$).

YKL-39 had an only slight stimulatory effect on the expression of the selected genes, however statistically significant difference was identified in case of stimulation with 1 μg/ml compared to the non-stimulated cells. The fold changes of these tested genes were summarized in Table.12. After 6 h of stimulation with YKL-39, minor but statistically significant changes in expression of TNFAIP6, HSD11B1, SGPP2, CD274, and CRIM1 were observed (Figure 20 A, B, C, D, G, and H). The highest stimulatory effect was found for TNFAIP6 (fold change 1.33). After 24 h of the stimulation with YKL-39, the statistically significant changes were found on TNFAIP6, HSD11B1, SGPP2, CRIM1, CD274, and CD82 (Figure 20 A, B, C, D, G, and H). The highest effect of YKL-39 after 24 h of stimulation was found on TNFAIP6 (fold change 2.56). The tendency of YKL-39 to stimulate expression of ABCA1 and ARRDC4 was also observed after 24 h (Figure 20 E and F).

Table 10. Fold change of selected YKL-39 induced genes by RT-qPCR validation.

	Fold change (6 h)	**Fold change (24 h)**
HSD11B1	1.22	1.46
TNFAIP6	1.33	2.56
SGPP2	1.29	1.81
ABCA1	0.99	1.35
ARRDC4	1.02	1.24
CD82	0.93	1.27
CD274	1.30	1.50
CRIM1	1.30	1.34

These data indicate that YKL-39 has only slight effect on the change in the transcriptional program of monocytes. However, the profile of the induced genes was unique, suggesting a specific role of YKL-39 in the activation of monocytes recruited from the circulation.

3.7 YKL-39 effect on MCF-7 cells proliferation and apoptosis

Since expression of YKL-39 in macrophages was found to be induced by TGF-beta, a multifunctional cytokine expressed in various types of cancer, including breast cancer, next question that we asked was whether YKL-39 affects the proliferation or apoptosis of tumor cells. The proliferation of human breast adenocarcinoma cells MCF-7 in response to YKL-39 was analyzed using EdU proliferation assay.

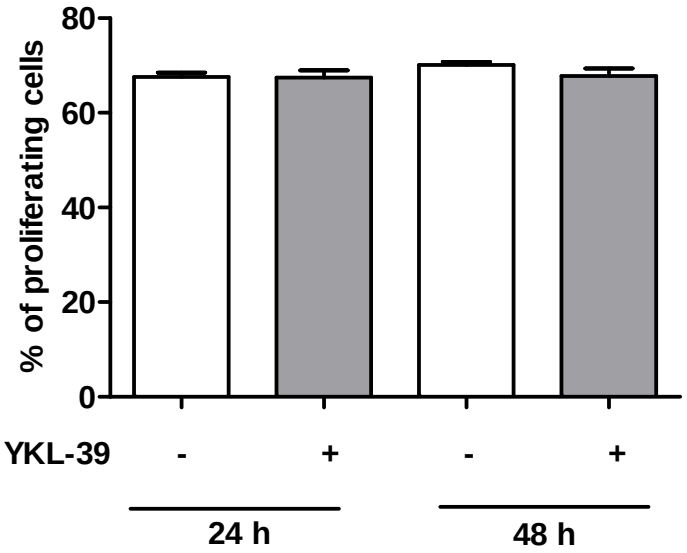

Figure 21. Proliferation assay for YKL-39 stimulated MCF-7 cells. MCF-7 breast cancer cell lines were incubated with 100 ng/ml YKL-39 for 24 h or 48 h. The percentage of proliferating cells was quantified with Click-iT EdU Alexa Fluor 488 Flow Cytometry Assay Kit.

MCF-7 cells were cultured in presence or absence of YKL-39 for 24 or 48 h. No difference in proliferative activity between non-stimulated and YKL-39-stimulated groups was observed at both time points (Figure 21).

To investigate the effects of YKL-39 on the apoptosis of MCF-7 cells, DNA fragmentation assay was performed. As a positive control for the induction of apoptosis, MCF-7 cells were stimulated with staurosporine. YKL-39 was used at the concentration of 100 ng/ml. Induction of apoptosis was tested after 6 h, 12 h, 24 h and 48 h of stimulation (Figure 22).

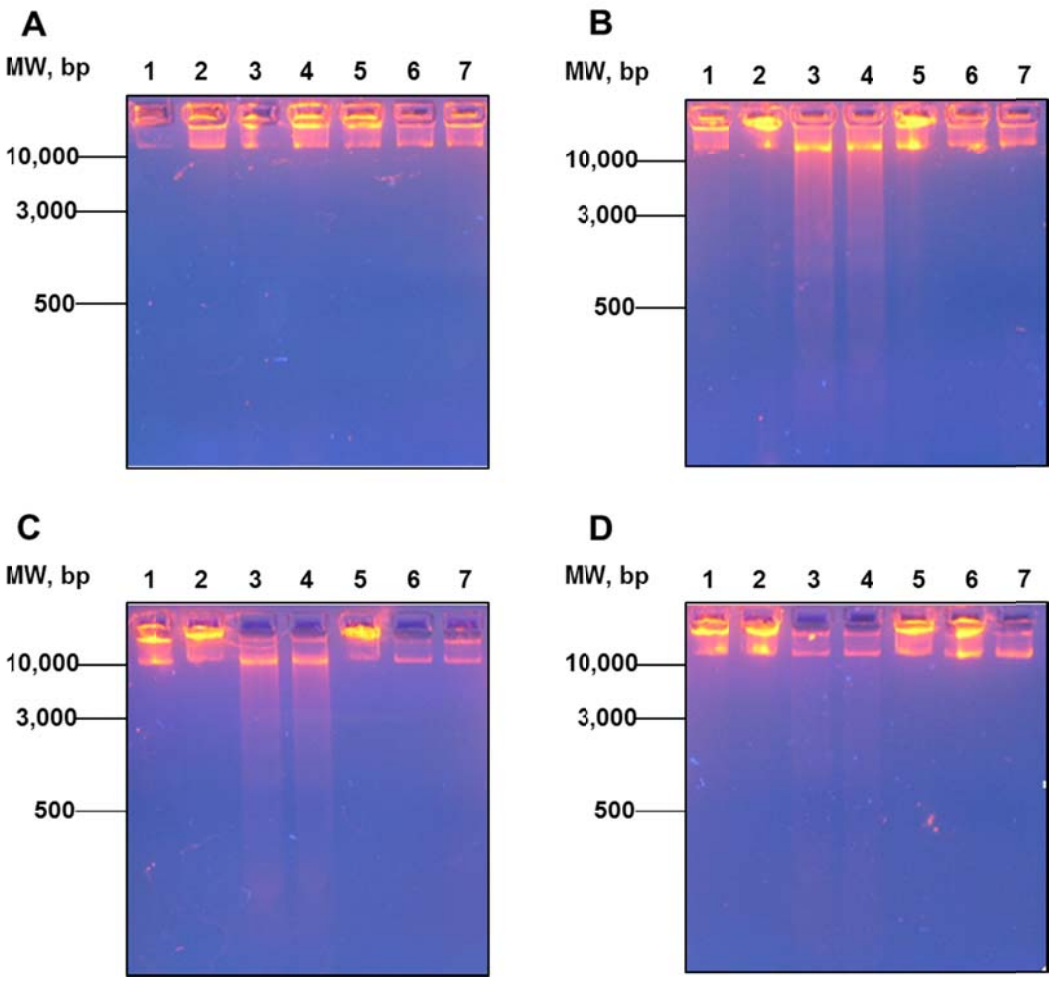

Figure 22. DNA fragmentation analysis in MCF-7 cells. MCF-7 were incubated with different stimulations, genomic DNA of each group was isolated. **A.** 6 h; **B.** 12 h**; C.** 24 h**; D.** 48 h after stimulation (Lane 1: Medium with 10 % FCS; Lane 2: Medium with 10 % FCS+5 µl DMSO; Lane 3: Medium with 10 % FCS+0.5 µM staurosporine; Lane 4: Medium with 10 % FCS+0.5 µM staurosporine +100 ng/ml YKL-39; Lane 5: Medium with 10 % FCS+100 ng/ml YKL-39; Lane 6: Medium without FCS; Lane 7: Medium without FCS +100 ng/ml YKL-39).

It was observed that staurosporine at the concentration of 0.5 µM induced apoptosis in MCF-7 cells after 12 and 24 h. The application of YKL-39 alone had no pro-apoptotic effect, and the addition of YKL-39 did not increase the pro-apoptotic effect of staurosporine (Figure 22).

4. Discussion

4.1 Expression of YKL-39 in macrophages

In this study, we analyzed the expression and secretion pattern of YKL-39 in long-term cultured macrophages *in vitro*. For the first time, it was demonstrated that in macrophages cultivated up to 24 days, the expression of YKL-39 is induced by TGF-beta in combination with IL-4, but not by IL-4 alone. These data suggest that YKL-39 acts as a marker for late-stage differentiation of macrophages in pathological conditions. During tumor growth and progression, a significant amount of TGF-beta is produced by cancer and stromal cells and secreted in the tumor microenvironment (Pickup et al., 2013). An increased expression of TGF-beta was shown to correlate with the malignancy of different cancers (Derynck et al., 2001; Katsuno et al., 2013). Therefore, TGF-beta is considered to play a major role in the initiation and progression of cancer by affecting proliferation, apoptosis, and differentiation of cancer cells in the tumor microenvironment (Cantelli et al., 2017).

Moreover, TGF-beta also involves in the development of atherosclerotic disease which is induced by the accumulation of macrophages (Loeffler and Wolf, 2014; Ramji et al., 2006). In this process, gene expression of mature human macrophages was up-regulated by TGF-beta. It was first demonstrated that the combination of IL-4 and TGF-beta induces the expression of IL-17 receptor B in macrophages (Gratchev et al., 2004). Next, using Affymetrix gene expression profiling assay, it was found in our laboratory that TGF-beta induce expressions of a wide array of genes in mature human macrophages, including transcriptional regulators, immune modulators, and genes associated with lipid processing which contributes to atherosclerotic plaque vulnerability (Gratchev et al., 2008a; Nurgazieva et al., 2015). However, less is known about the effect of TGF-beta on human macrophages in the tumor microenvironment. In the present work, it was demonstrated that TGF-beta induces the production of chitinase-like protein YKL-39 in human primary macrophages. Therefore, investigation of the secretion mode and biological functions of YKL-39 was the further focus of this project.

4.2 Localization, sorting and secretory mechanisms of YKL-39

SI-CLP was found to be sorted by stabilin-1 and secreted via lysosomes in alternatively activated macrophages (Kzhyshkowska et al., 2006b). In the present study, the question was raised whether YKL-39 is sorted via a similar pathway in macrophages in this study.

It was found that YKL-39 is sorted into LAMP-1 positive and secretion-committed CD63 positive lysosomes in IL-4+TGF-beta stimulated macrophages. A similar pattern of intracellular distribution was discovered for SI-CLP in our previous study (Kzhyshkowska et al., 2006b). In HEK293-YKL-39-FLAG cell line, YKL-39 is miss-sorted into the globular structures and localized in the nuclear area. Transient overexpression of recombinant stabilin-1 in this model cell line resulted in the re-distribution of YKL-39 into the cytoplasm, and this effect was similar to our previously published data demonstrating the role of stabilin-1 in the intracellular sorting of SI-CLP in H1299 cell model (Kzhyshkowska et al., 2006b). Using a pull-down assay fasciclin domain 7 of stabilin-1 was found to mediate the interaction with YKL-39, which is also consistent with our previous results demonstrating the interaction of stabilin-1 and SI-CLP (Kzhyshkowska et al., 2006b). Therefore, YKL-39, similarly to the SI-CLP, can be targeted by stabilin-1 into the lysosomal secretory pathway in human alternatively activated macrophages.

Lysosomes are organelles with complex functions involved in cell death, immunity, signaling, and stress responses (Holtzman, 2013; Piao and Amaravadi, 2015), which not only participate in digesting extracellular material internalized by endocytosis and intracellular components sequestered by autophagy, but also secrete their contents by fusing with the plasma membrane (Piao and Amaravadi, 2015). Two types of lysosomes contained proteins are necessary for their functions: soluble hydrolases and integral lysosomal membrane proteins. More than 60 hydrolases have been identified and characterized, some of which play an important implication on tumor progress (Piao and Amaravadi, 2016; Schröder et al., 2010). The best investigated lysosomal hydrolases are the cathepsin proteases, which are subdivided into three groups based on the active site of the amino acids and the catalytic activity: serine cathepsins (cathepsins A and G), cysteine cathepsins (cathepsins B, C, F and H) and aspartic cathepsins (cathepsins D and E) (Krikorian et al., 2015). It was suggested that cathepsins could either promote or suppress the tumor growth; the cytosolic cathepsins inhibit tumor growth by activating the apoptotic pathway (Olson and Joyce, 2015). In contrast, the extracellular cathepsins promote tumor growth through degradation of basement membrane and activation of other pro-tumorigenic proteins (Repnik et al., 2012). Cathepsins B and E were proved involved in cancer progression and metastasis in different types of cancer, such as breast cancer and pancreatic cancer (Bengsch et al., 2014; Keliher et al., 2013). Glyco_18 domain containing proteins were also found by us and others to be sorted via the endosomal/lysosomal system and secreted by activated macrophages (Kzhyshkowska et al., 2007; Kzhyshkowska et al., 2006b; Renkema et al., 1997). Chitotriosidase was seen

comparable to cathepsin D in lysosomal vesicles in macrophages (Renkema et al., 1997). SI-CLP was demonstrated to be sorted by stabilin-1 via a lysosomal pathway in alternatively activated macrophages (Kzhyshkowska et al., 2006b). In this study, it was demonstrated that YKL-39, similar to SI-CLP, is sorted into the lysosomal secretory pathway. Considering the fact that YKL-39 expression is strongly induced by TGF-beta, an essential regulatory cytokine of the tumor microenvironment, it was important to identify biological activities of YKL-39, which can implicate in the cancer progression.

4.3 Functional analysis of YKL-39

4.3.1 YKL-39 promotes monocyte migration

Monocytes are intensively recruited into growing tumors by chemotactic factors secreted by tumor cells and stromal cells in the tumor microenvironment (Quail and Joyce, 2013; Riabov et al., 2014). TAMs serve as a source of chemotactic factors, such as CCL2, CCL17, CCL18, and CCL22, which attract circulating monocytes (Bingle et al., 2002; Sierra-Filardi et al., 2014; Young and Singh, 2016). For example, CCL2 is a key chemokine which is responsible for the recruitment of circulating monocytes to the site of the tumor or inflamed tissue (Deshmane et al., 2009; Partridge and Siddiqui, 2017). Chitinase-like proteins also belong to the macrophage-secreted factors that have chemotactic activity towards different cell types. (Kawada et al., 2012; Owhashi et al., 2000). YM1 was described as a chemotactic factor towards eosinophils, T lymphocytes and polymorph nuclear leukocytes (Owhashi et al., 2000). YKL-40 has a chemotactic activity towards macrophages in colorectal cancer; also, it was reported that YKL-40 is highly up-regulated in the atherosclerotic plaque which is characterized by the infiltration of monocytes (Boot et al., 1999).

Therefore, it was hypothesized that YKL-39 could also have chemotactic activity. Effect of YKL-39 on the induction of migration of freshly isolated human CD14+ monocytes was analyzed in the trans-well system and compared to the effects of CCL2. The concentration of YKL-39 (100 ng/ml) was used according to biologically active concentrations of YKL-40 90.3±8.2 ng/ml in patients with hip OA (Conrozier et al., 2000). It was found that YKL-39 significantly promotes migration of monocytes after 1 and 3 h. After 1 h, the effect of YKL-39 had approximately 10 % of CCL2 in mediating monocytes recruitment. After 3 h, the effect of YKL-39 was even more pronounced and constituted 65% of the chemotactic activity of CCL2, which indicated the biological significance of YKL-39 mediated recruitment of monocytes.

Monocytes recruited to the tumor site by YKL-39 or other chemoattractants differentiate into tumor-associated macrophages under the influence of the local microenvironment, where TGF-beta can induce secretion of YKL-39 in macrophages. The next question was raised whether in addition to the recruitment of monocytes; YKL-39 can have a direct effect on the transcriptional program of newly infiltrated monocytes. Therefore, the effects of YKL-39 on the gene expression profile in monocytes were analyzed in this study.

4.3.2 Gene expression profile of monocytes stimulated with YKL-39

To model the effects of YKL-39 on the programming of monocytes recruited from the circulation, freshly isolated human CD14+ monocytes were stimulated for 6 and 24 h with YKL-39, gene expression was analyzed by Affymetrix microarray (24 h) and validated by RT-qPCR (6 h and 24 h). It was found that 8 genes were up-regulated by YKL-39. However, only modest differences in the gene expression (from 1.24 up to 2.56 fold at 24 h time point) were identified. For 6 genes, the differences confirmed by RT-qPCR had statistical significance, and these genes are discussed below.

TNFAIP6 (also known as TSG-6) is a secreted protein with a hyaluronan-binding domain which is involved in extracellular matrix stability and cell migration (Lee et al., 1993). TNFAIP6 is known to interact with a variety of matrix associated molecules, such as versican, aggrecan, and fibronectin (Kuznetsova et al., 2008). Even though it was demonstrated in migration assay that YKL-39 showed a chemotactic effect after a short time, the up-regulation of TNFAIP6 could still improve the adhesion abilities of monocytes to other cell types, and indirectly promote the migratory ability of monocytes.

HSD11B1, known as enzyme 11β-hydroxysteroid dehydrogenase type 1, plays an essential role in acute and chronic inflammation (Chapman et al., 2013). There is no HSD11B1 expression in human monocytes, but it is induced during the differentiation process of monocytes toward resting or naive macrophages (Thieringer et al., 2001). The polarization of naive macrophages to M1 phenotype will further induce the expression of HSD11B1, whereas polarization to M2 phenotype has no effect (Chapman et al., 2013). The reason behind this is still unknown, but might be associated with the different energy metabolism between M1 and M2 macrophages (Rodríguez-Prados et al., 2010). It was demonstrated in this study that the expression of HSD11B1 is up-regulated in monocytes in response to YKL-39, that can be produced by IL-4+TGF-beta stimulate macrophages, and can be considered as an M2 marker. It can be hypothesized that YKL-39 stimulates very early step of monocytes to naive macrophage differentiation, and expression analysis of HSD11B1 in subtypes of

tumor-associated macrophages has to be performed in future. Additionally, recent studies revealed that glucose metabolism can directly alter the macrophages polarization (Haschemi et al., 2012). The influences of HSD11B1 expression on macrophage glucose metabolism was reported in several studies. Through the coupling of HSD11B1 oxo-reductase activity to hexose 6-phosphate activity in the endoplasmic reticulum, HSD11B1 may directly affect polarization or the extent of activation of macrophages (Haschemi et al., 2012). The dynamic regulation of HSD11B1 in macrophages can be essential to regulate the ongoing inflammatory response, through indirect diversion of glucose-6-phosphate.

CRM1 (chromosomal maintenance 1) is known for the ability to promote HMGB1 expression (Tang et al., 2007). Immune cells such as monocytes, macrophages, and dendritic cells secrete HMGB1, which acts as a cytokine mediator of inflammation (Bonaldi et al., 2003; Xu et al., 2016). Therefore, the induction effect of YKL-39 on CRM1 expression in monocytes can also contribute to the up-regulation of HMGB1, which may affect the inflammatory process in the tumor microenvironment.

YKL-39 slightly up-regulates other genes expression such as SGPP2, CD274, and CD82, which are associated with various biological processes. SGPP2 (Sphingosine-1-Phosphate Phosphatase 2) is induced during inflammatory responses and contributes to the metabolism of sphingolipids (Kunkel et al., 2013; Mechtcheriakova et al., 2007). CD274 is also known as programmed death-ligand 1 (PD-L1), interacting with its receptor to inhibit T-cells activation and cytokine production, which contributes to immune escape of tumor cells through the cytotoxic T-cell inactivation in tumor microenvironment (Huang et al., 2017; Topalian et al., 2015). CD82 is used as a differentiation marker of monocytes into macrophages (Lebel-Binay et al., 1995; Yang et al., 2016). The regulatory effects of YKL-39 on these genes suggest its role in sphingolipids metabolism, T-cell activation, and macrophages differentiation.

4.3.3 Effect of YKL-39 on angiogenesis

Tumor angiogenesis is a crucial process for supplying rapidly growing tumors with essential nutrients and oxygen (Riabov et al., 2014). Monocytes recruited to the tumor site and programmed by tumor cells are known as TAMs, which is the primary source of pro-angiogenic factors (Nishida et al., 2006; Riabov et al., 2014). TAMs produce a variety of pro-angiogenic factors under the hypoxic condition in tumor site, for example, VEGF, which promotes migration of endothelial cells and macrophages towards tumor areas (Casazza et al., 2014; Corliss et al., 2016; Wang et al., 2011).

Chitinase-like protein YKL-40 has already been shown to be involved in tumor angiogenesis in several studies. It was reported that gp38k (porcine homolog protein of YKL-40) promotes the migration and spreading of vascular smooth muscle cells *in vitro* (Nishikawa and Millis, 2003). The expression of YKL-40 in MDA-MB-231 breast cancer cells and HCT-116 colon cancer cells is also associated with tumor formation in an extensive angiogenic phenotype mice model (Shao et al., 2009). Recombinant YKL-40 protein was also found to induce angiogenesis of vascular endothelial cell *in vitro* (Shao, 2014). A correlation of blood vessel density and YKL-40 expression has also been observed in human breast cancer patients (Shao et al., 2011). Therefore, it was considered that YKL-40 acts as a pro-angiogenic factor in cancer.

YKL-39 has a high structural similarity to YKL-40. To analyze whether YKL-39 exerts the same angiogenesis effect through direct activation of vascular endothelial cells, tube formation assay using HUVEC cells was performed. It was confirmed that 100 ng/ml and 1 µg/ml of recombinant YKL-39 protein significantly induced tube formation in HUVEC cells *in vitro*. This data supports the hypothesis that YKL-39 can directly induce angiogenesis, and that YKL-39 expressing TAMs can serve as a source of angiogenic factors in the tumor microenvironment.

4.3.4 Effect of YKL-39 on tumor cells

The role of YKL-40 in tumor cell proliferation was described in several studies. Induced colony formation was observed in YKL-40 overexpressed U373-MG cells *in vitro*, while the deletion of YKL-40 in U87-MG cells inhibited the colony forming ability (Ku et al., 2011). However, another chitinase-like protein SI-CLP had not effect on the proliferation of murine breast adenocarcinoma cells TS/A (Wang, 2012). In our laboratory, the expression of YKL-39 was found in TAMs in the primary tumor of breast cancer patients (unpublished data), which suggest that YKL-39 may also affect the biological function of tumor cells. The results of this study have shown that YKL-39 has no effect on the proliferation and apoptosis in MCF-7 cells.

In summary, the biological activities of YKL-39 have been identified in this study: chemotactic activity towards monocytes and pro-angiogenic effect. Considering that YKL-39 is induced by TGF-beta, a multifunctional regulator of the tumor microenvironment, we can hypothesize that YKL-39 can be expressed by tumor-associated macrophages and can contribute to the programming of tumor microenvironment and tumor progression. Since YKL-39 is absent in rodents and present only in humans, analysis of the correlation of

YKL-39 levels with clinical parameters of tumor progression is a promising approach to identify the role of YKL-39 in cancer.

5. Summary

YKL-39 contains a Glyco_18 domain and belongs to the family of mammalian chitinase-like proteins. Macrophages are the primary source of several chitinase-like proteins in cancer and chronic inflammatory conditions. Chitinase-like proteins YKL-40 and YM1/2 combine properties of growth factors and chemotactic factors for immune cells. Moreover, YKL-40 was demonstrated to be a potent pro-angiogenic factor in tumors. However, the role of YKL-39 in immune cell recruitment and angiogenesis has not been studied to date. The aims of the thesis project included the analysis of the regulation of YKL-39 production in primary human macrophages, investigation of the intracellular sorting mechanism of YKL-39, and the identification of YKL-39 biological effects related to the tumor progression. Using RT-qPCR and immunofluorescence/confocal microscopy it was shown that YKL-39 gene expression and protein production are strongly up-regulated by multifunctional cytokine TGF-beta in combination with IL-4, but not by IL-4 alone. Confocal microscopy analysis demonstrated that endogenous YKL-39 is sorted into the lysosomal secretory pathway in primary human macrophages. Using *in vitro* pull-down assays and HEK293-cell based model system, it was shown that stabilin-1 directly interacts with YKL-39 via fasciclin domain 7 and mediates its intracellular sorting. Furthermore, YKL-39 was demonstrated to be secreted by human macrophages under IL-4+TGF-beta stimulation in long-term culture condition. YKL-39 affected neither proliferation nor apoptosis of tumor cells. However, analysis of the biological activity of YKL-39 revealed that it has a strong inducing effect on the recruitment of primary human monocytes and on the tube formation by HUVEC cells *in vitro*. Affymetrix microarray analysis, validated by RT-qPCR, demonstrated that YKL-39 has only minor effect on the transcriptional program in primary human monocytes by slight induction of genes related to the regulation of migration and inflammation, suggesting that chemotactic effect of YKL-39 on monocytes is not mediated by their transcriptional activation. In summary, it was demonstrated that master cytokine of tumor microenvironment TGF-beta is a key factor inducing YKL-39 production in macrophages. The biological activity of YKL-39 is related to the two essential processes in tumor microenvironment: monocytes recruitment and angiogenesis. In perspective, analysis of the expression of YKL-39 in tumor-associated macrophages and analysis of the correlation of YKL-39 with tumor growth and metastasis has to be performed to consider YKL-39 as a potential target for therapy.

6. References

Aggarwal, N., and Sloane, B.F. (2014). Cathepsin B: multiple roles in cancer. PROTEOMICS-Clinical Applications 8, 427-437.

Alberts, B., Johnson, A., Lewis, J., Raff, M., Roberts, K., and Walter, P. (2002). Transport from the Trans Golgi Network to the Cell Exterior: Exocytosis.

Areshkov, P.A., and Kavsan, V.M. (2010). Chitinase 3-like protein 2 (CHI3L2, YKL-39) activates phosphorylation of extracellular signal-regulated kinases ERK1/ERK2 in human embryonic kidney (HEK293) and human glioblastoma (U87 MG) cells. Cytology and genetics 44, 1-6.

Areshkov, P.O., Avdieiev, S.S., Balynska, O.V., LeRoith, D., and Kavsan, V.M. (2012). Two closely related human members of chitinase-like family, CHI3L1 and CHI3L2, activate ERK1/2 in 293 and U373 cells but have the different influence on cell proliferation. Int J Biol Sci 8, 39-48.

Babst, M. (2004). GGAing ubiquitin to the endosome. Nature cell biology 6, 175-177.

Bain, C.C., and Mowat, A.M. (2012). CD200 receptor and macrophage function in the intestine. Immunobiology 217, 643-651.

Bakırcı, E.M., Ünver, E., Değirmenci, H., Kıvanç, T., Günay, M., Hamur, H., Büyüklü, M., Ceyhun, G., Topal, E., and Çoban, T. (2015). Serum YKL-40/chitinase 3-like protein 1 level is an independent predictor of atherosclerosis development in patients with obstructive sleep apnea syndrome. Turk Kardiyol Dern Ars 43, 333-339.

Baldacci, F., Lista, S., Cavedo, E., Bonuccelli, U., and Hampel, H. (2017a). Diagnostic function of the neuroinflammatory biomarker YKL-40 in Alzheimer's disease and other neurodegenerative diseases. Expert Review of Proteomics 14, 285-299.

Baldacci, F., Toschi, N., Lista, S., Zetterberg, H., Blennow, K., Kilimann, I., Teipel, S., Cavedo, E., Dos Santos, A.M., and Epelbaum, S. (2017b). Two-level diagnostic classification using cerebrospinal fluid YKL-40 in Alzheimer's disease. Alzheimer's & Dementia.

Baran, A., Myśliwiec, H., Szterling-Jaworowska, M., Kiluk, P., Świderska, M., and Flisiak, I. (2017). Serum YKL-40 as a potential biomarker of inflammation in psoriasis. Journal of Dermatological Treatment, 1-21.

Bengsch, F., Buck, A., Günther, S., Seiz, J., Tacke, M., Pfeifer, D., Von Elverfeldt, D., Sevenich, L., Hillebrand, L., and Kern, U. (2014). Cell type-dependent pathogenic functions of overexpressed human cathepsin B in murine breast cancer progression. Oncogene 33, 4474-4484.

Bigg, H.F., Wait, R., Rowan, A.D., and Cawston, T.E. (2006). The mammalian chitinase-like lectin, YKL-40, binds specifically to type I collagen and modulates the rate of type I collagen fibril formation. Journal of Biological Chemistry 281, 21082-21095.

Bingle, L., Brown, N., and Lewis, C. (2002). The role of tumour□associated macrophages in tumour progression: implications for new anticancer therapies. The Journal of pathology 196, 254-265.

Blott, E.J., and Griffiths, G.M. (2002). Secretory lysosomes. Nature reviews Molecular cell biology 3, 122-131.

Bonaldi, T., Talamo, F., Scaffidi, P., Ferrera, D., Porto, A., Bachi, A., Rubartelli, A., Agresti, A., and Bianchi, M.E. (2003). Monocytic cells hyperacetylate chromatin protein HMGB1 to redirect it towards secretion. The EMBO journal 22, 5551-5560.

Boot, R.G., Blommaart, E.F., Swart, E., Ghauharali-van der Vlugt, K., Bijl, N., Moe, C., Place, A., and Aerts, J.M. (2001). Identification of a novel acidic mammalian chitinase distinct from chitotriosidase. Journal of Biological Chemistry 276, 6770-6778.

Boot, R.G., van Achterberg, T.A., van Aken, B.E., Renkema, G.H., Jacobs, M.J., Aerts, J.M., and de Vries, C.J. (1999). Strong induction of members of the chitinase family of proteins in atherosclerosis. Arteriosclerosis, thrombosis, and vascular biology 19, 687-694.

Braulke, T., and Bonifacino, J.S. (2009). Sorting of lysosomal proteins. Biochimica et Biophysica Acta (BBA)-Molecular Cell Research 1793, 605-614.

Cantelli, G., Crosas-Molist, E., Georgouli, M., and Sanz-Moreno, V. (2017). TGFB-induced transcription in cancer. Paper presented at: Seminars in Cancer Biology (Elsevier).

Casazza, A., Di Conza, G., Wenes, M., Finisguerra, V., Deschoemaeker, S., and Mazzone, M. (2014). Tumor stroma: a complexity dictated by the hypoxic tumor microenvironment. Oncogene 33, 1743-1754.

Chang, N.-C.A., Hung, S.-I., Hwa, K.-Y., Kato, I., Chen, J.-E., Liu, C.-H., and Chang, A.C. (2001). A macrophage protein, Ym1, transiently expressed during inflammation is a novel mammalian lectin. Journal of Biological Chemistry 276, 17497-17506.

Chapman, K.E., Coutinho, A.E., Zhang, Z., Kipari, T., Savill, J.S., and Seckl, J.R. (2013). Changing glucocorticoid action: 11β-hydroxysteroid dehydrogenase type 1 in acute and chronic inflammation. The Journal of steroid biochemistry and molecular biology 137, 82-92.

Cintin, C., Johansen, J., Christensen, I.J., Price, P., Sørensen, S., and Nielsen, H.J. (1999). Serum YKL-40 and colorectal cancer. British journal of cancer 79, 1494.

Colton, C.A., Mott, R.T., Sharpe, H., Xu, Q., Van Nostrand, W.E., and Vitek, M.P. (2006). Expression profiles for macrophage alternative activation genes in AD and in mouse models of AD. Journal of neuroinflammation 3, 1.

Comabella, M., Fernández, M., Martin, R., Rivera-Vallvé, S., Borrás, E., Chiva, C., Julià, E., Rovira, A., Cantó, E., and Alvarez-Cermeño, J.C. (2010). Cerebrospinal fluid chitinase 3-like 1 levels are associated with conversion to multiple sclerosis. Brain 133, 1082-1093.

Conrozier, T., Carlier, M., Mathieu, P., Colson, F., Debard, A., Richard, S., Favret, H., Bienvenu, J., and Vignon, E. (2000). Serum levels of YKL-40 and C reactive protein in patients with hip osteoarthritis and healthy subjects: a cross sectional study. Annals of the rheumatic diseases 59, 828-831.

Corliss, B.A., Azimi, M.S., Munson, J.M., Peirce, S.M., and Murfee, W.L. (2016). Macrophages: an inflammatory link between angiogenesis and lymphangiogenesis. Microcirculation 23, 95-121.

Cox, T. (2001). Gaucher disease: understanding the molecular pathogenesis of sphingolipidoses. Journal of inherited metabolic disease 24, 107-123.

Craig-Schapiro, R., Perrin, R.J., Roe, C.M., Xiong, C., Carter, D., Cairns, N.J., Mintun, M.A., Peskind, E.R., Li, G., and Galasko, D.R. (2010). YKL-40: a novel prognostic fluid biomarker for preclinical Alzheimer's disease. Biological psychiatry 68, 903-912.

David, C., Nance, J.P., Hubbard, J., Hsu, M., Binder, D., and Wilson, E.H. (2012). Stabilin-1 expression in tumor associated macrophages. Brain research 1481, 71-78.

Dehne, N., Mora, J., Namgaladze, D., Weigert, A., and Brüne, B. (2017). Cancer cell and macrophage cross-talk in the tumor microenvironment. Current Opinion in Pharmacology 35, 12-19.

Derynck, R., Akhurst, R.J., and Balmain, A. (2001). TGF-β signaling in tumor suppression and cancer progression. Nature genetics 29, 117-129.

Deshmane, S.L., Kremlev, S., Amini, S., and Sawaya, B.E. (2009). Monocyte chemoattractant protein-1 (MCP-1): an overview. Journal of interferon & cytokine research 29, 313-326.

Di Rosa, M., Distefano, G., Zorena, K., and Malaguarnera, L. (2016). Chitinases and immunity: ancestral molecules with new functions. Immunobiology 221, 399-411.

Di Rosa, M., Malaguarnera, G., De Gregorio, C., Drago, F., and Malaguarnera, L. (2013). Evaluation of CHI3L-1 and CHIT-1 expression in differentiated and polarized macrophages. Inflammation 36, 482-492.

Donnelly, L.E., and Barnes, P.J. (2004). Acidic mammalian chitinase–a potential target for asthma therapy. Trends in pharmacological sciences 25, 509-511.

Duque, G.A., and Descoteaux, A. (2015). Macrophage cytokines: involvement in immunity and infectious diseases. Secretion of Cytokines and Chemokines by Innate Immune Cells, 6.

Elias, J.A., Homer, R.J., Hamid, Q., and Lee, C.G. (2005). Chitinases and chitinase-like proteins in T H 2 inflammation and asthma. Journal of Allergy and Clinical Immunology 116, 497-500.

Epelman, S., Lavine, K.J., Beaudin, A.E., Sojka, D.K., Carrero, J.A., Calderon, B., Brija, T., Gautier, E.L., Ivanov, S., and Satpathy, A.T. (2014a). Embryonic and adult-derived resident cardiac macrophages are maintained through distinct mechanisms at steady state and during inflammation. Immunity 40, 91-104.

Epelman, S., Lavine, K.J., and Randolph, G.J. (2014b). Origin and functions of tissue macrophages. Immunity 41, 21-35.

Faibish, M., Francescone, R., Bentley, B., Yan, W., and Shao, R. (2011). A YKL-40–neutralizing antibody blocks tumor angiogenesis and progression: a potential therapeutic agent in cancers. Molecular cancer therapeutics 10, 742-751.

Francescone, R.A., Scully, S., Faibish, M., Taylor, S.L., Oh, D., Moral, L., Yan, W., Bentley, B., and Shao, R. (2011). Role of YKL-40 in the angiogenesis, radioresistance, and progression of glioblastoma. Journal of Biological Chemistry 286, 15332-15343.

Fusetti, F., Pijning, T., Kalk, K.H., Bos, E., and Dijkstra, B.W. (2003). Crystal structure and carbohydrate-binding properties of the human cartilage glycoprotein-39. Journal of Biological Chemistry 278, 37753-37760.

Ghosh, P., Dahms, N.M., and Kornfeld, S. (2003a). Mannose 6-phosphate receptors: new twists in the tale. Nature reviews Molecular cell biology 4, 202-213.

Ghosh, P., Griffith, J., Geuze, H.J., and Kornfeld, S. (2003b). Mammalian GGAs act together to sort mannose 6-phosphate receptors. The Journal of cell biology 163, 755-766.

Ginhoux, F., Greter, M., Leboeuf, M., Nandi, S., See, P., Gokhan, S., Mehler, M.F., Conway, S.J., Ng, L.G., and Stanley, E.R. (2010). Fate mapping analysis reveals that adult microglia derive from primitive macrophages. Science 330, 841-845.

Ginhoux, F., and Jung, S. (2014). Monocytes and macrophages: developmental pathways and tissue homeostasis. Nature Reviews Immunology 14, 392-404.

Ginhoux, F., Schultze, J.L., Murray, P.J., Ochando, J., and Biswas, S.K. (2016). New insights into the multidimensional concept of macrophage ontogeny, activation and function. Nature immunology 17, 34-40.

Gisterå, A., and Hansson, G.K. (2017). The immunology of atherosclerosis. Nature Reviews Nephrology 13, 368-380.

Goerdt, S., Bhardwaj, R., and Sorg, C. (1993). Inducible expression of MS-1 high-molecular-weight protein by endothelial cells of continuous origin and by dendritic cells/macrophages in vivo and in vitro. The American journal of pathology 142, 1409.

Goerdt, S., Walsh, L.J., Murphy, G.F., and Pober, J.S. (1991). Identification of a novel high molecular weight protein preferentially expressed by sinusoidal endothelial cells in normal human tissues. J Cell Biol 113, 1425-1437.

Gordon, S. (2003). Alternative activation of macrophages. Nature Reviews Immunology 3, 23-35.

Goswami, K.K., Ghosh, T., Ghosh, S., Sarkar, M., Bose, A., and Baral, R. (2017). Tumor promoting role of anti-tumor macrophages in tumor microenvironment. Cellular Immunology.

Gratchev, A., Kzhyshkowska, J., Duperrier, K., Utikal, J., Velten, F., and Goerdt, S. (2004). The Receptor for Interleukin□17E is Induced by Th2 Cytokines in Antigen□Presenting Cells. Scandinavian journal of immunology 60, 233-237.

Gratchev, A., Kzhyshkowska, J., Kannookadan, S., Ochsenreiter, M., Popova, A., Yu, X., Mamidi, S., Stonehouse-Usselmann, E., Muller-Molinet, I., and Gooi, L. (2008a). Activation of a TGF-β-specific multistep gene expression program in mature macrophages requires glucocorticoid-mediated surface expression of TGF-β receptor II. The Journal of Immunology 180, 6553-6565.

Gratchev, A., Kzhyshkowska, J., Köthe, K., Muller-Molinet, I., Kannookadan, S., Utikal, J., and Goerdt, S. (2006). Mφ1 and Mφ2 can be re-polarized by Th2 or Th1 cytokines, respectively, and respond to exogenous danger signals. Immunobiology 211, 473-486.

Gratchev, A., Schmuttermaier, C., Mamidi, S., Gooi, L., Goerdt, S., and Kzhyshkowska, J. (2008b). Expression of osteoarthritis marker YKL-39 is stimulated by transforming growth factor beta (TGF-beta) and IL-4 in differentiating macrophages. Biomarker insights 3.

Guo, Y., Sirkis, D.W., and Schekman, R. (2014). Protein sorting at the trans-Golgi network. Annual review of cell and developmental biology 30, 169-206.

Hasanagic, M., Waheed, A., and Eissenberg, J.C. (2015). Chapter Three-Different Pathways to the Lysosome: Sorting out Alternatives. International review of cell and molecular biology 320, 75-101.

Haschemi, A., Kosma, P., Gille, L., Evans, C.R., Burant, C.F., Starkl, P., Knapp, B., Haas, R., Schmid, J.A., and Jandl, C. (2012). The sedoheptulose kinase CARKL directs macrophage polarization through control of glucose metabolism. Cell metabolism 15, 813-826.

Hashimoto, D., Chow, A., Noizat, C., Teo, P., Beasley, M.B., Leboeuf, M., Becker, C.D., See, P., Price, J., and Lucas, D. (2013). Tissue-resident macrophages self-maintain locally throughout adult life with minimal contribution from circulating monocytes. Immunity 38, 792-804.

Hinsinger, G., Galéotti, N., Nabholz, N., Urbach, S., Rigau, V., Demattei, C., Lehmann, S., Camu, W., Labauge, P., and Castelnovo, G. (2015). Chitinase 3-like proteins as diagnostic and prognostic biomarkers of multiple sclerosis. Multiple Sclerosis Journal 21, 1251-1261.

Hoeffel, G., Wang, Y., Greter, M., See, P., Teo, P., Malleret, B., Leboeuf, M., Low, D., Oller, G., and Almeida, F. (2012). Adult Langerhans cells derive predominantly from embryonic fetal liver monocytes with a minor contribution of yolk sac–derived macrophages. Journal of Experimental Medicine, jem. 20120340.

Høgdall, E.V., Ringsholt, M., Høgdall, C.K., Christensen, I.J., Johansen, J.S., Kjaer, S.K., Blaakaer, J., Ostenfeld-Møller, L., Price, P.A., and Christensen, L.H. (2009). YKL-40 tissue expression and plasma levels in patients with ovarian cancer. BMC cancer 9, 8.

HogenEsch, H., Dunham, A., Seymour, R., Renninger, M., and Sundberg, J.P. (2006). Expression of chitinase□like proteins in the skin of chronic proliferative dermatitis (cpdm/cpdm) mice. Experimental dermatology 15, 808-814.

Holtzman, E. (2013). Lysosomes (Springer Science & Business Media).

Hormigo, A., Gu, B., Karimi, S., Riedel, E., Panageas, K.S., Edgar, M.A., Tanwar, M.K., Rao, J.S., Fleisher, M., and DeAngelis, L.M. (2006). YKL-40 and matrix metalloproteinase-9 as potential serum biomarkers for patients with high-grade gliomas. Clinical Cancer Research 12, 5698-5704.

Hu, B., Trinh, K., Figueira, W.F., and Price, P.A. (1996). Isolation and sequence of a novel human chondrocyte protein related to mammalian members of the chitinase protein family. Journal of Biological Chemistry 271, 19415-19420.

Huang, B., Zhang, H., Gu, L., Ye, B., Jian, Z., Stary, C., and Xiong, X. (2017). Advances in Immunotherapy for Glioblastoma Multiforme. Journal of Immunology Research 2017.

Iwamoto, F.M., Hottinger, A.F., Karimi, S., Riedel, E., Dantis, J., Jahdi, M., Panageas, K.S., Lassman, A.B., Abrey, L.E., and Fleisher, M. (2011). Serum YKL-40 is a marker of prognosis and disease status in high-grade gliomas. Neuro-oncology 13, 1244-1251.

Jin, H., Copeland, N., Gilbert, D., Jenkins, N., Kirkpatrick, R., and Rosenberg, M. (1998). Genetic characterization of the murine Ym1 gene and identification of a cluster of highly homologous genes. Genomics 54, 316-322.

Johansen, J.S., Brasso, K., Iversen, P., Teisner, B., Garnero, P., Price, P.A., and Christensen, I.J. (2007). Changes of biochemical markers of bone turnover and YKL-40 following hormonal treatment for metastatic prostate cancer are related to survival. Clinical Cancer Research 13, 3244-3249.

Johansen, J.S., Milman, N., Hansen, M., Garbarsch, C., Price, P.A., and Graudal, N. (2005). Increased serum YKL-40 in patients with pulmonary sarcoidosis—a potential marker of disease activity? Respiratory medicine 99, 396-402.

Junker, N., Johansen, J.S., Andersen, C.B., and Kristjansen, P.E. (2005). Expression of YKL-40 by peritumoral macrophages in human small cell lung cancer. Lung Cancer 48, 223-231.

Katsuno, Y., Lamouille, S., and Derynck, R. (2013). TGF-β signaling and epithelial–mesenchymal transition in cancer progression. Current opinion in oncology 25, 76-84.

Kavsan, V., Dmitrenko, V., Boyko, O., Filonenko, V., Avdeev, S., Areshkov, P., Marusyk, A., Malisheva, T., Rozumenko, V., and Zozulya, Y. (2008). Overexpression of YKL-39 gene in glial brain tumors. Scholarly Research Exchange.

Kavsan, V., Shostak, K., Dmitrenko, V., Zozulya, Y., Rozumenko, V., and Demotes-Mainard, J. (2004). Characterization of genes with increased expression in human glioblastomas. TSitologiia i genetika 39, 37-49.

Kawada, M., Chen, C.-C., Arihiro, A., Nagatani, K., Watanabe, T., and Mizoguchi, E. (2008). Chitinase 3-like-1 enhances bacterial adhesion to colonic epithelial cells through the interaction with bacterial chitin-binding protein. Laboratory investigation 88, 883-895.

Kawada, M., Seno, H., Kanda, K., Nakanishi, Y., Akitake, R., Komekado, H., Kawada, K., Sakai, Y., Mizoguchi, E., and Chiba, T. (2012). Chitinase 3-like 1 promotes macrophage recruitment and angiogenesis in colorectal cancer. Oncogene 31, 3111-3123.

Keliher, E.J., Reiner, T., Earley, S., Klubnick, J., Tassa, C., Lee, A.J., Ramaswamy, S., Bardeesy, N., Hanahan, D., and DePinho, R.A. (2013). Targeting cathepsin E in pancreatic cancer by a small molecule allows in vivo detection. Neoplasia 15, 684IN681-693IN683.

Kienzle, C., and von Blume, J. (2014). Secretory cargo sorting at the trans-Golgi network. Trends in cell biology 24, 584-593.

Kim, K., Ahn, Y., Kim, D., Kim, H.-S., and Kim, D. (2017). Elevated serum YKL-40 levels in patients with Kawasaki disease. Biomarkers 22, 326-330.

Knorr, T., Obermayr, F., Bartnik, E., Zien, A., and Aigner, T. (2003). YKL-39 (chitinase 3-like protein 2), but not YKL-40 (chitinase 3-like protein 1), is up regulated in osteoarthritic chondrocytes. Annals of the rheumatic diseases 62, 995-998.

Krikorian, A., Patel, R., Rodriguez, A., Yasmeen, T., and Drever, E.D. (2015). Cathepsins are a diverse group of proteases that are increasingly being recognized for their role in various disease states. The focus of this article is to review the data regarding the activity of cathepsin K and cathepsin S in adipocyte differentiation and function as well as glucose metabolism. Data from animal and human studies have shown up-regulation of cathepsin K expression in white adipose. Clinical Reviews in Bone and Mineral Metabolism 13, 36-42.

Ku, B.M., Lee, Y.K., Ryu, J., Jeong, J.Y., Choi, J., Eun, K.M., Shin, H.Y., Kim, D.G., Hwang, E.M., and Park, J.Y. (2011). CHI3L1 (YKL□40) is expressed in human gliomas and regulates the invasion, growth and survival of glioma cells. International journal of cancer 128, 1316-1326.

Kumagai, E., Mano, Y., Yoshio, S., Shoji, H., Sugiyama, M., Korenaga, M., Ishida, T., Arai, T., Itokawa, N., and Atsukawa, M. (2016). Serum YKL-40 as a marker of liver fibrosis in patients with non-alcoholic fatty liver disease. Scientific reports 6.

Kunkel, G.T., Maceyka, M., Milstien, S., and Spiegel, S. (2013). Targeting the sphingosine-1-phosphate axis in cancer, inflammation and beyond. Nature Reviews Drug Discovery 12, 688-702.

Kunz, L., van't Wout, E., van Schadewijk, A., Postma, D., Kerstjens, H., Sterk, P., and Hiemstra, P. (2015). Regulation of YKL-40 expression by corticosteroids: effect on pro-inflammatory macrophages in vitro and its modulation in COPD in vivo. Respiratory research 16, 154.

Kurz, T., Terman, A., Gustafsson, B., and Brunk, U.T. (2008). Lysosomes in iron metabolism, ageing and apoptosis. Histochemistry and cell biology 129, 389-406.

Kuznetsova, S.A., Mahoney, D.J., Martin-Manso, G., Ali, T., Nentwich, H.A., Sipes, J.M., Zeng, B., Vogel, T., Day, A.J., and Roberts, D.D. (2008). TSG-6 binds via its CUB_C domain to the cell-binding domain of fibronectin and increases fibronectin matrix assembly. Matrix Biology 27, 201-210.

Kzhyshkowska, J. (2010). Multifunctional receptor stabilin-1 in homeostasis and disease. The Scientific World Journal 10, 2039-2053.

Kzhyshkowska, J., Gratchev, A., and Goerdt, S. (2006a). Stabilin□1, a homeostatic scavenger receptor with multiple functions. Journal of cellular and molecular medicine 10, 635-649.

Kzhyshkowska, J., Gratchev, A., and Goerdt, S. (2007). Human chitinases and chitinase-like proteins as indicators for inflammation and cancer. Biomarker insights 2, 128.

Kzhyshkowska, J., Gratchev, A., Martens, J.-H., Pervushina, O., Mamidi, S., Johansson, S., Schledzewski, K., Hansen, B., He, X., and Tang, J. (2004). Stabilin-1 localizes to endosomes and the trans-Golgi network in human macrophages and interacts with GGA adaptors. Journal of leukocyte biology 76, 1151-1161.

Kzhyshkowska, J., Gratchev, A., Schmuttermaier, C., Brundiers, H., Krusell, L., Mamidi, S., Zhang, J., Workman, G., Sage, E.H., and Anderle, C. (2008). Alternatively activated macrophages regulate extracellular levels of the hormone placental lactogen via receptor-mediated uptake and transcytosis. The Journal of Immunology 180, 3028-3037.

Kzhyshkowska, J., Gudima, A., Moganti, K., Gratchev, A., and Orekhov, A. (2016a). Perspectives for Monocyte/Macrophage-Based Diagnostics of Chronic Inflammation. Transfusion Medicine and Hemotherapy 43, 66-77.

Kzhyshkowska, J., and Krusell, L. (2009). Cross-talk between endocytic clearance and secretion in macrophages. Immunobiology 214, 576-593.

Kzhyshkowska, J., Mamidi, S., Gratchev, A., Kremmer, E., Schmuttermaier, C., Krusell, L., Haus, G., Utikal, J., Schledzewski, K., and Scholtze, J. (2006b). Novel stabilin-1 interacting chitinase-like protein (SI-CLP) is up-regulated in alternatively activated macrophages and secreted via lysosomal pathway. Blood 107, 3221-3228.

Kzhyshkowska, J., Neyen, C., and Gordon, S. (2012). Role of macrophage scavenger receptors in atherosclerosis. Immunobiology 217, 492-502.

Kzhyshkowska, J., Workman, G., Cardó-Vila, M., Arap, W., Pasqualini, R., Gratchev, A., Krusell, L., Goerdt, S., and Sage, E.H. (2006c). Novel function of alternatively activated macrophages: stabilin-1-mediated clearance of SPARC. The Journal of Immunology 176, 5825-5832.

Kzhyshkowska, J., Yin, S., Liu, T., Riabov, V., and Mitrofanova, I. (2016b). Role of chitinase-like proteins in cancer. Biological chemistry 397, 231-247.

Lebel-Binay, S., Lagaudriere, C., Fradelizi, D., and Conjeaud, H. (1995). CD82, tetra-span-transmembrane protein, is a regulated transducing molecule on U937 monocytic cell line. Journal of leukocyte biology 57, 956-963.

Lee, C.G., Da Silva, C.A., Dela Cruz, C.S., Ahangari, F., Ma, B., Kang, M.-J., He, C.-H., Takyar, S., and Elias, J.A. (2011). Role of chitin and chitinase/chitinase-like proteins in inflammation, tissue remodeling, and injury. Annual review of physiology 73, 479-501.

Lee, T.H., Klampfer, L., Shows, T., and Vilcek, J. (1993). Transcriptional regulation of TSG6, a tumor necrosis factor-and interleukin-1-inducible primary response gene coding for a secreted hyaluronan-binding protein. Journal of Biological Chemistry 268, 6154-6160.

Létuvé, S., Kozhich, A., Arouche, N., Grandsaigne, M., Reed, J., Dombret, M.-C., Kiener, P.A., Aubier, M., Coyle, A.J., and Pretolani, M. (2008). YKL-40 is elevated in patients with chronic obstructive pulmonary disease and activates alveolar macrophages. The Journal of Immunology 181, 5167-5173.

Libreros, S., Garcia-Areas, R., Keating, P., Carrio, R., and Iragavarapu-Charyulu, V.L. (2013). Exploring the role of CHI3L1 in "pre-metastatic" lungs of mammary tumor-bearing mice.

Libreros, S., and Iragavarapu-Charyulu, V. (2015). YKL-40/CHI3L1 drives inflammation on the road of tumor progression. Journal of leukocyte biology 98, 931-936.

Liu, J., Sukhova, G.K., Sun, J.-S., Xu, W.-H., Libby, P., and Shi, G.-P. (2004). Lysosomal cysteine proteases in atherosclerosis. Arteriosclerosis, thrombosis, and vascular biology 24, 1359-1366.

Loeffler, I., and Wolf, G. (2014). Transforming growth factor-β and the progression of renal disease. Nephrology Dialysis Transplantation 29, i37-i45.

Low, D., Subramaniam, R., Lin, L., Aomatsu, T., Mizoguchi, A., Ng, A., DeGruttola, A.K., Lee, C.G., Elias, J.A., and Andoh, A. (2015). Chitinase 3-like 1 induces survival and proliferation of intestinal epithelial cells during chronic inflammation and colitis-associated cancer by regulating S100A9. Oncotarget 6, 36535.

Luzio, J.P., Hackmann, Y., Dieckmann, N.M., and Griffiths, G.M. (2014). The biogenesis of lysosomes and lysosome-related organelles. Cold Spring Harbor perspectives in biology 6, a016840.

Ma, B., Herzog, E.L., Lee, C.G., Peng, X., Lee, C.-M., Chen, X., Rockwell, S., Koo, J.S., Kluger, H., and Herbst, R.S. (2015). Role of Chitinase 3–like-1 and Semaphorin 7a in Pulmonary Melanoma Metastasis. Cancer research 75, 487-496.

Mantovani, A., Biswas, S.K., Galdiero, M.R., Sica, A., and Locati, M. (2013). Macrophage plasticity and polarization in tissue repair and remodelling. The Journal of pathology 229, 176-185.

Mantovani, A., Sica, A., Sozzani, S., Allavena, P., Vecchi, A., and Locati, M. (2004). The chemokine system in diverse forms of macrophage activation and polarization. Trends in immunology 25, 677-686.

Martinez, F.O., and Gordon, S. (2014). The M1 and M2 paradigm of macrophage activation: time for reassessment. F1000Prime Rep 6, 12703.

Mechtcheriakova, D., Wlachos, A., Sobanov, J., Kopp, T., Reuschel, R., Bornancin, F., Cai, R., Zemann, B., Urtz, N., and Stingl, G. (2007). Sphingosine 1-phosphate phosphatase 2 is induced during inflammatory responses. Cellular signalling 19, 748-760.

Meng, G., Zhao, Y., Bai, X., Liu, Y., Green, T.J., Luo, M., and Zheng, X. (2010). Structure of human stabilin-1 interacting chitinase-like protein (SI-CLP) reveals a saccharide-binding cleft with lower sugar-binding selectivity. Journal of Biological Chemistry 285, 39898-39904.

Michelsen, A.E., Rathcke, C.N., Skjelland, M., Holm, S., Ranheim, T., Krohg-Sørensen, K., Klingvall, M.F., Brosstad, F., Øie, E., and Vestergaard, H. (2010). Increased YKL-40 expression in patients with carotid atherosclerosis. Atherosclerosis 211, 589-595.

Mills, C.D., Lenz, L.L., and Harris, R.A. (2016). A breakthrough: macrophage-directed cancer immunotherapy. Cancer research 76, 513-516.

Miyatake, K., Tsuji, K., Yamaga, M., Yamada, J., Matsukura, Y., Abula, K., Sekiya, I., and Muneta, T. (2013). Human YKL39 (chitinase 3-like protein 2), an osteoarthritis-associated gene, enhances proliferation and type II collagen expression in ATDC5 cells. Biochemical and biophysical research communications 431, 52-57.

Møllgaard, M., Degn, M., Sellebjerg, F., Frederiksen, J., and Modvig, S. (2016). Cerebrospinal fluid chitinase□3□like 2 and chitotriosidase are potential prognostic biomarkers in early multiple sclerosis. European journal of neurology 23, 898-905.

Mondal, S., Baksi, S., Koris, A., and Vatai, G. (2016). Journey of enzymes in entomopathogenic fungi. Pacific Science Review A: Natural Science and Engineering 18, 85-99.

Murphy, J., Summer, R., Wilson, A.A., Kotton, D.N., and Fine, A. (2008). The prolonged life-span of alveolar macrophages. American journal of respiratory cell and molecular biology 38, 380-385.

Murray, P.J., Allen, J.E., Biswas, S.K., Fisher, E.A., Gilroy, D.W., Goerdt, S., Gordon, S., Hamilton, J.A., Ivashkiv, L.B., and Lawrence, T. (2014). Macrophage activation and polarization: nomenclature and experimental guidelines. Immunity 41, 14-20.

Muszyński, P., Groblewska, M., Kulczyńska-Przybik, A., Kułakowska, A., and Mroczko, B. (2017). YKL-40 as a potential biomarker and a possible target in therapeutic strategies of Alzheimer's disease. Current neuropharmacology.

Muzzarelli, R.A. (2013). Chitin (Elsevier).

Nishida, N., Yano, H., Nishida, T., Kamura, T., and Kojiro, M. (2006). Angiogenesis in cancer. Vascular health and risk management 2, 213.

Nishikawa, K.C., and Millis, A.J. (2003). gp38k (CHI3L1) is a novel adhesion and migration factor for vascular cells. Experimental cell research 287, 79-87.

Nøjgaard, C., Johansen, J.S., Christensen, E., Skovgaard, L.T., Price, P.A., Becker, U., and Group, E. (2003). Serum levels of YKL-40 and PIIINP as prognostic markers in patients with alcoholic liver disease. Journal of hepatology 39, 179-186.

Nurgazieva, D., Mickley, A., Moganti, K., Ming, W., Ovsyi, I., Popova, A., Awad, K., Wang, N., Bieback, K., and Goerdt, S. (2015). TGF-β1, but not bone morphogenetic proteins, activates Smad1/5 pathway in primary human macrophages and induces expression of proatherogenic genes. The Journal of Immunology 194, 709-718.

Olson, O.C., and Joyce, J.A. (2015). Cysteine cathepsin proteases: regulators of cancer progression and therapeutic response. Nature Reviews Cancer 15, 712-729.

Owhashi, M., Arita, H., and Hayai, N. (2000). Identification of a novel eosinophil chemotactic cytokine (ECF-L) as a chitinase family protein. Journal of Biological Chemistry 275, 1279-1286.

Partridge, N.C., and Siddiqui, J.A. (2017). CCL2/MCP-1 and Parathyroid Hormone Action on Bone. Frontiers in Endocrinology 8, 49.

Patel, S., and Goyal, A. (2017). Chitin and chitinase: Role in pathogenicity, allergenicity and health. International Journal of Biological Macromolecules.

Pellicoro, A., Ramachandran, P., Iredale, J.P., and Fallowfield, J.A. (2014). Liver fibrosis and repair: immune regulation of wound healing in a solid organ. Nature Reviews Immunology 14, 181-194.

Piao, S., and Amaravadi, R.K. (2015). Targeting the lysosome in cancer. Annals of the New York Academy of Sciences.

Piao, S., and Amaravadi, R.K. (2016). Targeting the lysosome in cancer. Annals of the New York Academy of Sciences 1371, 45-54.

Pickup, M., Novitskiy, S., and Moses, H.L. (2013). The roles of TGF [beta] in the tumour microenvironment. Nature Reviews Cancer 13, 788-799.

Politz, O., Gratchev, A., McCOURT, P.A., Schledzewski, K., Guillot, P., Johansson, S., Svineng, G., Franke, P., Kannicht, C., and Kzhyshkowska, J. (2002). Stabilin-1 and− 2 constitute a novel family of fasciclin-like hyaluronan receptor homologues. Biochemical Journal 362, 155-164.

Ponpuak, M., Mandell, M.A., Kimura, T., Chauhan, S., Cleyrat, C., and Deretic, V. (2015). Secretory autophagy. Current opinion in cell biology 35, 106-116.

Quail, D.F., and Joyce, J.A. (2013). Microenvironmental regulation of tumor progression and metastasis. Nature medicine 19, 1423-1437.

Qureshi, A.M., Hannigan, A., Campbell, D., Nixon, C., and Wilson, J.B. (2011). Chitinase-like proteins are autoantigens in a model of inflammation-promoted incipient neoplasia. Genes & cancer 2, 74-87.

Ramji, D., Singh, N., Foka, P., Irvine, S., and Arnaoutakis, K. (2006). Transforming growth factor-β-regulated expression of genes in macrophages implicated in the control of cholesterol homoeostasis (Portland Press Limited).

Ranok, A., Wongsantichon, J., Robinson, R.C., and Suginta, W. (2015). Structural and thermodynamic insights into chitooligosaccharide binding to human cartilage chitinase 3-like protein 2 (CHI3L2 or YKL-39). Journal of Biological Chemistry 290, 2617-2629.

Raskovalova, T., Deegan, P.B., Yang, R., Pavlova, E., Stirnemann, J., Labarère, J., Zimran, A., Mistry, P.K., and Berger, M. (2017). Plasma chitotriosidase activity versus CCL18 level for assessing type I Gaucher disease severity: protocol for a systematic review with meta-analysis of individual participant data. Systematic Reviews 6, 87.

Recklies, A.D., White, C., and Hua, L. (2002). The chitinase 3-like protein human cartilage glycoprotein 39 (HC-gp39) stimulates proliferation of human connective-tissue cells and activates both extracellular signal-regulated kinase-and protein kinase B-mediated signalling pathways. Biochemical Journal 365, 119-126.

Rehli, M., Krause, S., and Andreesen, R. (1997). Molecular characterization of the gene for human cartilage gp-39 (CHI3L1), a member of the chitinase protein family and marker for late stages of macrophage differentiation. Genomics 43, 221-225.

Rehli, M., Niller, H.-H., Ammon, C., Langmann, S., Schwarzfischer, L., Andreesen, R., and Krause, S.W. (2003). Transcriptional regulation of CHI3L1, a marker gene for late stages of macrophage differentiation. Journal of Biological Chemistry 278, 44058-44067.

Renkema, G.H., Boot, R.G., Au, F.L., Donker□Koopman, W.E., Strijland, A., Muijsers, A.O., Hrebicek, M., and Aerts, J.M. (1998). Chitotriosidase, a chitinase, and the 39□kDa human cartilage glycoprotein, a chitin□binding lectin, are homologues of family 18 glycosyl hydrolases secreted by human macrophages. European Journal of Biochemistry 251, 504-509.

Renkema, G.H., Boot, R.G., Strijland, A., Donker□Koopman, W.E., Berg, M., Muijsers, A.O., and Aerts, J.M. (1997). Synthesis, sorting, and processing into distinct isoforms of human macrophage chitotriosidase. European Journal of Biochemistry 244, 279-285.

Repnik, U., Stoka, V., Turk, V., and Turk, B. (2012). Lysosomes and lysosomal cathepsins in cell death. Biochimica et Biophysica Acta (BBA)-Proteins and Proteomics 1824, 22-33.

Rhee, I. (2016). Diverse macrophages polarization in tumor microenvironment. Archives of pharmacal research 39, 1588-1596.

Riabov, V., Gudima, A., Wang, N., Mickley, A., Orekhov, A., and Kzhyshkowska, J. (2014). Role of tumor associated macrophages in tumor angiogenesis and lymphangiogenesis. The regulation of angiogenesis by tissue cell-macrophage interactions, 63.

Riabov, V., Yin, S., Song, B., Avdic, A., Schledzewski, K., Ovsiy, I., Gratchev, A., Verdiell, M.L., Sticht, C., and Schmuttermaier, C. (2016). Stabilin-1 is expressed in human breast cancer and supports tumor growth in mammary adenocarcinoma mouse model. Oncotarget 7, 31097.

Robinson, D.G., and Neuhaus, J.-M. (2016). Receptor-mediated sorting of soluble vacuolar proteins: myths, facts, and a new model. Journal of experimental botany 67, 4435-4449.

Rodríguez-Prados, J.-C., Través, P.G., Cuenca, J., Rico, D., Aragonés, J., Martín-Sanz, P., Cascante, M., and Boscá, L. (2010). Substrate fate in activated macrophages: a comparison between innate, classic, and alternative activation. The Journal of Immunology 185, 605-614.

Rőszer, T. (2015). Understanding the mysterious M2 macrophage through activation markers and effector mechanisms. Mediators of inflammation 2015.

Salamon, J., Hoffmann, T., Elies, E., Peldschus, K., Johansen, J.S., Lüers, G., Schumacher, U., and Wicklein, D. (2014). Antibody directed against human YKL-40 increases tumor volume in a human melanoma xenograft model in scid mice. PloS one 9, e95822.

Sanfilippo, C., Nunnari, G., Calcagno, A., Malaguarnera, L., Blennow, K., Zetterberg, H., and Di Rosa, M. (2017). The chitinases expression is related to Simian Immunodeficiency Virus Encephalitis (SIVE) and in HIV encephalitis (HIVE). Virus research 227, 220-230.

Schimpl, M., Rush, C.L., Betou, M., Eggleston, I.M., Recklies, A.D., and Van Aalten, D.M. (2012). Human YKL-39 is a pseudo-chitinase with retained chitooligosaccharide-binding properties. Biochemical Journal 446, 149-157.

Schledzewski, K., Falkowski, M., Moldenhauer, G., Metharom, P., Kzhyshkowska, J., Ganss, R., Demory, A., Falkowska□Hansen, B., Kurzen, H., and Ugurel, S. (2006). Lymphatic endothelium□specific hyaluronan receptor LYVE□1 is expressed by stabilin□1+, F4/80+, CD11b+ macrophages in malignant tumours and wound healing tissue in vivo and in bone marrow cultures in vitro: implications for the assessment of lymphangiogenesis. The Journal of pathology 209, 67-77.

Schmidt, H., Johansen, J.S., Gehl, J., Geertsen, P.F., Fode, K., and von der Maase, H. (2006). Elevated serum level of YKL□40 is an independent prognostic factor for poor survival in patients with metastatic melanoma. Cancer 106, 1130-1139.

Schneider, C., Nobs, S.P., Kurrer, M., Rehrauer, H., Thiele, C., and Kopf, M. (2014). Induction of the nuclear receptor PPAR-[gamma] by the cytokine GM-CSF is critical for the differentiation of fetal monocytes into alveolar macrophages. Nature immunology 15, 1026-1037.

Schröder, B.A., Wrocklage, C., Hasilik, A., and Saftig, P. (2010). The proteome of lysosomes. Proteomics 10, 4053-4076.

Shao, R. (2014). YKL-40 acts as an angiogenic factor to promote tumor angiogenesis. The regulation of angiogenesis by tissue cell-macrophage interactions 7.

Shao, R., Cao, Q., Arenas, R., Bigelow, C., Bentley, B., and Yan, W. (2011). Breast cancer expression of YKL-40 correlates with tumour grade, poor differentiation, and other cancer markers. British journal of cancer 105, 1203-1209.

Shao, R., Hamel, K., Petersen, L., Cao, Q., Arenas, R.B., Bigelow, C., Bentley, B., and Yan, W. (2009). YKL-40, a secreted glycoprotein, promotes tumor angiogenesis. Oncogene 28, 4456-4468.

Sierra-Filardi, E., Nieto, C., Domínguez-Soto, Á., Barroso, R., Sánchez-Mateos, P., Puig-Kroger, A., López-Bravo, M., Joven, J., Ardavín, C., and Rodríguez-Fernández, J.L. (2014). CCL2 shapes macrophage polarization by GM-CSF and M-CSF: identification of CCL2/CCR2-dependent gene expression profile. The Journal of Immunology 192, 3858-3867.

Sohn, M.H., Kang, M.-J., Matsuura, H., Bhandari, V., Chen, N.-Y., Lee, C.G., and Elias, J.A. (2010). The chitinase-like proteins breast regression protein-39 and YKL-40 regulate

hyperoxia-induced acute lung injury. American journal of respiratory and critical care medicine 182, 918-928.

Stahlschmidt, W., Robertson, M.J., Robinson, P.J., McCluskey, A., and Haucke, V. (2014). Clathrin terminal domain-ligand interactions regulate sorting of mannose 6-phosphate receptors mediated by AP-1 and GGA adaptors. Journal of Biological Chemistry 289, 4906-4918.

Steck, E., Breit, S., Breusch, S.J., Axt, M., and Richter, W. (2002). Enhanced expression of the human chitinase 3-like 2 gene (YKL-39) but not chitinase 3-like 1 gene (YKL-40) in osteoarthritic cartilage. Biochemical and biophysical research communications 299, 109-115.

Stout, R.D., and Suttles, J. (2004). Functional plasticity of macrophages: reversible adaptation to changing microenvironments. Journal of leukocyte biology 76, 509-513.

Tamoutounour, S., Guilliams, M., Sanchis, F.M., Liu, H., Terhorst, D., Malosse, C., Pollet, E., Ardouin, L., Luche, H., and Sanchez, C. (2013). Origins and functional specialization of macrophages and of conventional and monocyte-derived dendritic cells in mouse skin. Immunity 39, 925-938.

Tang, D., Shi, Y., Kang, R., Li, T., Xiao, W., Wang, H., and Xiao, X. (2007). Hydrogen peroxide stimulates macrophages and monocytes to actively release HMGB1. Journal of leukocyte biology 81, 741-747.

Tang, H., Sun, Y., Shi, Z., Huang, H., Fang, Z., Chen, J., Xiu, Q., and Li, B. (2013). YKL-40 induces IL-8 expression from bronchial epithelium via MAPK (JNK and ERK) and NF-κB pathways, causing bronchial smooth muscle proliferation and migration. The Journal of Immunology 190, 438-446.

Tharanathan, R.N., and Kittur, F.S. (2003). Chitin—the undisputed biomolecule of great potential.

Thieringer, R., Le Grand, C.B., Carbin, L., Cai, T.-Q., Wong, B., Wright, S.D., and Hermanowski-Vosatka, A. (2001). 11β-Hydroxysteroid dehydrogenase type 1 is induced in human monocytes upon differentiation to macrophages. The Journal of Immunology 167, 30-35.

Thongsom, S., Chaocharoen, W., Silsirivanit, A., Wongkham, S., Sripa, B., Choe, H., Suginta, W., and Talabnin, C. (2016). YKL-40/chitinase-3-like protein 1 is associated with poor prognosis and promotes cell growth and migration of cholangiocarcinoma. Tumor Biology 37, 9451-9463.

Topalian, S.L., Drake, C.G., and Pardoll, D.M. (2015). Immune checkpoint blockade: a common denominator approach to cancer therapy. Cancer cell 27, 450-461.

van de Laar, L., Saelens, W., De Prijck, S., Martens, L., Scott, C.L., Van Isterdael, G., Hoffmann, E., Beyaert, R., Saeys, Y., and Lambrecht, B.N. (2016). Yolk sac macrophages, fetal liver, and adult monocytes can colonize an empty niche and develop into functional tissue-resident macrophages. Immunity 44, 755-768.

Varol, C., Mildner, A., and Jung, S. (2015). Macrophages: development and tissue specialization. Annual review of immunology 33, 643-675.

Vind, I., Johansen, J., Price, P., and Munkholm, P. (2003). Serum YKL-40, a potential new marker of disease activity in patients with inflammatory bowel disease. Scandinavian journal of gastroenterology 38, 599-605.

Volck, B., Price, P.A., Johansen, J.S., Sørensen, O., Benfield, T.L., Nielsen, H.J., Calafat, J., and Borregaard, N. (1997). YKL-40, a mammalian member of the chitinase family, is a matrix protein of specific granules in human neutrophils. Proceedings of the Association of American Physicians 110, 351-360.

Vos, K., Steenbakkers, P., Miltenburg, A., Bos, E., van Den Heuvel, M., Van Hogezand, R., De Vries, R., Breedveld, F., and Boots, A. (2000). Raised human cartilage

glycoprotein-39 plasma levels in patients with rheumatoid arthritis and other inflammatory conditions. Annals of the rheumatic diseases 59, 544-548.

Wan, G., Xiang, L., Sun, X., Wang, X., Li, H., Ge, W., and Cao, F. (2017). Elevated YKL-40 expression is associated with a poor prognosis in breast cancer patients. Oncotarget 8, 5382.

Wang, N. (2012). Analysis of biological activity and mechanism of secretion of chitinase-like protein SI-CLP. In Department of Dermatology, Venerology and Allergology of the Medical Faculty of Mannheim (Mannheim, Germany: Medical Faculty Mannheim of the University of Heidelberg), pp. 111.

Wang, Y., Zang, Q.S., Liu, Z., Wu, Q., Maass, D., Dulan, G., Shaul, P.W., Melito, L., Frantz, D.E., and Kilgore, J.A. (2011). Regulation of VEGF-induced endothelial cell migration by mitochondrial reactive oxygen species. American Journal of Physiology-Cell Physiology 301, C695-C704.

Xiao, W., Meng, G., Zhao, Y., Yuan, H., Li, T., Peng, Y., Zhao, Y., Luo, M., Zhao, W., and Li, Z. (2014). Human Secreted Stabilin□1− Interacting Chitinase‐like Protein Aggravates the Inflammation Associated With Rheumatoid Arthritis and Is a Potential Macrophage Inflammatory Regulator in Rodents. Arthritis & Rheumatology 66, 1141-1152.

Xu, M., Zhou, G.-m., Wang, L.-h., Zhu, L., Liu, J.-m., Wang, X.-d., Li, H.-t., and Chen, L. (2016). Inhibiting High-Mobility Group Box 1 (HMGB1) Attenuates inflammatory cytokine expression and neurological deficit in ischemic brain injury following cardiac arrest in rats. Inflammation 39, 1594-1602.

Xue, J., Schmidt, S.V., Sander, J., Draffehn, A., Krebs, W., Quester, I., De Nardo, D., Gohel, T.D., Emde, M., and Schmidleithner, L. (2014). Transcriptome-based network analysis reveals a spectrum model of human macrophage activation. Immunity 40, 274-288.

Yang, W.S., Yi, Y.-S., Kim, D., Kim, M.H., Park, J.G., Kim, E., Lee, S.Y., Yoon, K., Kim, J.-H., and Park, J. (2016). Nuclear factor kappa-B-and activator protein-1-mediated immunostimulatory activity of compound K in monocytes and macrophages. Journal of Ginseng Research.

Yona, S., Kim, K.-W., Wolf, Y., Mildner, A., Varol, D., Breker, M., Strauss-Ayali, D., Viukov, S., Guilliams, M., and Misharin, A. (2013). Fate mapping reveals origins and dynamics of monocytes and tissue macrophages under homeostasis. Immunity 38, 79-91.

Young, K., and Singh, G. (2016). Cancer-Induced Inflammation. In Oncodynamics: Effects of Cancer Cells on the Body (Springer), pp. 73-84.

Zhao, J., Lv, Z., Wang, F., Wei, J., Zhang, Q., Li, S., Yang, F., Zeng, X., Wu, X., and Wu, Z. (2013). Ym1, an eosinophilic chemotactic factor, participates in the brain inflammation induced by Angiostrongylus cantonensis in mice. Parasitology research 112, 2689-2695.

Zhu, Z., Zheng, T., Homer, R.J., Kim, Y.-K., Chen, N.Y., Cohn, L., Hamid, Q., and Elias, J.A. (2004). Acidic mammalian chitinase in asthmatic Th2 inflammation and IL-13 pathway activation. Science 304, 1678-1682.

7. Curriculum Vitae

PERSONAL

Name:	Tengfei Liu
Date of birth:	11.08.1987
Nationality:	China
Family status:	Married
Father:	Lei Liu
Mother:	Jianmei Liu

EDUCATIONAL BACKGROUND

09.2003-06.2006	Gaobeidian No.1 High School, Baoding, Hebei, China
06.2006	Degree: High School Diploma

UNIVERSITY BACKGROUND

10.2013 – present	Post-graduate study at Ruprecht–Karls University of Heidelberg, Institute of Transfusion Medicine and Immunology, Germany
09.2010 - 06.2013	Hebei University, Baoding, Hebei, China Major: Pharmaceutical Analysis Minor: Cell Pharmacology
06.2013	Degree: Master of Science Master's thesis title: "The anti-inflammatory effects of short chain fatty acids and their analogues". Master thesis score: excellent
09.2006-06.2010	Hebei University, Baoding, Hebei, China Major: Pharmaceutical Sciences Minor: Biochemical Pharmacy
06.2010	Degree: Bachelor of Science Bachelor's thesis title: "Antitumor activity studies on four kinds of novel Thiochromanone derivatives". Bachelor thesis score: excellent

8. Acknowledgements

First, I express my deep sense of gratitude to my supervisor Prof. Dr. Julia Kzhyshkowska for her excellent guidance and support from the initial to the final steps of my Ph.D. project, for helping to develop an understanding of the subject, for encouragement and valuable scientific and general advice, for her attentive review of my thesis.

I would like to acknowledge Prof. Dr. Harald Klüter, director of the Institute of Transfusion Medicine and Immunology, University of Heidelberg, for permitting me and providing me all necessary facilities to complete my thesis.

I would also like to acknowledge the support of China Scholar Council and the Chinese Government, for providing the finance and education opportunity during my thesis. I would also like to acknowledge the Graduate Academy of Heidelberg University and DKFZ, for providing the necessary courses and training and all the wonderful lectures and symposiums.

I am warmly thankful to Ms. Christina Schmuttermaier, Ms. Stefanie Uhlig and Ms. Susanne Elvers-Hornung for their excellent technical assistance, good advice, as well as for the creation of a comfortable and friendly atmosphere in the laboratory. I am also grateful to Prof. Dr. Karen Bieback for giving me valuable advice and assisting me in RT-qPCR data analysis. I am extremely grateful to Dr. Elisabeth Kremmer, Institute for Molecular Immunology, Helmholtz Center Munich, for the co-operation in the generation of monoclonal anti-YKL- 39 antibodies.

I would like to thank Ms. Carolina De La Torre and Dr. Carsten Sticht from the Affymetrix Core Facility of Medical Research Center, Medical Faculty Mannheim, University of Heidelberg for assistance with hybridization of the gene expression microarrays and statistical analysis of the data.

I would like to thank my friends and colleagues Vladimir Riabov, Julia Michel, Amanda Mickley, Shuiping Yin, Dandan Xu, Kondaiah Moganti, Michael Balduff, Laura Matuschik, Feng Li, Maria Llopis Verdiell, Marije Mossel and Bin Song for their advice and for providing many enjoyable moments in and outside the laboratory.

My warmest thanks go to my wife Kun Xie for her constant support, encouragement and all the help throughout my work. Finally, yet importantly, I would like to thank my family for the inspiration of my activities and creation of comfort in my life.